The School of Engineering

THE UNIVERSITY OF AUCKLAND
NEW ZEALAND

Department of Civil and Environmental Engineering

# Design of Ductile Reinforced Concrete Moment Resisting Frames Using Grade 500E Reinforcement

by

**Nicholas Brooke**
Les Megget
Dr. Jason Ingham

April 2005

School of Engineering
Report No. 617

**Whakapukahatanga Taiao**
New Zealand Maori for
Strengthening the environment - built and natural

**For further information contact:**
Department of Civil and Environmental Engineering, School of Engineering
The University of Auckland, Private Bag 92019, Auckland, New Zealand
Telephone 64-9-3737599 ext.88166 or ext. 85715 Facsimile 64-9-3737462
Web www.cee.auckland.ac.nz Email cee-enquiries@auckland.ac.nz

# Design of Ductile Reinforced Concrete Moment Resisting Frames Using Grade 500E Reinforcement

by

**Nicholas Brooke**

Les Megget

Dr. Jason Ingham

**School of Engineering Report No. 617**

Department of Civil and Environmental Engineering
The University of Auckland
New Zealand

April 2005

# Summary

This report describes a series of four interior beam-column joint tests conducted at the University of Auckland. These tests were funded by the Earthquake Commission research foundation. The purpose of the tests was to provide data on the seismic performance of beam-column joints with grade 500E beam longitudinal reinforcement of large diameters. In particular the tests examined the occurrence of bond failure and reinforcement slip in such joints.

The test units were representative of an interior beam-column joint from a typical, monolithic moment resisting frame. The units were approximately two thirds of full size, and of similar size to five beam-column joints previously tested at the University of Auckland that used smaller diameter beam longitudinal reinforcement. The test units were designed using the capacity design procedures of NZS 3101:1995. However, to promote bond failure the units did not follow the requirements limiting the ratio of beam longitudinal reinforcement diameter to column depth.

The four beam-column joint sub-assemblies were subjected to a cyclic load history. Load steps of increasing storey drift were applied. Despite none of the units meeting New Zealand design requirements for the prevention of bond failure, at drift levels equivalent to those allowed in New Zealand the performance of all four units was good, with no strength loss, and no significant reinforcement slip. At greater drift angles bond failure occurred in only two of the four tests, despite testing reaching storey drift angles that were approximately twice those allowed in New Zealand and. It is believed that the reason for the exceptionally good performance of two of the units was the large excess vertical joint shear and column moment capacity. The tests described re-emphasised the high yield drift angles, and hence low appropriate design ductility levels, of moment resisting frames including grade 500E beam longitudinal reinforcement.

This report also shows that the use of grade 500E longitudinal reinforcement in the beams of moment resisting frames is not an effective design solution. A comparison was made of beam-column joints designed for equal forces using grade 300E and grade 500E beam longitudinal reinforcement. It was found that in most cases the use of grade 500E reinforcement requires at least twice as many bars, resulting in worse reinforcement congestion in the joints, where congestion has always been a problem. This situation would be worsened if realistic allowance was made for the higher forces that the frame reinforced with grade 500E longitudinal reinforcement would have to sustain, due to the lower ductility inherent in the design.

It was concluded that current New Zealand design rules for the prevention of bond failure in frames reinforced with grade 500E beam longitudinal reinforcement are currently mildly conservative. This was considered a satisfactory situation. However, it is recommended that designers do not use grade 500E longitudinal reinforcement in the beams of moment resisting frames.

# Contents

# List of Figures

# List of Tables

# Notation

| | | |
|---|---|---|
| $A_g$ | = | Gross area of column section |
| $A_s$ | = | Area of larger of top or bottom beam reinforcement areas |
| $A_s'$ | = | Area of smaller of top or bottom beam reinforcement areas |
| $C_c$ | = | Concrete compression force opposing tension force in steel area $A_s$ |
| $C'_c$ | = | Concrete compression force opposing tension force in steel area $A_s'$ |
| $C''_c$ | = | Column concrete compression force |
| $C'''_c$ | = | Column concrete compression force |
| $C_s$ | = | Reinforcement compression force opposing tension force in steel area $A_s$ |
| $C'_s$ | = | Reinforcement compression force opposing tension force in steel area $A_s'$ |
| $C''_s$ | = | Column reinforcement compression force |
| $C'''_s$ | = | Column reinforcement compression force |
| $d_b$ | = | Diameter of reinforcement that is part of $A_s$ |
| $d_b'$ | = | Diameter of reinforcement that is part of $A_s'$ |
| Dxx | = | Designation of deformed reinforcing bar of diameter xx mm and nominal yield strength of 300 MPa |
| $E_c$ | = | Young's modulus for concrete |
| $E_{steel}$ | = | Young's modulus for reinforcing steel taken as 200,000 MPa |
| F | = | NZS 3101 factor to increase the required column depth when high strength reinforcement is used in beams |
| $F_B$ | = | Change in reinforcement force per unit length over width of joint |
| $f_B$ | = | Change in reinforcement stress per unit length over width of joint |
| $f_{BMax}$ | = | Maximum change in reinforcement stress per unit length before bond failure occurs |
| $f'_c$ | = | Unconfined compressive strength of concrete |
| $F_n$ | = | Actuator force required to develop nominal yield strength of a beam |
| $f_u$ | = | Ultimate tensile strength of reinforcement |
| $f_y$ | = | Yield strength of reinforcement area $A_s$ |
| $f'_y$ | = | Yield strength of reinforcement area $A_s'$ |
| $F_{3/4Fn}$ | = | Actuator force at peak of $¾F_n$ half-cycle |
| HDxx | = | Designation of deformed reinforcing bar of diameter xx mm and nominal yield strength of 500 MPa |
| $h_b$ | = | Depth of beam section |
| $h_c$ | = | Depth of column section |
| HRxx | = | Designation of plain reinforcing bar of diameter xx mm and nominal yield strength of 500 MPa |
| $I_e$ | = | Effective moment of inertia of a concrete section |
| $I_g$ | = | Gross moment of inertia of a concrete section |

| | | |
|---|---|---|
| $l_b$ | = | Length of beam between column centres (or actuators) |
| $l_c$ | = | Length of column between beam centres (or column restraints) |
| $M_{col}$ | = | Bending moment in column |
| $M_n$ | = | Nominal moment capacity of a section calculated according to NZS 3101:1995 |
| $M_o$ | = | Beam overstrength moment supported by $A_s$, $C_s$ and $C_c$ |
| $M'_o$ | = | Beam overstrength moment supported by $A_s'$, $C'_s$ and $C'_c$ |
| $M_y$ | = | Predicted yield strength of beams, calculated as a doubly reinforced section |
| $N^*$ | = | Column axial force |
| Rxx | = | Designation of plain reinforcing bar of diameter xx mm and nominal yield stress of 300 MPa |
| T | = | Tension force in reinforcement area $A_s$ |
| T' | = | Tension force in reinforcement area $A'_s$ |
| T'' | = | Tension force in column reinforcement |
| T''' | = | Tension force in column reinforcement |
| $V_b$ | = | Beam shear force generating |
| $V_{col}$ | = | Column shear force |
| $V_{jh}$ | = | Horizontal joint shear force |
| $V_{jv}$ | = | Vertical joint shear force |
| $\alpha_f$ | = | A factor accounting for the reduction in bond strength expected when beams frame into a joint in two planes |
| $\alpha_o$ | = | Reinforcement overstrength factor |
| $\alpha_p$ | = | A factor to account for the influence of column axial load on bond strength |
| $\alpha_s$ | = | A factor to account for the more severe bond conditions experienced by reinforcement that is part of $A_s'$ |
| $\alpha_t$ | = | A factor to account for the negative influence on bond strength of having a large depth of fresh concrete beneath a reinforcing bar |
| $\beta$ | = | Ratio of smaller to larger beam reinforcement areas |
| $\gamma$ | = | A joint shear deformation |
| $\Delta_y$ | = | Estimated beam tip displacement at first yielding of beam reinforcement |
| $\Delta_{3/4Fn}$ | = | Beam tip displacement at peak of $¾F_n$ half-cycle |
| $\delta_c$ | = | Calculated design interstorey deflection |
| $\delta_m$ | = | Maximum permissible design interstorey drift |
| $\delta_x$ | = | Change of length of portal gauge number x |
| $\varepsilon_y$ | = | Yield strain of reinforcement |
| $\theta_y$ | = | Interstorey drift at point of first yield |
| $\mu$ | = | Displacement ductility factor |
| $\rho$ | = | Beam reinforcement ratio |
| $\varphi_y$ | = | Yield curvature of a section |

# 1 Introduction

In New Zealand there have traditionally been two grades of steel reinforcement. Over time the yield strength of these materials has gradually increased. Most recently the yield strength of the higher strength reinforcement was increased from 430 MPa to 500 MPa (Grade 500E). This resulted in changes to the way reinforced concrete structures must be designed. The research presented here looked at the impact of the higher strength reinforcement on the occurrence of bond failure in beam-column joints

Reinforced concrete is a composite material. For structural purposes compressive forces are typically carried by the concrete, and tensile forces by the steel reinforcement. This takes advantage of the properties of both materials. In order for structures to function correctly it is vital that forces can be transferred between the concrete and reinforcement. One mechanism by which this occurs is the bond that forms at the interface between the reinforcement and the concrete. This bond mechanism is particularly important in interior beam-column joints.

Like any material the bond between steel and concrete has a finite strength. If the maximum bond stress is exceeded and the bond between the beam longitudinal reinforcement and the concrete in the joint is broken, the reinforcement can slip freely through the concrete and the stiffness of the beam-column joint is reduced significantly. This is unlikely to cause a catastrophic failure, but will increase the deflection of the building if it is subjected to further loading. The failure of the bond mechanism is dependent on concrete strength and confinement, reinforcement strength and diameter, and the length over which the force transfer can occur (column size in beam-column joints).

Previous research at the University of Auckland [1, 2] indicated that New Zealand design rules did not provide sufficient protection against bond failure of high strength reinforcement in beam-column joints. In order to rectify this situation a database of interior beam-column joint test results was previously assembled to determine appropriate design criteria [3]. An amendment to NZS 3101:1995 [4] based on this database was released in late 2003. However, previous beam-column joint tests in New Zealand that used grade 500 reinforcement all contained beam longitudinal reinforcement of 20 mm diameter or smaller. It was therefore felt to be desirable to investigate the effect of using larger diameter high strength beam reinforcement on the bond performance of beam-column joints. The four tests described herein provide information on this subject.

# 2 Literature Review

This literature review focuses on bond failure in interior beam-column joints and gives an overview of previous reinforced concrete beam-column joint testing, particularly considering tests that investigated bond failure in interior joints. Additionally, the review traces the development of New Zealand standard requirements for the prevention of bond failure in interior beam-column joints.

## *2.1 Beam-column joints*

A moment resisting frame is a structural form consisting of vertical columns and horizontal beams, typically joined together in a grid type pattern. The points at which these elements meet are defined as beam-column joint regions. The role of the beam-column joint is to transfer forces (shear, moment and axial force) between the beams and columns of the frame.

Depending on the type of frame and the location of the joint within the frame, a beam-column joint can have between one and four beams framing into it. Joints are generally divided into exterior and interior joints, and frames into perimeter and space frames. Exterior joints are comprised of either one (perimeter frame) or two (uniform frame) beams meeting the column, and interior joints have at least two beams framing into the joint on parallel faces. Examples of these joint types can be seen in Figure 2-1. At the top floor of a building similar joints to those below exist, but without a column extending above the joint.

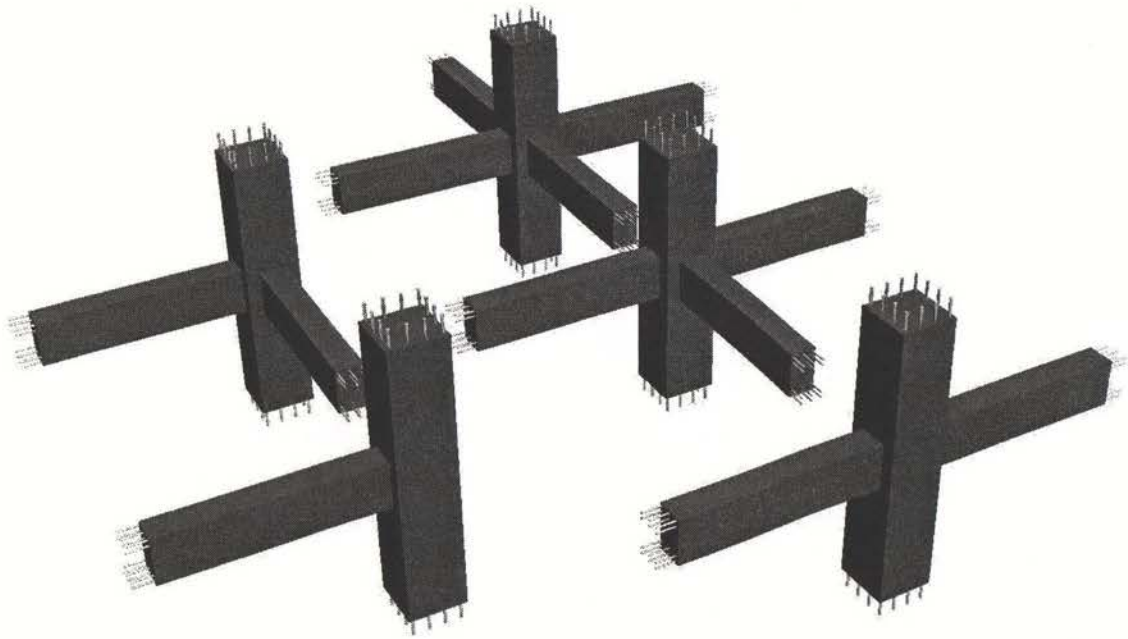

**Figure 2-1 Possible configurations of exterior (left row) and interior (right row) beam-column joints**

Aside from plastic hinge formation adjacent to the joint region, there are two predominant failure modes for interior beam-column joints [5], these being a shear failure associated with the provision of insufficient joint shear reinforcement, and bond or anchorage failure of the longitudinal beam reinforcement. This second failure mode occurs due to the high bond stresses that typically develop in interior beam-column joints [6].

## 2.2 Initial investigations into beam-column joint performance

Although the importance of the role of beam-column joints in the seismic performance of reinforced concrete moment resisting frames is widely recognised today, this has not always been the case. The need to properly detail reinforced concrete beam-column joints is not given special attention by Blume et al. [7] in their landmark textbook of 1961.

The inadequacies of then-current methods of detailing beam-column joints was revealed by a series of serious earthquakes during the 1960's. Failure of beam-column joints was identified as one of the primary causes in cases where moment resisting frames performed poorly [8]. This led Hanson and Connor to conduct the first significant research investigating the seismic performance of reinforced concrete exterior [8] and interior [9] beam-column joints. These tests revealed that reinforced concrete moment resisting frames with well confined beam-column joints were able to meet the required performance standards of the time, i.e. avoiding visible damage during moderate earthquakes and surviving more serious seismic events without collapse [7] - design goals that are closely related to the current philosophy of limit state design [10].

Following these initial tests assessing the seismic response of beam-column joints many more researchers began investigating ways of improving the seismic performance of both interior and exterior beam-column joints. The introduction and acceptance of capacity design [6, 11] as a requirement for satisfactory seismic design increased the emphasis placed on ensuring that beam-column joints were able to transfer the maximum (overstrength) actions that could be imposed on them by the surrounding members.

## 2.3 Interior beam-column joint testing

The actions on interior beam-column joints differ quite substantially from those on exterior joints [6]. For cases where beam details are similar, the shear strength of interior beam-column joints must be greater than exterior joints, since the presence of beams framing into the joint on opposite sides leads to significantly greater shear forces compared to exterior joints [6]. With reference to Figure 2-2, the horizontal shear force on a beam-column joint when yielding occurs adjacent to the joint is:

$$V_{jh} = T + C'_c + C'_s - V_{col} \qquad \textbf{eq. 1}$$

where T, $C'_c$ and $C'_s$ are the tension and compression forces on opposite sides of the joint and $V_{col}$ is the shear force acting in the column above the joint. For an interior joint with equal positive and negative beam longitudinal reinforcement ($A_s$=$A'_s$):

$$C'_c + C'_s \approx T \qquad \text{eq. 2}$$

while for an exterior joint both $C'_c$ and $C'_s$ are zero (since there is no beam framing into the joint on the opposite side of the joint). It is therefore evident that for an interior beam column joint the horizontal joint shear will be almost twice that of an exterior joint. It is also accepted that the bond within the joint between the concrete and the longitudinal reinforcement occurs under more adverse conditions [6, 12]. These adverse conditions occur because of the greater change in reinforcement stress across the width of an interior joint compared to an exterior joint. Seismic induced axial loading of the columns is normally less critical than in exterior joints, due to the balancing effect of approximately equal beam shear forces being applied in opposing directions by the two beams on opposite faces of the joint (see Figure 2-2).

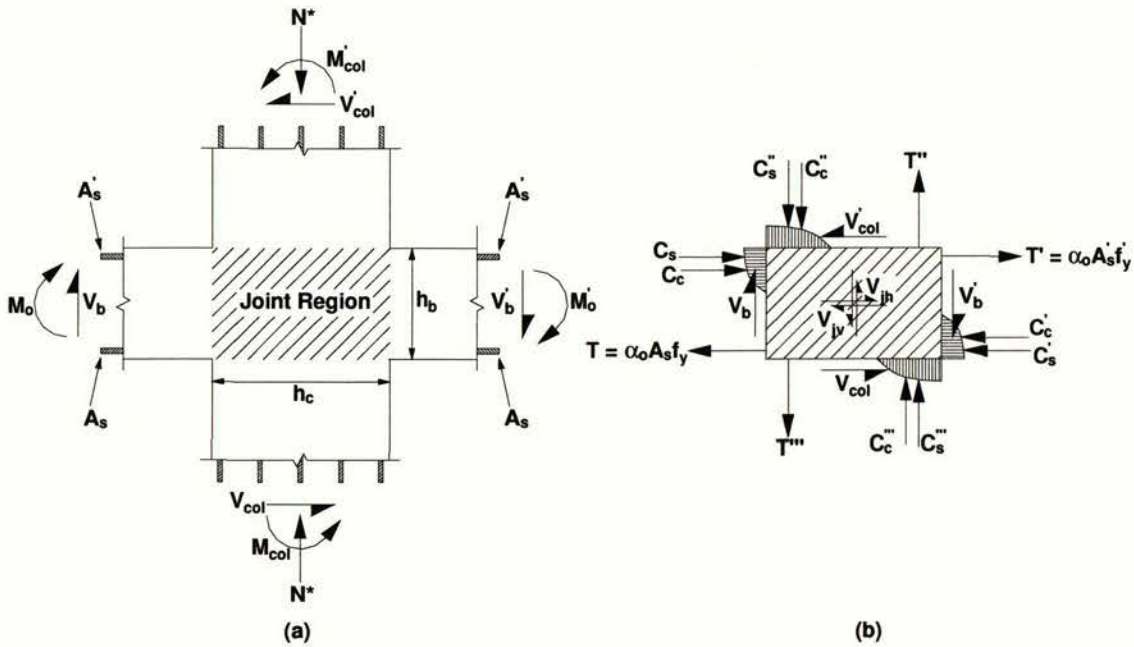


**Figure 2-2 External & internal actions on an interior beam-column joint (after NZS 3101:1995 [4])**

It has been determined from analysis of previous test results that it is possible to develop and sustain very high bond stresses within a beam-column joint provided that reinforcement does not yield [13]. For most moment resisting frames, designers in New Zealand are obliged to employ a capacity design philosophy to ensure that in a seismic event yielding can only occur in the beam flexural reinforcement [10]. By preventing the yielding of column reinforcement, the formation of a less ductile column sway collapse mechanism is avoided [6]. A secondary effect of this design philosophy is to significantly reduce the likelihood that the column reinforcement anchorage in the joint region will fail [4, 13]. For this reason, the current study focused on the failure of bond between the beam reinforcement and the surrounding concrete.

A reduction of stiffness and energy dissipation are characteristic of anchorage failure in interior joints [5]. This form of failure is less likely than joint shear failure to cause structural collapse [3]. In addition, it has proven difficult to formulate a model of bond slip behaviour that is both accurate and suitably simple for routine design [14], and it is widely believed that some level of bond failure is inevitable in joints experiencing seismic attack [14-16].

The absence of a validated bond slip model, as mentioned in the previous paragraph, has resulted in a high level of empiricism being included in the formulation of design provisions to prevent bond failure in interior beam-column joints. It is not surprising therefore that, despite more than three decades of experimental and analytical investigation of the problem, there are still significant differences in the bond strength provisions of the world's various concrete design codes [15, 16].

Bond failure was noticed during the earliest cyclic testing of an interior beam-column joint. Hanson noted that failure of longitudinal reinforcement anchorage increased the flexibility of the test unit, but did not reduce the moment capacity. This maintenance of strength was attributed to the ability of the beam reinforcement to find anchorage in the beam concrete on the opposite side of the joint [9].

Between that finding and the present time innumerable interior beam-column joint tests have been undertaken, but only those of particular note are discussed here.

Park and Paulay [6] discussed the problem of bond failure, noting that the precise effects of bond failure were difficult to quantify due to the limited experimental data available. In discussing the results of Hanson [9] they postulated that the anchorage of beam reinforcement in the opposite beam would lead to a reduction in ductility capacity of the beams framing into the column. They also suggested that interior beam-column joints could be expected to perform better if numerous small reinforcing bars were used in place of fewer large bars. These views on bond performance in interior beam-column joints were echoed by ACI-ASCE committee 352 in their beam-column joint design provisions [17].

Despite the lack of direction given in design codes before the late 1970's on how to prevent anchorage failure, some tests conducted at this time did not show signs of bond failure [18]. This was attributed to a combination of the low yield strength reinforcement typical of the era and the likelihood of a more significant failure (plastic hinge zone, column confinement or joint shear failure for example) occurring at an early stage. However, when Fenwick and Irvine tested four beam-column joint units, complete bond failure was noted in two of these [19].

The two units tested by Fenwick and Irvine that did not experience bond failure showed the potential of a different method of detailing interior beam-column joints. In contrast to relying on the bond between reinforcement and concrete in the joint region, these units included steel plates welded to

both the beam and column longitudinal reinforcement [19]. When combined with additional reinforcement welded to the beam longitudinal reinforcement within the joint region to prevent yield penetration into the joint, these anchor plates ensured perfect anchorage of the longitudinal reinforcement [19]. However, despite relieving congestion of the joint region (by allowing the use of fewer, large diameter reinforcing bars), it was soon recognised that assembling the reinforcement of such a joint would be very difficult [13]. Two other methods of alleviating the problem of bond failure in interior beam-column joints were presented by Galunic et al. [20]. Both these methods aimed to relocate the plastic hinges away from the column face, which helps prevent bond failure. This same goal was discussed by Blakeley et al. [21] who tested a sub-assembly that incorporated haunched beams. The side effect of relocating the plastic hinge zone away from the column face is that the rotation required at each hinge is increased. This can be achieved, but requires careful detailing of the beams.

A significant effort to improve understanding of the bond-slip relationships was made at the University of California at Berkeley in the late 1970's and early 1980's [12, 22-27]. Lead by Popov and Bertero, this investigation began by conducting a series of experiments that reemphasised the high likelihood of bond failure occurring in interior beam-column joints.[12, 26]. Based on the results of these and other tests an analytical model for predicting the bond-slip behaviour of reinforcing bars was developed and described by Viwathanatepa et al. [27], Ciampi et al. [22] and Eligehausen et al. [24]. Ciampi et al. [22] also suggested that the minimum bond length (and hence column depth) should be severely restricted. They suggested that the development length should be between 25 and 40 bar diameters, and also noted that use of high strength concrete allowed a relaxation of these limits proportional to the tensile strength of the concrete. Filippou et al. [25] integrated the aforementioned bond-slip model into a model for beam-column joint sub-assemblies. They then used this model to assess the effects of various parameters on bond-slip behaviour, and thus on the hysteretic performance of beam-column joints. They concluded that the ratio of top to bottom reinforcement ($\beta$), bar diameter and yield strength, load history and specimen size all affected the bond-slip behaviour of beam-column joints. These Berkeley studies played a significant role in the development of the Paulay/Priestley relationship between bar diameter and column depth [14], subsequently adopted in the New Zealand design standard [4] and discussed further in section 2.4.

Since the 1970's, numerous studies have investigated aspects of the performance of interior beam-column joints. The bond strength developed in these tests has assisted the progressive refinement of design code requirements related to bond strength, as described in section 2.4. Recent work overseas has focussed largely on developing computational models for predicting reinforcement slip and its effect on the response of beam-column joints and moment resisting frames [28-36]. Although these studies allow considerably more accuracy in the analysis of the seismic response of reinforced concrete moment resisting frames, they are not relevant to this study, and hence are not detailed here. An exception to this statement is the investigation conducted by Leon [37]. This consisted of

testing four half-scale beam-column joints, all of which had identical beam longitudinal reinforcement. The purpose of this research was to investigate the effect of column depth on joint performance. The column depth of the units varied between 16 and 28 bar diameters, and the reinforcement used had a yield strength of 414 MPa. Leon concluded that an anchorage length of 28 bar diameters ($d_b/h_c \leq 1/28$) was required to ensure adequate joint performance.

Details of recent University of Auckland investigations into bond strength in interior beam-column joints are given in section 2.5.

## 2.4 Design Code Requirements in New Zealand for the Prevention of Bond Failure

It was mentioned in section 2.2 that prior to 1970 little attention was paid to the seismic response of beam-column joints. This lack of awareness of the importance of beam-column joints in relation to the performance of a structure was reflected in the seismic design codes of the time. As a result, early New Zealand concrete design codes did not incorporate specific design requirements for beam-column joint regions [38]. Users of these codes were referred to then-current American codes, notably those of the Structural Engineers Association of California (SEAOC) and the American Concrete Institute (ACI).

Although these American codes included some guidance on providing adequate shear strength and confinement in the joint region, the provisions dealing with longitudinal reinforcement anchorage in interior joints was limited. For instance, in their article discussing beam-column joint design provisions to be used in conjunction with ACI 318-71 (the 1971 edition of the ACI concrete design code, which was widely used in New Zealand [39, 40]) ACI-ASCE committee 352 emphasised the fact that bond stresses in interior beam-column joints may be very high [17]. However, they felt there was insufficient data to allow design rules to be formulated, and stated only that bond deterioration could be reduced by using smaller diameter reinforcing bars [17].

The lack of direction provided in overseas design codes, and an apparent contradiction of the design examples presented by ACI-ASCE committee 352 (as discussed by Paulay et al. [41]) led to the organisation of a discussion group of the New Zealand Society for Earthquake Engineering, tasked with formulating interim measures for the prevention of anchorage failure in interior beam-column joints [42]. Although covering grade 275 reinforcement only, the recommendation that beam reinforcement bar diameter should be limited to $1/25^{th}$ of the depth of the column through which it passed [42] represented the first firm guidance on anchoring of reinforcing bars in interior joints.

The restriction on bar sizes proposed by the discussion group was retained in the 1982 revision of the New Zealand concrete design code[43]. A new limit was introduced further restricting the bar diameter that could be used when grade 380 MPa reinforcement was specified (to $1/35^{th}$ of the

column depth). Both this limit and that for grade 275 reinforcement were based on a more general limit (eq. 3) discussed by Paulay and Park [44].

$$\frac{d_b}{h_c} \leq \frac{12}{f_y} \qquad \textbf{eq. 3}$$

In eq. 3 $d_b$ is the bar diameter of the beam longitudinal reinforcement, $h_c$ the column depth, and $f_y$ the yield strength of the beam longitudinal reinforcement. Some relaxation of this strict requirement was permitted if the column carried a large axial load [43]. It is important to note that eq. 3 has existed in two forms, that shown above and an earlier form with $11/f_y$ in place of $12/f_y$. This change was necessitated by a change in the way reinforcement strength was rated in New Zealand (discussed below).

The theoretical basis of eq. 3 is straightforward. If it is conservatively assumed that the overstrength capacity of a reinforcing bar is developed on either side of a beam-column joint (tension yielding on one side and compression yielding on the other), then the change of force per unit length ($F_B$) of bonded reinforcement in the joint region is:

$$F_B = \frac{2\alpha_o f_y A_s}{h_c} \qquad \textbf{eq. 4}$$

where $\alpha_o$ is the overstrength factor for the reinforcement, $A_s$ is the area of the reinforcing bar, and other symbols are as for eq. 3. Converting this force to a bond stress ($f_B$), and defining $A_s$ in terms of bar diameter gives:

$$f_B = \frac{2\alpha_o f_y \frac{\pi d_b^2}{4}}{\pi d_b h_c} \qquad \textbf{eq. 5}$$

Simplifying this and assuming that $f_B$ is a limiting bond stress (i.e. the maximum stress that can be sustained before bond failure) gives:

$$f_{B.Max} \geq \frac{\alpha_o f_y d_b}{2h_c} \qquad \textbf{eq. 6}$$

Finally this can be rearranged to give:

$$\frac{d_b}{h_c} \leq \frac{2f_{B.Max}}{\alpha_o f_y} \qquad \textbf{eq. 7}$$

which is clearly related to eq. 3. Through calibration with existing test data it was determined that $2f_{B.Max}/\alpha_o$ was approximately equal to eleven for the reinforcement used at the time. Since this time all New Zealand design standards have included equations for the prevention of bond failure of this form, i.e.

$$\frac{d_b}{h_c} \leq \frac{K}{f_y} \qquad \textbf{eq. 8}$$

where K is a constant, which has grown in complexity each time a revised standard has been released.

It was recognised that the restrictions represented by eq. 3 were conservative [14]. Eq. 3 assumed that the full over-strength capacity of the reinforcing bar developed in compression and tension on the two sides of the joint [14], and was based on tests where the concrete strength used was low ($f'_c$~20-25 MPa) [14].

Possibly because of the severity of eq. 3 the American Concrete Institute decided on different limits (bar size to be less than $1/20^{th}$ of the column depth, irrespective of reinforcement yield stress) when they revised their beam-column joint design recommendations [45]. It was recognised by the committee that limited bar slip would occur when this less restrictive design criteria was used [45]; this was felt to be more desirable than the large column sizes that would result from using the New Zealand design guideline [43]. This limit remains in the latest ACI design code [46].

Progress towards less conservative design for the prevention of bond failure in beam-column joints was also made in New Zealand. Park and Ruitong [47] proposed that the New Zealand design code requirements [43] be replaced with an equation that reduces to the following:

$$\frac{d_b}{h_c} \leq \frac{6.7\sqrt{f'_c}}{(1+\beta)\alpha_o f_y} \qquad \textbf{eq. 9}$$

Note that eq. 9 differs slightly from the equation published by Park and Ruitong. This is due to the subsequent change to the way reinforcement is described in New Zealand (see section 2.5). In eq. 9 $d_b$, $h_c$, $\alpha_o$ and $f_y$ have the same meaning as previously, $\beta$ represents $A_s'/A_s$ ($\beta \leq 1.0$), the ratio of the smaller to larger areas of reinforcement (i.e. areas of top and bottom reinforcement) and $f'_c$ is the compressive strength of the concrete (It has long been realised that bond strength depends on the tensile strength of concrete [6, 24], which is proportional to the square root of $f'_c$). Park and Ruitong felt it was important to include a term allowing for situations where the areas of top and bottom reinforcement differed ($\beta$) since bars that are a part of the larger reinforcement area place lower demand on the concrete-steel bond than bars that or part of the smaller reinforcement area, or where the two reinforcement areas are equal. This occurs because the tension force developed by the smaller reinforcement area will be insufficient to cause the larger reinforcement area to yield in compression if all reinforcement is of equal yield strength.

Park and Ruitong's equation was calibrated so that for the severe conditions on which the existing design criteria [43] were based ($f'_c$ = 20 MPa, equal areas of top and bottom reinforcement, i.e. $\beta$ = 1.0), eq. 9 would give the same ratio of allowable bar size to column depth as eq. 3. The advantage of eq. 9 lay in its ability to account for more favourable bond conditions that might be encountered in design.

Before the methods of Park and Ruitong could be considered for inclusion in a revised edition of the New Zealand concrete design code, a further advance in complexity was proposed by Paulay and Priestley [14]. Their model took into account column axial load, depth of fresh concrete cast under a bar and the poorer bond conditions when plastic hinges form simultaneously at all four faces of a column (as may occur in space frames, see Figure 2-1), in addition to the tensile strength of the concrete and the yield strength and over-strength of the beam reinforcement.

This model was included with minor changes when the New Zealand concrete design standard was revised in 1995 [4]:

$$\frac{d_b}{h_c} \le 6\left(\frac{\alpha_t \alpha_p}{\alpha_s}\right)\alpha_f \frac{\sqrt{f'_c}}{\alpha_o f_y} \qquad \textbf{eq. 10}$$

In eq. 10 $\alpha_p$ is a factor allowing for the positive effect of column axial load, $\alpha_t$ is a factor allowing for the depth of fresh concrete under a reinforcing bar when the joint is cast, $\alpha_s$ accounts for the ratio of positive to negative beam reinforcement ($\beta=A_s'/A_s$, $0.75\le\beta\le1.0$), $\alpha_f$ allows for the case when plastic hinges can form at all four faces of the column, and other symbols have the same meaning as in eq. 9.

There is a significant difference between eq. 9 and eq. 10 in the manner in which they deal with unequal areas of top and bottom reinforcement. In eq. 9, proposed by Park and Ruitong [47], it is assumed that $\beta = 1.0$ for reinforcement belonging to the group of bars (top or bottom) that has <u>smaller</u> total area ($A_s'$). In eq. 10 $\alpha_s = 2.55-\beta$, and it is assumed that $\beta = 1.0$ for reinforcement belonging to the <u>larger</u> area of (top or bottom) reinforcement. This results in a fundamental difference in the way $\beta$ affects the allowable bar diameter. For both eq. 9 and eq. 10 $\beta = 1.0$ gives a "reference" allowable bar diameter, at which the bar diameter allowed for reinforcement in both groups is equal. However, from this reference point, eq. 9 increases the allowable diameter of reinforcement that is part the larger reinforcement group ($A_s$), while eq. 10 reduces the allowable diameter of bars that are part of $A_s'$. This is illustrated in Figure 2-3. It is useful to relate this "reference" bar diameter to the diameter of a bar affected by changing the value of $\beta$. Doing this the following relationships are obtained:

$$\frac{d_b}{d_b'} = \frac{2}{1+\beta} \qquad \text{(a)}$$

$$\frac{d_b}{d_b'} = \frac{2.55-\beta}{1.55} \qquad \text{(b)}$$

**eq. 11**

Eq. 11 (a) & (b) represent the ratios of allowable reinforcement diameter for a bar in the larger reinforcement group divided by that of a bar in the smaller reinforcement group, according to Park and Ruitong [47] and NZS 3101:1995 [4] respectively. The ratio is similar for realistic values of $\beta$, despite the different forms of this relationship (hyperbolic vs linear) as can be seen in Figure 2-4. It is noted that the relations shown in Figure 2-3 & Figure 2-4 are independent of materials strengths.

As can be seen in Figure 2-5, the differences discussed above result in quite different allowable bar diameters for the case shown; by extension these differences will exist for all combinations of materials strengths. It appears that the method of Park and Ruitong [47] is more conservative except for situations where there is a significant difference between $A_s$ and $A_s'$. However, it is important to note that the relationship used in NZS 3101:1995 (eq. 10) includes other variables to take account of situations where bond performance is likely to be poor.

Although there are clearly significant differences between the methods of Park and Ruitong [47] and NZS 3101:1995 (originally Paulay and Priestley [14]), it is not clear from published research whether a direct comparison of the methods has been made, and hence it is not possible to state which method is most realistic. It is probably safe to assume that the method included in NZS 3101:1995 is superior, since one of the authors of each method (Park and Paulay respectively) were amongst the group responsible for producing NZS 3101:1995.

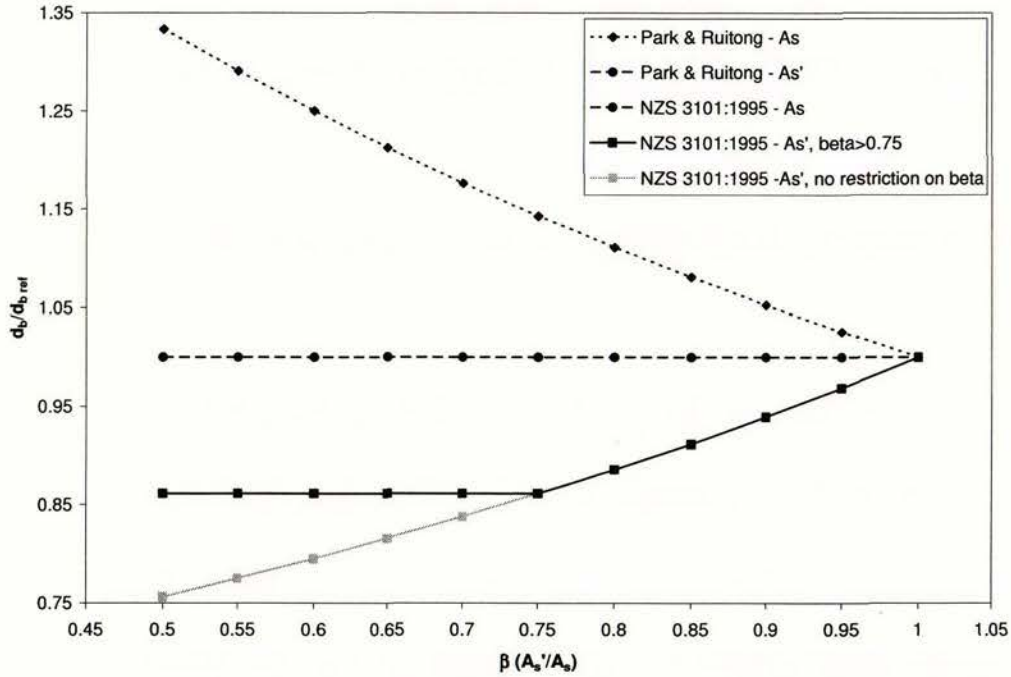


**Figure 2-3 The effect of β on allowable bar sizes for different design methods**

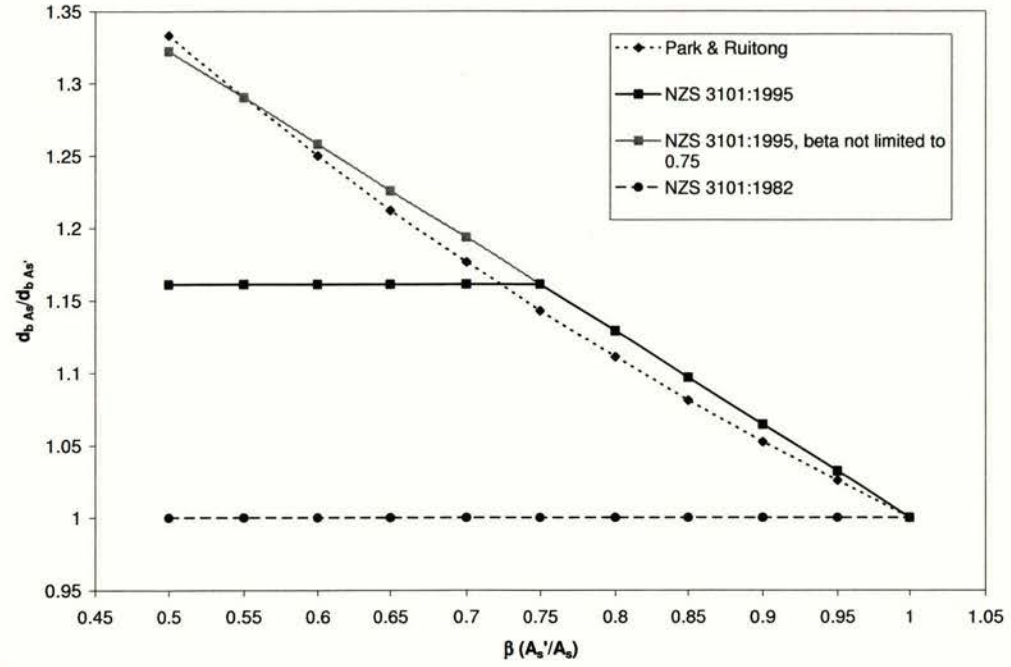


**Figure 2-4 Ratio of allowable size of top and bottom reinforcement for different design methods**

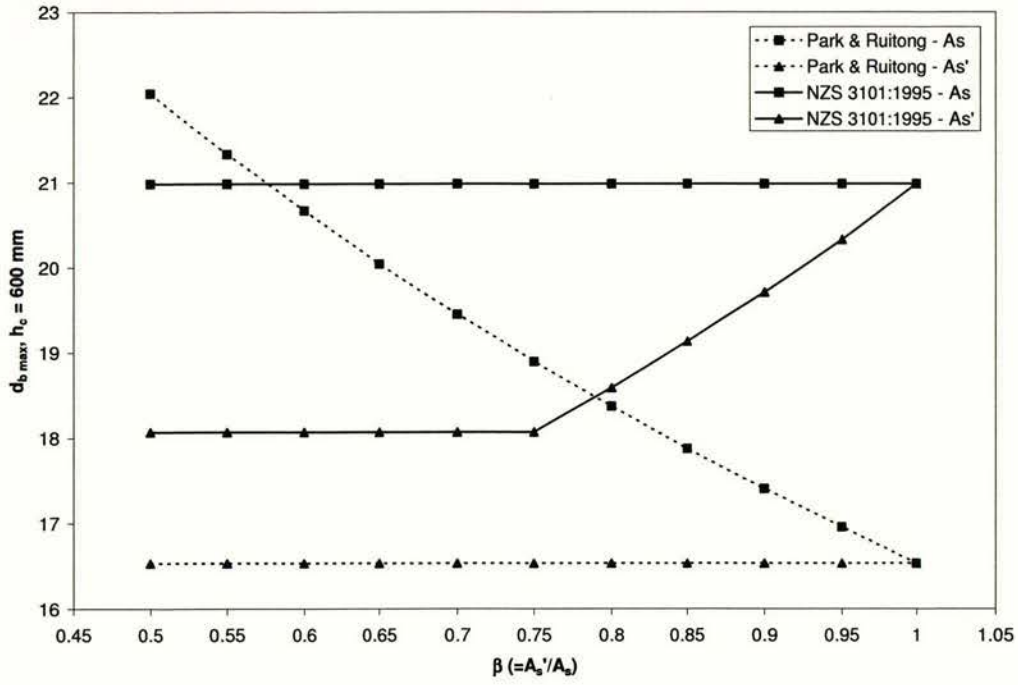


**Figure 2-5 Allowable bar diameters for $A_s$ & $A_s'$ according to Park & Ruitong and NZS 3101:1995, $f'_c$ = 40 MPa, $f_y$ = 500 MPa**

In addition to the detailed method of defining the limiting ratio of bar diameter to column depth (eq. 10), a less complicated equation was also given in NZS 3101:1995 [4]. In order to simplify the design procedure, many of the factors included in eq. 10 were assumed to have unfavourable values. These assumptions gave the following:

$$\frac{d_b}{h_c} \leq 3.3\alpha_f \frac{\sqrt{f'_c}}{\alpha_o f_y} \qquad \textbf{eq. 12}$$

where all variables have the same meaning as above. Comparison of allowable bar diameter resulting from the use of different beam-column joint anchorage design criteria is given in section 3.

## 2.5 Recent University of Auckland Studies on Reinforcement Anchorage in Interior Beam-Column Joints

Since the 1970's the strength of reinforcement used for structural purposes in New Zealand has gradually increased. Initially two grades were commonly specified, mild (275 MPa nominal yield strength) and high strength (380 MPa nominal yield strength). These strengths were minimum yield strength values. A revised specification for steel reinforcement [48] introduced the use of lower characteristic (fifth percentile) yield strength for designating steel reinforcement. This lead to grade 275 reinforcement being re-designated as grade 300 reinforcement. Subsequently, grade 380 reinforcement was replaced with a new 430 MPa steel that was both stronger and more ductile. More recently a desire to standardise material properties and design standards with those used in Australia has led to the somewhat controversial [49] introduction of 500 MPa (grade 500E) reinforcement in place of grade 430.

In 1998 Young [1] revisited the concept of avoiding anchorage failure through the use of anchor plates. This research utilised Reidbar reinforcement, a proprietary threaded reinforcing bar onto which anchor plates could be screwed. This solution avoided many of the difficulties associated with the use of welded anchor plates [1]. Importantly, Reidbar had a yield strength of 500 MPa.

In addition to re-emphasising the good performance of beam-column joints including anchor plates, Young's study revealed that the existing design requirements for the prevention of anchorage failure in beam-column joints (see eq. 10 and eq. 12) were non-conservative when applied to 500 MPa reinforcement. As a means of assessing the performance of the test unit including anchor plates, a second beam-column joint was built. This control test unit was designed according to NZS 3101:1995 [4]. However, when tested, anchorage failure occurred and significant slip of the beam longitudinal reinforcement was noted.

Despite concerns being expressed over the suitability of high strength reinforcement for use in beams of ductile moment resisting frames [49-52], it was considered unsatisfactory that the new grade of reinforcing steel appeared to be incompatible with the New Zealand concrete design standard. Therefore, four further beam-column joint tests were conducted by Megget et al. [2] at the University

of Auckland. These four test units were all designed in accordance with NZS 3101:1995 [4], and included small diameter (<20 mm) grade 500 longitudinal reinforcement in the beams [2]. In particular, the column depths exceeded those required. In all four of these tests bond failure occurred at ductilities significantly lower than the maximum value of six specified in the New Zealand concrete design standard [2].

In order to reconcile the previously noted bond failures of beam-column joints [1, 2] designed in accordance with NZS 3101:1995 [4], Fenwick and Megget conducted an analytical study of previous beam-column joint tests in order to determine if it was necessary to alter the design provisions for the prevention of bond failure in NZS 3101:1995. This study [3] analysed the results of 59 beam-column joint tests and established whether anchorage failure occurred in each test. By correlating the yield strength of the beam reinforcement, the column size and the inter-storey drift level at which bond failure occurred, they came to the conclusion that the New Zealand concrete design standard was non-conservative with respect to the prevention of bond failure in beam-column joints.

To rectify this problem an amendment to NZS 3101:1995 was released late in 2003. This amendment is discussed in more detail in section 3.

# 3 NZS 3101:1995 Amendment No.3

## *3.1 Amendment No.3 and its Effects*

Over its ten year lifespan NZS 3101:1995 [4] has been amended three times to correct mistakes and to include new research findings. The most recent (and final) amendment was released in late 2003. The primary reasons for this amendment were the need to address research indicating problems with the design of precast flooring [53] and to take into account a new standard for reinforcing steel, released in 2001 [54].

There were a number of additional changes made to NZS 3101:1995 [4] with the release of this amendment. Among these was a change to the rules governing design to prevent anchorage failure in interior beam-column joints. As mentioned previously (see section 2.5 above) this change was made as a result of work carried out by Fenwick and Megget at the University of Auckland [3].

To account for the poor bond performance of beam-column joints containing grade 500 reinforcement [2] a modification factor for the allowable ratio of bar diameter to column depth was introduced. The amended clause reads as follows:

> The maximum diameter of Grades 300 and 500 longitudinal beam bars passing through an interior joint shall be computed from either eq. 10 or eq. 12 above provided one of the conditions, (i) to (v) below is satisfied:
>
> (i) Grade 300 reinforcement is used;
>
> (ii) Inter-storey deflections are calculated using the time history method and satisfy the limits of clause 2.5.4.5 of NZS 4203 [10];
>
> (iii) The inter-storey deflection divided by the storey height (the inter-storey drift ratio) at the ultimate limit state do not exceed 1.2% when calculated using the equivalent static or modal response spectrum methods;
>
> (iv) The beam-column joint zone is protected from plastic hinge formation at the faces of the column;
>
> (v) The plastic hinge rotation at either face of the column does not exceed 0.006 radians
>
> If none of these conditions is satisfied the permissible diameter of Grade 500 beam reinforcement passing through an interior joint shall be determined by multiplying the diameter given by eq. 10 or eq. 12 above by F.
>
> $$F = \left( 2.2 - 1.5\frac{\delta_c}{\delta_m} \right), \text{ but not greater than 1.0} \qquad \textbf{eq. 13}$$
>
> Where:
>
> $\delta_c$ = Calculated inter-storey deflections given by clause 4.7 of NZS 4203 [10].

$\delta_m$ = Maximum permissible inter-storey drift given by clause 2.5.4.5 of NZS 4203 [10].

It is planned that this amended clause will be included unchanged in the new New Zealand Concrete design standard, currently available in draft form as DZ 3101 [55].

Irrespective of the actual drift limit ($\delta_m$) it can be readily determined that the limiting upper value of F=1.0 is reached when $\delta_c$ is 80% of the maximum allowable drift. At the other extreme, F=0.7 when the design drift level is equal to the maximum allowed - i.e. when $\delta_c=\delta_m$ the maximum reinforcement diameter allowed is only 70% of that indicated by either eq. 10 or eq. 12.

Reducing bar diameter by 30% results in a 51% reduction in bar cross-sectional area, and hence bar strength. Therefore twice as many bars will be required to carry a given tension force. This additional reinforcement will obviously lead to significantly increased reinforcement congestion. This will be particularly severe at the beam-column joints, where reinforcement congestion has always been a problem. The other means of meeting the requirements of the amendment are to use the same (pre-amendment 3) reinforcement diameter and to increase the column width by 43% (1/0.7), or to use grade 300 reinforcement.

## *3.2 Comparison of Historical New Zealand Methods of Determining Maximum Bar Diameter in Interior Beam-Column Joints*

Figure 3-1 presents a comparison of the different methods used at times in New Zealand for the determination of the maximum bar diameter passing through an interior beam-column joint.

In Figure 3-1 it is assumed that an interior joint from a perimeter frame (i.e. two beams framing into a column from opposite sides, see Figure 2-1, bottom right) is being designed, for a worst case of no column axial load. No account is made for the depth of fresh concrete beneath the bars in question (meaning that more conservative restrictions will apply for some bars designed using NZS 3101:1995 or DZ 3101, both of which require a 15% reduction in bar diameter for bars with more than 300 mm of fresh concrete beneath them when the concrete surrounding the bar is poured), and it is assumed that equal areas of top and bottom reinforcement are to be placed in the beams. Grade 300E and 500E reinforcement is considered, along with a range of concrete strengths from 20 MPa to 70 MPa. Finally, the column depth has been selected as 600 mm. Note that the values given for DZ 3101 [55] are identical to values that would be calculated using NZS 3101:1995 after the release of amendment 3 (discussed previously).

The most obvious change since NZS 3101:1982 [43] is the increase in bar diameter allowed where high strength concrete is used. For low strength concrete, the maximum bar diameter is similar whichever relationship is used. It can also be seen that NZS 3101:1995 [4] (without amendment 3) is the least conservative of the relationships plotted. The other noteworthy feature is the great

difference in allowable bar diameter allowed by DZ 3101 (and NZS 3101:1995 with amendment 3) depending on whether grade 300E or 500E reinforcement is used.

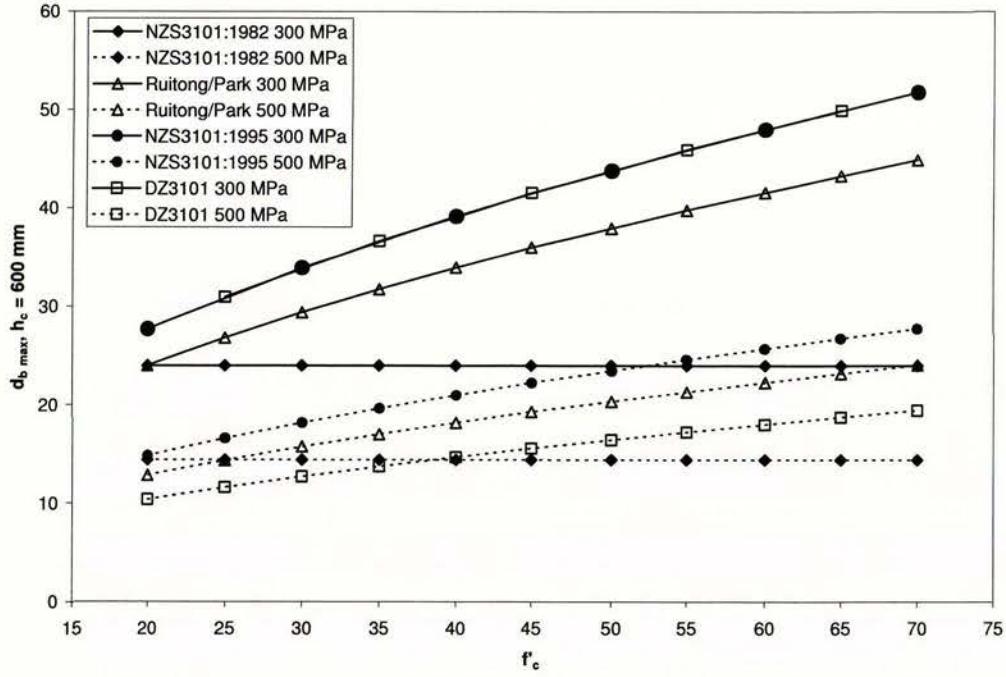


**Figure 3-1 Comparison of bar diameter restrictions for different design methods**

## 3.3 The Use of Grade 500E Beam Longitudinal Reinforcement in Moment Resisting Frames

As mentioned above, amendment 3 to NZS 3101:1995 (and DZ 3101) requires the diameter of a grade 500E reinforcing bar to be significantly greater than the diameter of a grade 300E reinforcing bar. Numerically, this difference is equal to

$$\frac{\alpha_{o,500E}}{\alpha_{o,300E}}\frac{1}{F}\frac{f_{y,500E}}{f_{y,300E}} = \frac{1.4}{1.25} * \frac{1}{0.7} * \frac{500}{300} = 2\frac{2}{3} \qquad \textbf{eq. 14}$$

i.e. the diameter of a grade 300E reinforcing bar is allowed to be 2.667 times the diameter of a grade 500E reinforcing bar if the column depth is equal.

This reduced allowable bar diameter has a large impact on the numbers of bars of different reinforcement grade required to resist a given tension force. Firstly, defining a constant:

$$K = 6\frac{\alpha_t \alpha_p \alpha_f}{\alpha_s}\sqrt{f'_c}\,h_c \qquad \textbf{eq. 15}$$

and referring to eq. 10 and eq. 13, the allowable bar diameters for grade 300E and 500E are:

$$d_{b300} = \frac{K}{1.25*300} \qquad \text{(a)} \qquad \textbf{eq. 16}$$

$$d_{b500} = \frac{0.7K}{1.4*500} \qquad \text{(b)}$$

Hence the force that can be carried by a bar of the maximum allowable size is:

$$F_{b300} = \frac{0.64K^2}{300}\frac{\pi}{4} \qquad \text{(a)}$$

**eq. 17**

$$F_{b500} = \frac{0.25K^2}{500}\frac{\pi}{4} \qquad \text{(b)}$$

The number of reinforcing bars, $N_b$, required to carry a tension force, T, is equal to the tension force divided by the force the bars can each sustain ($N_b=T/F_b$). The ratio of the number of grade 500E reinforcing bars required to the number of grade 300E bars required is thus:

$$\frac{N_{b500}}{N_{b300}} = \frac{F_{b300}}{F_{b500}} = \frac{0.64*500}{0.25*300} = 4.267 \qquad \text{(a)} \quad \textbf{eq. 18}$$

i.e. more than four grade 500E reinforcing bars may be required for every grade 300E reinforcing bar, despite the apparent strength advantage of grade 500E reinforcement, despite the apparent strength advantage of grade 500E reinforcement.

The figure of 4.267 arrived at above represents close to the maximum increase in the number of bars required if grade 500E reinforcement was chosen in place of grade 300E. Table 3-1 shows the influence that different parameters have on the ratio given in eq. 18. In the table various required tension forces, column depths and concrete strengths were chosen. Maximum bar diameters were calculated for grade 300E and 500E reinforcement and from these, useable bar sizes from the Pacific steel range[I] were selected. The whole number of bars required to carry the selected tension force was then calculated[II], along with the ratio of the number of grade 500E to 300E bars required.

While Table 3-1 represents a relatively small range of beam-column joints, it is evident that the ratios calculated are all equal to or less than the result of eq. 18 (with the exception of the first row, where unrealistically small grade 500 reinforcement is required), and that in all cases at least twice as many reinforcing bars are required when using grade 500E reinforcement. Table 3-1 is a sample of a much larger selection of beam-column joints analysed at the University of Auckland. For this larger study, the ranges of variables investigated was:

| | |
|---|---|
| Tension Force, T | 200 kN – 1500 kN (~3D16 – 6D32), 100 kN steps |
| Concrete Strength, $f'_c$ | 30 MPa – 70 MPa, 5 MPa steps |

[I] It was assumed that deformed bars of 10, 12, 16, 20, 25 and 32 mm diameter were available in both grade 300E and grade 500E types.

[II] In calculating the number of reinforcing bars required to carry the tension force an allowance was made that if the strength of a number of reinforcing bars was within 5% of the required strength this would be sufficient. This allowance is in line with common design practice.

Column Depth, $h_c$ 300 mm – 1000 mm, 100 mm steps

These ranges were considered to include all beam-column joints likely to be designed in New Zealand at present. Combining these variables in all combinations gave a total of 1008 beam-column joints that were analysed. A breakdown of the results of these analyses is given in Table 3-2.

**Table 3-1 Effect of changing design parameters on number of reinforcing bars required**

| Vary | T | $h_c$ | $f'_c$ | $d_{b\ max}$ G300E | $d_{b\ used}$ G300E | No. bars G300E | $d_{b\ max}$ G500E | $d_{b\ used}$ G500E | No. bars G500E | $\frac{N_{b500}}{N_{b300}}$ |
|---|---|---|---|---|---|---|---|---|---|---|
| | (kN) | (mm) | (MPa) | (mm) | (mm) | | (mm) | (mm) | | |
| $h_c$ | 600 | 400 | 30 | 22.6 | 20 | 7 | 8.5 | 6* | 41* | 5.9* |
| | | 500 | | 28.3 | 25 | 4 | 10.6 | 10 | 15 | 3.8 |
| | | 600 | | 33.9 | 32 | 3 | 12.7 | 12 | 11 | 3.7 |
| | | 700 | | 39.6 | 32 | 3 | 14.8 | 12 | 11 | 3.7 |
| | | 800 | | 45.2 | 32 | 3 | 17.0 | 16 | 6 | 2.0 |
| $f'_c$ | 600 | 600 | 30 | 33.9 | 32 | 3 | 12.7 | 12 | 11 | 3.7 |
| | | | 40 | 39.2 | 32 | 3 | 14.7 | 12 | 11 | 3.7 |
| | | | 50 | 43.8 | 32 | 3 | 16.4 | 16 | 6 | 2.0 |
| | | | 60 | 48.0 | 32 | 3 | 18.0 | 16 | 6 | 2.0 |
| | | | 70 | 51.8 | 32 | 3 | 19.4 | 16 | 6 | 2.0 |
| T | 400 | 600 | 30 | 33.9 | 32 | 2 | 12.7 | 12 | 7 | 3.5 |
| | 500 | | | 33.9 | 32 | 2 | 12.7 | 12 | 9 | 4.5 |
| | 600 | | | 33.9 | 32 | 3 | 12.7 | 12 | 11 | 3.7 |
| | 700 | | | 33.9 | 32 | 3 | 12.7 | 12 | 12 | 4.0 |
| | 800 | | | 33.9 | 32 | 4 | 12.7 | 12 | 14 | 3.5 |
| *6 mm grade 500E reinforcement is not a standard size – shown for comparison only | | | | | | | | | | |

**Table 3-2 Summary of beam-column joints analyses**

| $\frac{N_{b500}}{N_{b300}}$ | Number of Joints | Proportion |
|---|---|---|
| NA | 168 | 16.7% |
| <1.0 | 12 | 1.2% |
| =1.0 | 158 | 15.7% |
| >1.0 | 670 | 66.5% |

Of the beam-column joints analysed, no ratio of the number of grade 500E bars required to the number of grade 300E bars required could be calculated for 17% (168) of the cases. These cases had combinations of column depth (small) and concrete strength (low) that made it impossible to

design an NZS 3101:1995 compliant joint using grade 500E reinforcement. For example, for a 300 mm deep column no acceptable grade 500E reinforcement size was available, even when using 70 MPa concrete.

The beam-column joints that resulted in a less congested or equally congested joint region (i.e. fewer or equal number of longitudinal reinforcing bars) if grade 500E reinforcement was used instead of grade 300 reinforcement were exclusively cases where the combination of concrete strength (high) and column depth (large) resulted in the diameter of grade 300E reinforcement used being governed by the largest available bar diameter rather than the largest allowable bar diameter (e.g. for grade 300E reinforcement, $d_{b\ allowed}$ is 86 mm when $f'_c$ is 70 MPa and $h_c$ is 1000 mm). The twelve joints for which the number of grade 500 bars required was less than the number of grade 300 bars were all combinations of the highest concrete strength and largest column size included (70 MPa and 1000 mm respectively). This combination allowed the use of 32 mm diameter grade 500 reinforcement.

Removing these categories left the beam-column joints for which a greater number of grade 500E reinforcing bars were required than grade 300E bars. Of these 670 joints, approximately 70% (480) required at least twice as many bars of grade 500E reinforcement, while some required as many as 4.5 times as many.

The analysis conducted is a somewhat chaotic calculation – i.e. small differences in the input variables can result in significantly different results. This is due to the need to use specific bar sizes and whole numbers of bars. In order to assess the influence of the particular values of the variables chosen, these were randomised within ranges that bisected the steps discussed above, i.e.

| | |
|---|---|
| Tension Force, T | 100 kN steps, ±50 kN |
| Concrete Strength, $f'_c$ | 5 MPa steps, ±2.5 MPa |
| Column Depth, $h_c$ | 100 mm steps, ±50 mm |

In addition the allowance mentioned in footnote II was varied between 0% and 5%.

Although it is difficult to quantify the impact of the randomizations described, the authors are confident that changing the variables does not have a significant impact on the proportions of joints listed in Table 3-2. For instance, the proportion of joints requiring a greater number of grade 500 bars than grade 300 bars was seen to vary between 62.5% and 75% when variables were randomised as described.

Further calculations were made to assess the impact of possible changes to the overstrength factor of grade 500E reinforcement or to the minimum value of F (see eq. 13). For each change the designs of

the full set of 1008 beam-column joints were reassessed. The results of these changes are summarised in Table 3-3. For convenience the first results in Table 3-3 are for the case analysed previously.

**Table 3-3 The impact of changes to overstrength and F factors**

| | | $\frac{N_{b500}}{N_{b300}}$ | | | |
|---|---|---|---|---|---|
| **$\alpha_o$ Grade 500E** | **Minimum F** | **NA** | **<1.0** | **=1.0** | **>1.0** |
| 1.4 | 0.7 | 168 | 12 | 158 | 670 |
| 1.35 | 0.7 | 140 | 24 | 187 | 657 |
| 1.4 | 0.8 | 98 | 72 | 236 | 602 |
| 1.35 | 0.8 | 70 | 84 | 253 | 601 |

It can be seen that changing the overstrength factor of grade 500E reinforcement has little impact on the results of the analysis. Increasing the minimum value of F has more effect, reducing the number of cases for which grade 500E reinforcement cannot be used, and increasing the number of cases for which the use of grade 500E reinforcement is advantageous or makes no impact, at least in terms of the number of reinforcing bars required. However, almost 60% of cases still require more grade 500E reinforcing bars.

From the observations made in this section, it seems the conclusion must be made that using grade 500E beam flexural reinforcement is not an attractive design solution when using amendment 3 to NZS 3101:1995 [4], or the forthcoming replacement of NZS 3101:1995.

# 4 Design and Construction of Test Units and Test Method

## *4.1 Design*

The four beam-column joint sub-assemblies tested during this research programme were all designed according to the New Zealand Concrete design standard [4]. In order to aid comparison with the results of previous beam-column joint tests [1, 2], dimensions were kept similar to those of the previous tests where possible. To avoid confusion with these previous units, the test units were designated units 1B-4B.

For all four units the beams had cross sectional dimensions of 500 mm depth and 200 mm width, the same as those used by Young [1] and Megget et al. [2]. Equal top and bottom beam longitudinal reinforcement was chosen as three 25 mm diameter bars of grade 500E steel. This was chosen to achieve close to the maximum allowable reinforcement ratio, and was significantly more reinforcement than included in the previous tests mentioned. In order to maximise the quantity of reinforcement that could be placed in the beams it was decided to reduce the concrete cover to the outside of the stirrups to 15 mm, which is less than that specified by NZS 3101:1995 [4]. It was felt this was acceptable since the lifespan of the test units was short, and they were constructed and tested in an indoor environment with no potential exposure to the elements.

In accordance with New Zealand standards [4, 10], the design of other aspects of the test units was determined by capacity design requirements so that the column flexural strength and the shear strength of the beams, columns and joint region were designed to exceed the actions that would be imposed *on* them by both beams simultaneously developing their ultimate (overstrength) strength.

The column depth of each unit was based *on* that required by eq. 10. At the time of design amendment 3 (see section 3 above) was not finalised and a draft of the amendment was used. This was similar to the final amendment, but instead of being determined by eq. 13, F had a constant value of 0.8. The use of the amendment required some very large column depths, and the depth of the first test unit (unit 1B) was reduced to allow the use of existing column restraints. The design of the column depths for units 1B-4B is summarised in Table 4-1.

**Table 4-1 Design of column depths, units 1B-4B**

| Unit | $d_b$ | $f_y$ | $f'_c$ | F | $\alpha_t$ | $\alpha_p$ | $\alpha_s$ | $\alpha_f$ | $\alpha_o$ | $h_c$ req. | $h_c$ used | $h_c$ used/req. |
|---|---|---|---|---|---|---|---|---|---|---|---|---|
| | (mm) | (MPa) | (MPa) | | | | | | | (mm) | (mm) | |
| 1B | 25 | 500 | 35 | 0.8 | 1.0 | 1.0 | 1.55 | 1.0 | 1.4 | 955 | 800 | 0.84 |
| 2B | 25 | 500 | 50 | 0.8 | 1.0 | 1.0 | 1.55 | 1.0 | 1.4 | 799 | 800 | 1.00 |
| 3B | 25 | 500 | 50 | 0.8 | 1.0 | 1.0 | 1.55 | 1.0 | 1.4 | 799 | 675 | 0.84 |
| 4B | 25 | 500 | 40 | 0.8 | 1.0 | 1.0 | 1.55 | 1.0 | 1.4 | 894 | 675 | 0.76 |

It can be seen in Table 4-1 that for three of the test units the column size used was less than that specified by the NZS 3101:1995, even when using a less conservative value of F than that in the final amendment. These reduced column depths were chosen to promote bond failure before the occurrence of other failures such as plastic hinge buckling. It is also worth noting that the overstrength factor, $\alpha_o$, used was 1.4, rather than the more typical value of 1.25 used for lower reinforcement grades. 1.4 is the value suggested by Bull and Allington [56], and has been adopted for use with grade 500E reinforcement in a draft revised concrete design standard [55].

The reinforcement used for all four units was similar, differing only in the column longitudinal reinforcement and the shear reinforcement in the joint region. Typical reinforcement detailing can be seen in Figure 4-1, and details of column and joint reinforcement are given in Table 4-2. Note that the column depth shown in Figure 4-1 applied only to units 1B&2B – the column depth of units 3B&4B was 675 mm as shown in Table 4-1.

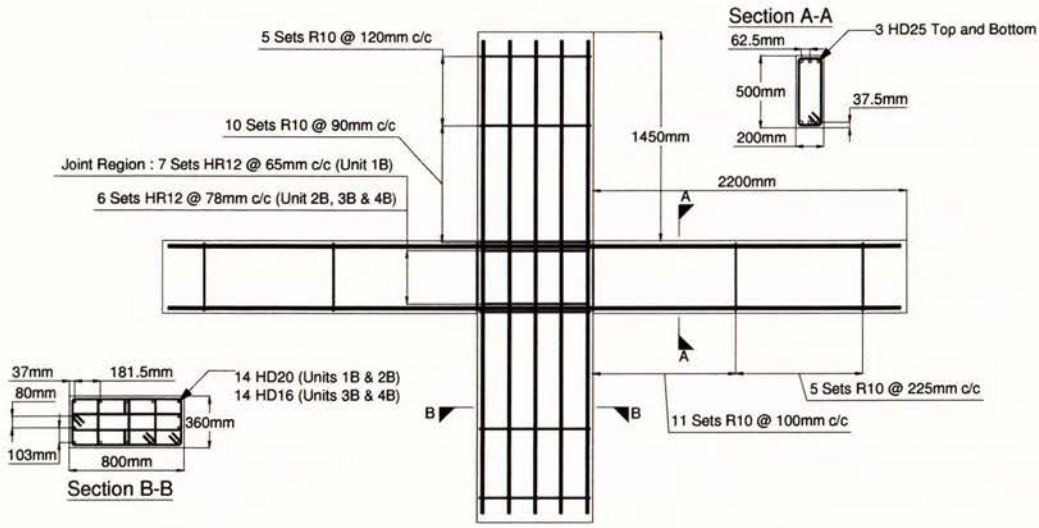


**Figure 4-1 Typical reinforcement detailing, units 1B-4B**

**Table 4-2 Test unit reinforcement details**

| Unit | Column Reinforcement | Joint Shear Reinforcement |
|---|---|---|
| 1B | 14-HD20 | 7 sets, 4 legged HR12 |
| 2B | 14-HD20 | 6 sets, 4 legged HR12 |
| 3B | 14-HD16 | 6 sets, 4 legged HR12 |
| 4B | 14-HD16 | 6 sets, 4 legged HR12 |

## *4.2 Construction*

Units 1B-4B were all constructed on site in the Civil Engineering Test Hall at the University of Auckland.

Reinforcement for the units was supplied by Pacific Steel and was delivered in two batches, the first including reinforcement for units 1B and 2B, the second that for the last two units. Additional reinforcement was ordered in each case so that the actual strength of the reinforcement could be measured (as opposed to the nominal yield strength, which is almost always lower than the actual strength). The measured reinforcement properties are shown in Table 4-3.

**Table 4-3 Measured reinforcement properties**

| Bar Type | Unit | $f_y$ | $f_u$ |
|---|---|---|---|
| | | (MPa) | (MPa) |
| HD25 | 1B, 2B | 552 | 682 |
| HD25 | 3B, 4B | 543 | 670 |
| HD16 | 3B, 4B | 584 | 717 |

No value for the strength of the column reinforcement of units 1B and 2B was obtained. 20 mm diameter Grade 300E reinforcement was ordered for this purpose. However, upon delivery it was found that grade 500E reinforcement had been delivered, and that no extra reinforcement had been included. It was decided to proceed with construction of units 1B and 2B using the higher strength reinforcement as it was envisaged this would have no significant effect on the performance of the unit.

Concrete for the four test units was supplied by a number of different companies. All concrete was delivered as a wet mix direct to the test hall. At the same time as the test units were cast at least six cylinders (100 mm diameter and 200 mm height) were also cast to allow the compressive strength of the concrete to be measured.

After pouring of the concrete the test units were covered with wet sacking and black polythene to ensure the concrete was kept moist during the initial stages of curing. The sacking was removed after two-three days, and the formwork was removed after approximately one week.

Measured concrete properties at the time of testing of each unit are shown in Table 4-4.

**Table 4-4 Measured concrete properties**

| Unit | $f'_c$ spec. | Age at test | $f'_c$ meas. | Standard Deviation |
|---|---|---|---|---|
| | (MPa) | (Days) | (MPa) | (MPa) |
| 1B | 35 | 55 | 31.2 | 2.3 |
| 2B | 50 | 26 | 40.6 | 0.9 |
| 3B | 50 | 33 | 44.8 | 0.2 |
| 4B | 40 | 28 | 42.8 | 1.0 |

## 4.3 Test Method

The method used during this series of tests was similar to that used by Young [1], Megget et al. [2] and other previous researchers at the University of Auckland.

The test setup used is shown in Figure 4-2. The units were tested horizontally, parallel to the strong floor of the Civil Engineering Test Hall. As is usual in New Zealand the units were tested under a simulated seismic loading regime. In order to apply these cyclic loads double acting hydraulic jacks were mounted to the end of each beam. The other end of these actuators was bolted to the strong floor via welded steel brackets.

No structurally significant axial load was applied to the columns of the test units. However, single acting hydraulic jacks were mounted at each end of the column and small ($N^* \sim 0.01 A_g f'_c$) forces were applied. These forces were to prevent movement of the unit that might occur if the forces in the double acting actuators were not balanced. The column ends were held laterally by steel frames bolted to the strong floor.

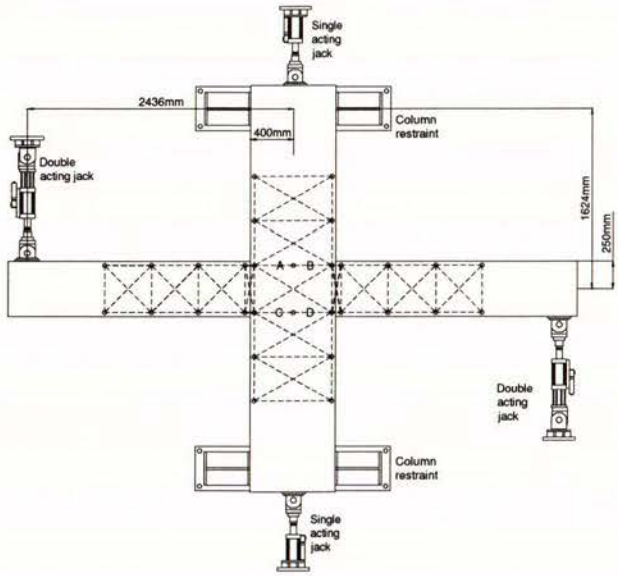


**Figure 4-2 Layout of portal gauges and hydraulic actuators**

The force in the single acting jacks was applied manually prior to testing using hand pumps. Control of the double acting jacks was by one of two methods. Initially a mechanical control system was used. Flow of hydraulic oil was directed to the appropriate end (push or pull) of each jack by tap type valves, and the force/displacement was controlled by manually operating a master valve. For later tests a computer controlled pump was developed. This allowed displacements to be input into the computer, which then operated valves to ensure the correct displacement was achieved. In theory this was a much superior system to the old manually operated pump, and should have allowed more accuracy of control. However, the system was only used briefly before problems were found requiring further development work.

Almost eighty gauges were mounted on each test unit. The majority of these were portal gauge transducers. These were attached to the unit by attaching suitable mounts to threaded studs that can be either glued into the concrete or (more commonly) welded to the reinforcing cage prior to pouring the concrete. Of particular note are the gauges marked A-D in Figure 4-2. These gauges were installed to monitor the slip of the beam longitudinal reinforcement through the joint region.

In addition to the portal gauge transducers, load cells were installed between each hydraulic actuator and the point where it met the test unit. These load cells allowed accurate measurement of the forces applied to the specimen. Turn potentiometer gauges were mounted over the stroke of each double acting actuator. These were used to measure the gross displacement of the beam ends relative to the strong floor and due to the importance of the measurement and the reputation of turn potentiometers for inaccuracy, it was felt to be prudent to provide redundancy and a check value by mounting large portal gauges at the same location. These gauges only had a capacity of ±50 mm, so had to be removed after the low displacement cycles were completed. The readings from the turn potentiometer gauges proved sufficiently reliable (see Figure 4-3) that the large portal gauges were omitted for the third and fourth tests. As a further redundancy steel rulers were mounted at the same point to allow visual checking of displacement, and to act as a record of progress if power failure interrupted testing.

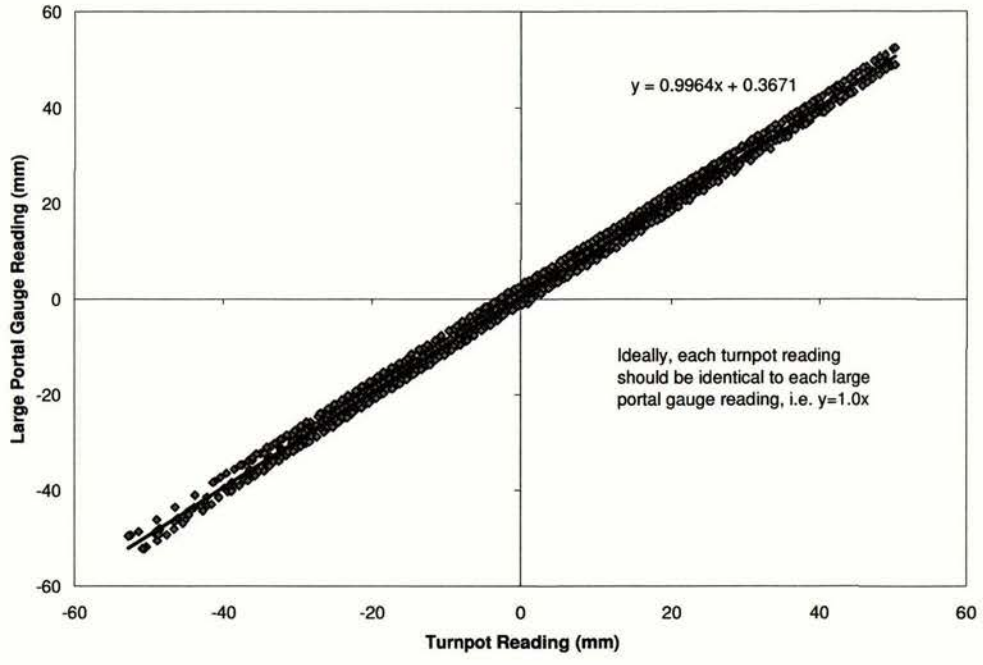


**Figure 4-3 Readings of turnpot vs. large portal gauge at beam ends**

The loading history applied to the units was based on one that has been used in New Zealand for many years and which was described by Park [57]. However, due to the increased inter-storey yield

drifts that are a characteristic of the use of high yield strength reinforcement [3], it was decided that load cycles would be inter-storey drift controlled instead of ductility controlled.

The loading history used, which is shown in Figure 4-4, began with a number of cycles to low inter-storey drift levels. These cycles all remained in the elastic range and differed between test units. Typically the unit would be loaded to a drift level of 0.5% in both directions. At this point testing would be paused and the results scrutinised to discern if all gauges seemed to be reading correctly.

If there were no apparent problems, loading was continued with two complete (i.e. positive peak to negative peak) loading cycles to 1.0% drift, followed by an increase of the drift level by 1.0% and two more complete cycles. This process was repeated until failure occurred.

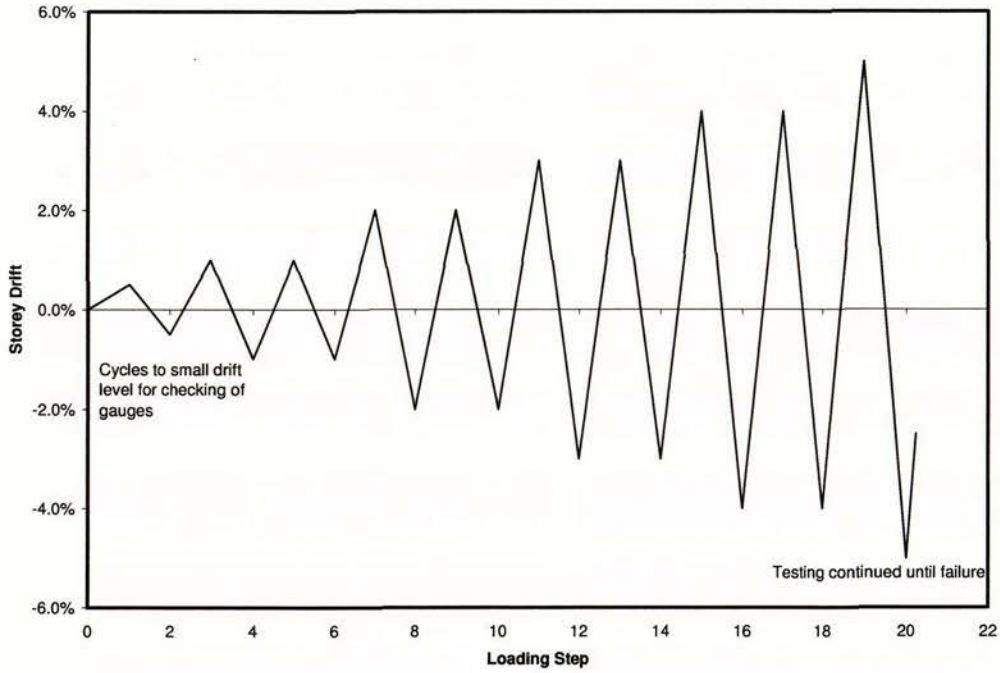


**Figure 4-4 Loading history used for units 1B-4B**

## *4.4 Definitions*

For the purposes of these tests, a positive force was defined as one that would result in an anti-clockwise movement of the load points about the joint. In measuring the translational movement of the joint relative to the floor, a positive movement was defined as upwards and to the right. These definitions are shown in Figure 4-5.

A push cycle was defined as one resulting in positive forces and displacements in contrast to a pull cycle, which resulted in a negative displacement of the load points. Loading began with a push cycle.

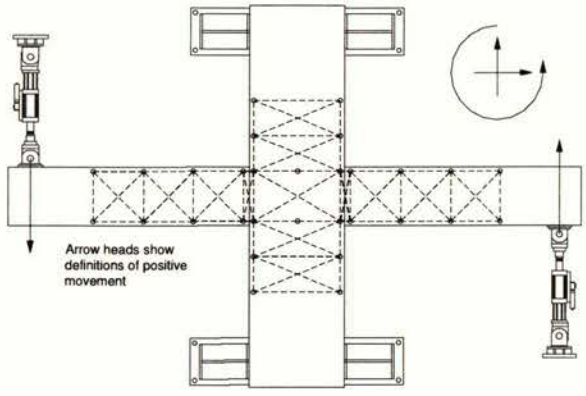


**Figure 4-5 Positive displacements of units 1B-4B**

Cracks that occurred during a push cycle were marked in red, and blue markings designated cracks that occurred during a pull cycle. All cracks were appropriately labelled, e.g. 2%$^{II}$ designated the second cycle to 2% drift in either the positive or negative direction, depending on the colour of the marking.

# 5 Test Observations

## *5.1 Unit 1B*

**¾ $F_n$ Push**

Immediately prior to testing, all gauges were checked to ensure that they were working correctly, and those that were not were replaced and rechecked. Finally, the reading on the steel rulers was noted, being 301 mm for the left hand beam and 272 mm for the right hand beam.

For this unit typical New Zealand practice was followed and a half-cycle to ¾ $F_n$ (¾ of the design strength of the unit) was planned in each direction. In this case ¾ $F_n$ corresponded with a load of 113 kN. During loading of the beams it was noted that the left beam was lagging behind the right beam, probably indicating more friction in the seals on the jack.

Neither beam appeared to achieve the required strength of 113 kN. The force measured in the right hand load cell stopped increasing significantly when it reached 87 kN. The cycle was continued beyond this point to see if the left hand beam would behave differently. It did not, and the force levelled off at 85 kN. The force on both beams increased slowly beyond this point, with the force displacement plots giving the appearance that the two beams had yielded.

This behaviour was found to be the result of a misidentification of the load cells measuring the applied force. This meant that the wrong calibration factors were input into the data acquisition software. This mistake was not established until after conclusion of the testing. Note however that all results are presented showing the corrected forces and that the actual strength achieved for this cycle was approximately 170 kN, equating to a face moment of 356 kNm.

The initial yield displacement for both beams was approximately 32 mm. This corresponded to a drift of 1.32%. Due to the desire to establish that the force had definitely stopped increasing, both beams had undergone significant inelastic type deformations, particularly the right hand beam, which reached yield first. For the left hand beam the final displacement at the end of the cycle was approximately 41 mm, and for the right beam 49 mm.

The impression that both beams had yielded was reinforced by the presence of extensive cracking (see Figure 5-1). Both beams showed flexural and shear cracks along their length, and the joint zone also exhibited shear cracking. In addition, some flexural cracking was noted in the column, and minor crushing of the concrete was seen at the beam-column interface.

Upon release of the load, the residual deformation for the left and right beams was approximately 15.4 mm and 21 mm respectively, again indicating yielding had occurred in the beams.

**Figure 5-1 Cracking of right hand beam during first cycle to 3/4 $M_n$**

Due to the disparity in actual and predicted strength, time was taken at this point to recheck that all gauges were registering correctly, and that the readings of the gauges at the load point matched those of the steel rulers. The reading of the left ruler was 258 mm, giving a difference of 43 mm, and the right ruler read 222 mm, a displacement of 50 mm. These readings verified that the displacements measured were accurate. Finally, the readings at the load points were compared with the combined displacements due to beam shear and flexure, column shear and flexure, joint shear and errors due to movement of the unit relative to the floor. These were found to be in reasonable agreement (see Figure 5-2 and Figure 5-3).

Following these checks it was decided that the next half-cycle would pull the beams to their apparent yield displacement (31 mm), assuming they behaved symmetrically as expected.

**31 mm Pull**

Strengths of 369 kNm and 344 kNm were achieved by the left-hand and right-hand beams respectively. The left hand beam achieved maximum strength at the maximum displacement, while the right hand beam appeared to yield at a displacement of around 26 mm. This was probably due to the larger residual displacement of the right hand beam after the push cycle.

As for the "¾ $F_n$" push cycle, extensive flexural and shear cracking was noted in both beams, with some shear cracks opening to a width of approximately one millimetre. The joint and columns

cracked as for the push cycle, and the overall crack pattern was similar to the push cycle but reversed as expected (see Figure 5-4). Residual displacements of approximately 4 mm were noted for both beams.

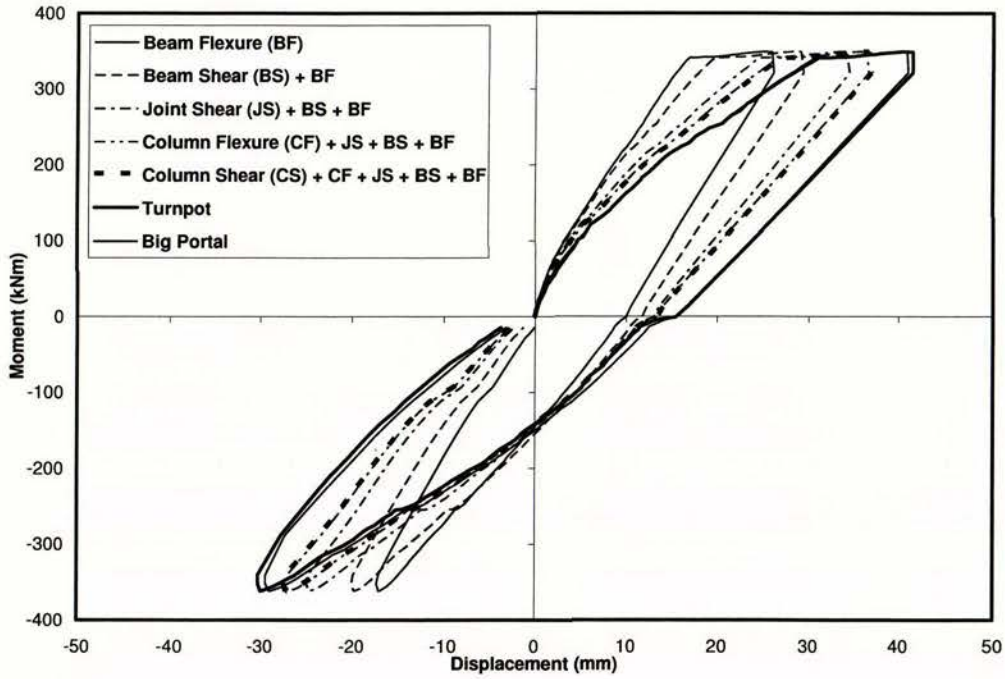


**Figure 5-2 Components of displacement for left hand beam, first cycle**

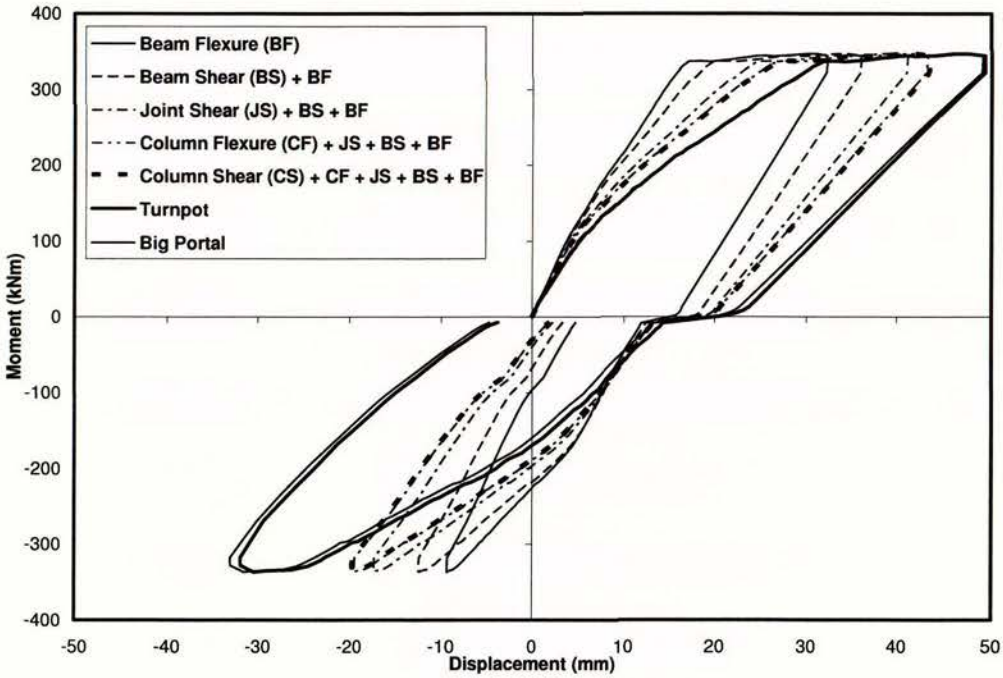


**Figure 5-3 Components of displacement for right hand beam, first cycle**

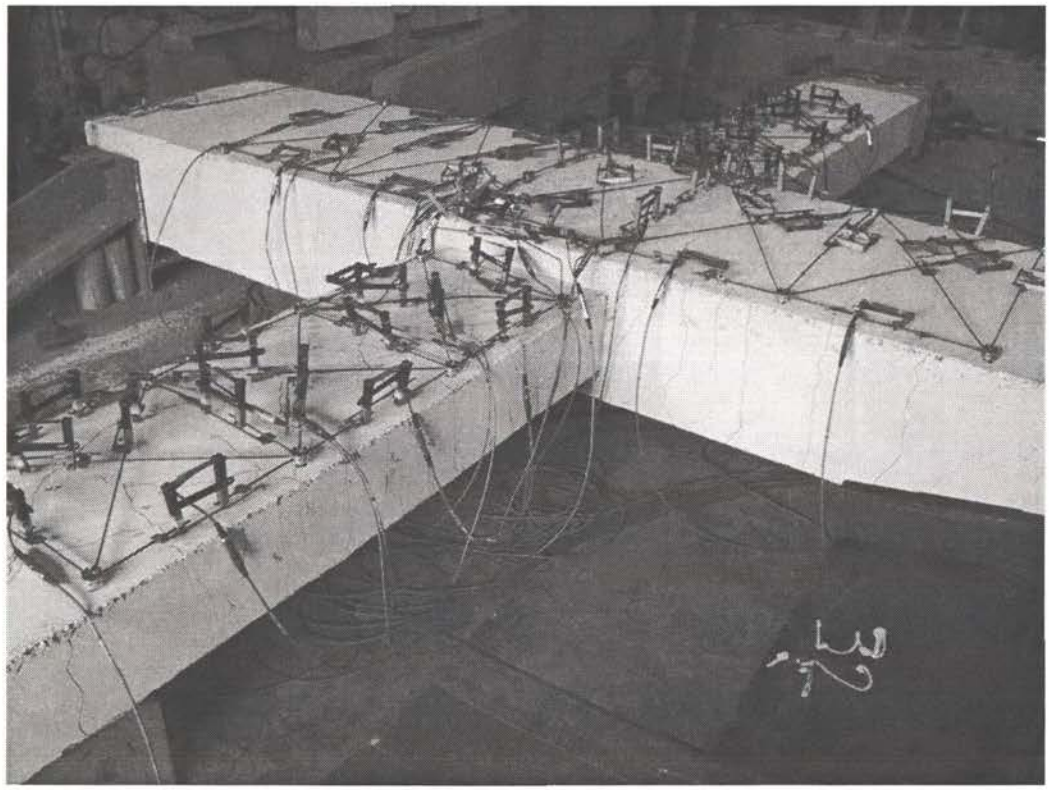

**Figure 5-4 Crack pattern after second cycle to 3/4 $M_n$**

**40 mm Push**

Due to the unexpected behaviour of unit 1B during the first cycle it was decided that the next cycle would be a push-pull pair to 40 mm. This was chosen since both beams had already experienced at least this deformation in the push direction.

During a brief analysis of the data from the previous pull half-cycle, it became apparent that there was a discrepancy in the readings for the right hand beam. From the lower right quadrant of Figure 5-3 it is obvious that the readings of the portal gauge and turnpot did not match the composite displacement calculated from the gauges measuring shear and flexure. It was determined that this was caused by a faulty gauge in the top of the plastic hinge region of the right hand beam.

Replacing this gauge required the initial reading to be recorded and a guess made of what the actual reading should be. It was estimated from observation of the corresponding gauges that the reading following release of the load would be approximately one millimetre. Adjusting the data such that this was the case gave a good match between the turnpot and composite measurements (see Figure 5-6).

Strengths developed during this cycle were 333 and 289 kNm for the left and right beam respectively. The strength developed by the right hand beam was significantly lower than during the first push

cycle. This can probably be attributed to the fact that the right hand beam had previously been displaced almost 50 mm in the push direction.

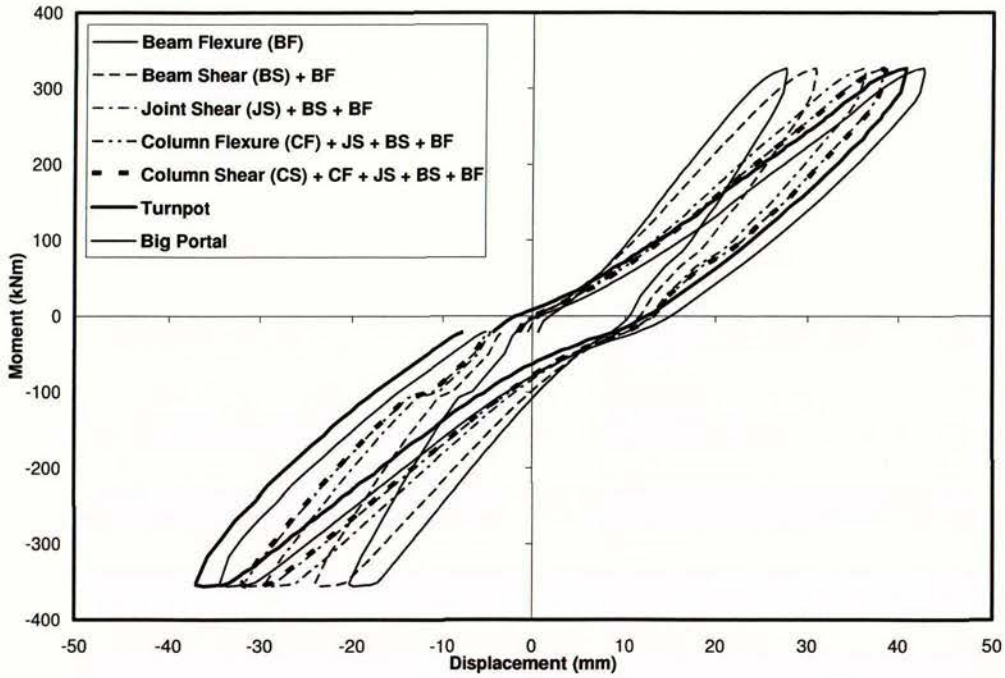


**Figure 5-5 Left hand beam displacements for 40 mm push and pull cycles**

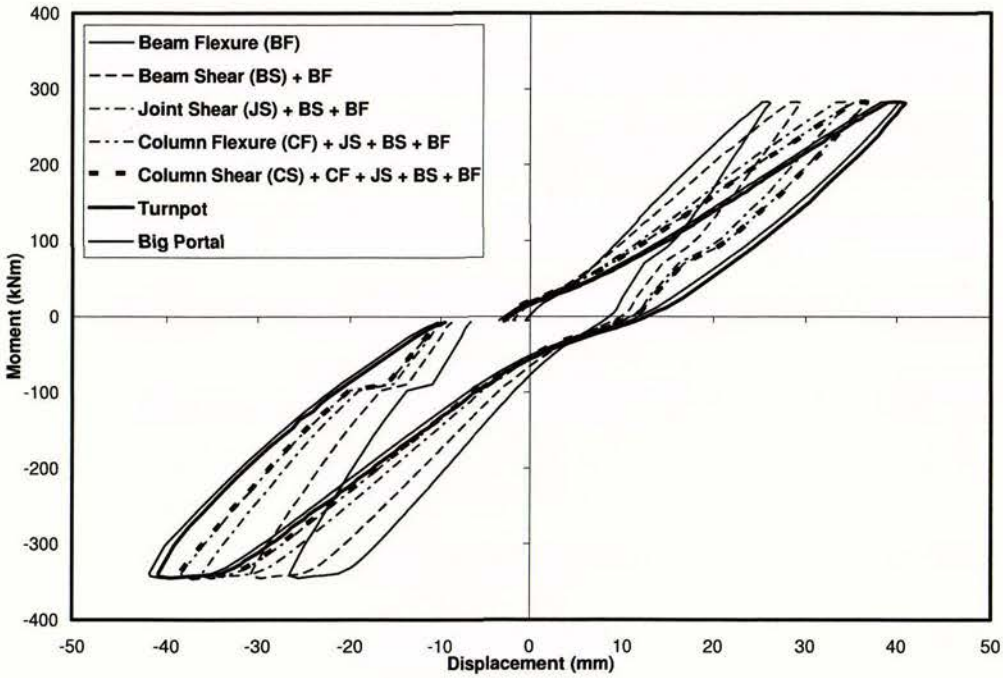


**Figure 5-6 Right hand beam displacements for 40 mm push and pull cycles**

During the 40 mm push half-cycle, few new cracks were noted. Existing shear and flexural cracks extended, particularly in the joint zone, and splitting cracks formed on the column faces adjacent to the beams. This was probably due to the thin layer of cover concrete provided in the design. Minor spalling was noted at the beam-column interface. It was not surprising that few new cracks formed as both beams had been displaced 40 mm or more previously.

**40 mm Pull**

This half-cycle was very similar to the 40 mm push. Strength development for the left beam was 363 kNm while the right beam achieved a strength of 352 kNm. More new cracks were noted than in the push half-cycle, due to the unit reaching higher displacements than it had previously done in the negative direction. Less spalling was evident than in the 40 mm push half-cycle.

Due to the low initial stiffness and the likelihood at the time that the test unit would not achieve it's design strength, it was decided to conduct a full set of four half-cycles to two percent drift (48.9 mm beam end displacement), followed by sets at three, four and five percent drift if the unit remained structurally capable of doing so.

**2% Push I**

The maximum strength achieved by the left beam was 350 kNm, and that of the right beam was 343 kNm. The crack at the column face of both beams had opened to approximately 4 mm at this stage, and well developed plastic hinges were apparent in both beams. Cracks within the plastic hinges were up to 1 mm in width.

**2% Pull I**

The strength developed by both beams was approximately 350 kNm during this half-cycle. Due to the large displacements required to achieve a drift level of 2% it was decided that the big portal gauges at the load points would be removed to prevent damage. From the next cycle onwards the gross displacement of the beams would be measured only by the turn potentiometers mounted at the same location. As these seemed to be recording accurately (see Figure 4-3) this was not felt to be a problem.

As was the case for the 2% push cycle, the cracks at the column face opened to between 4 and 5 mm during this half-cycle. The left hand plastic hinge zone in particular was extensively cracked (see Figure 5-7).

The right hand plastic hinge zone was less cracked overall, but was crossed by a large crack of approximately 2 mm width. Some concrete was lost from both plastic hinge zones, covering an area of approximately 1000 $mm^2$ on the right hand beam. However, the concrete loss at this stage was purely cosmetic.

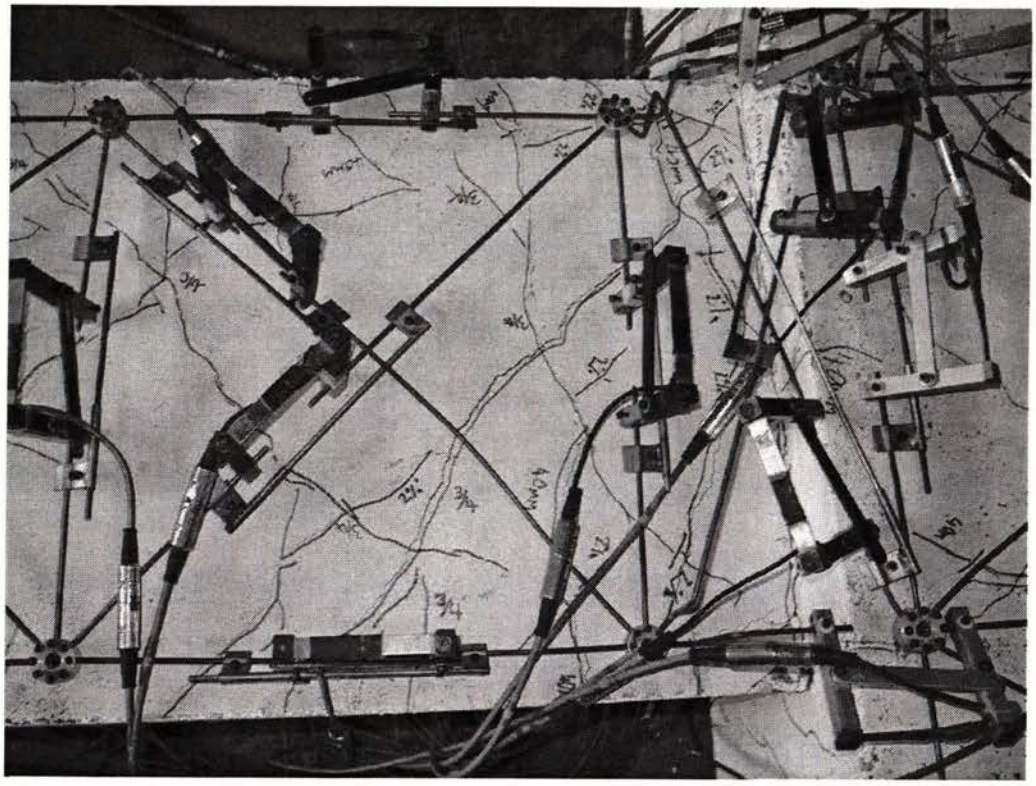

**Figure 5-7 Left-hand plastic hinge zone at end of first 2% pull half-cycle**

**2% Push II**

During this half-cycle the strength developed in the left beam was 363 kNm and in the right beam was 342 kNm. Cracks in both halves of the column extended by small amounts, and splitting cracks formed on the tension side of both beams. The shear cracks that had formed much earlier in the test now extended right across the depth of both beams.

**2% Pull II**

The left beam reached a strength of 376 kNm and the right 357 kNm. No significant new damage was noted.

**3% Push I**

The plastic hinge zones of both beams were extensively damaged at the end of this cycle. The primary crack at the column face of both beams was approximately 7 mm wide. The left hand hinge zone featured a second crack of 4 mm width, and several others up to 1 mm wide, while the right hand hinge contained several cracks of 2-3 mm width. The damage to the plastic hinge zones is shown in Figure 5-8 and Figure 5-9.

Little new damage was visible in either the column or joint zone of the unit. This indicated that the weak beam design philosophy was performing as expected.

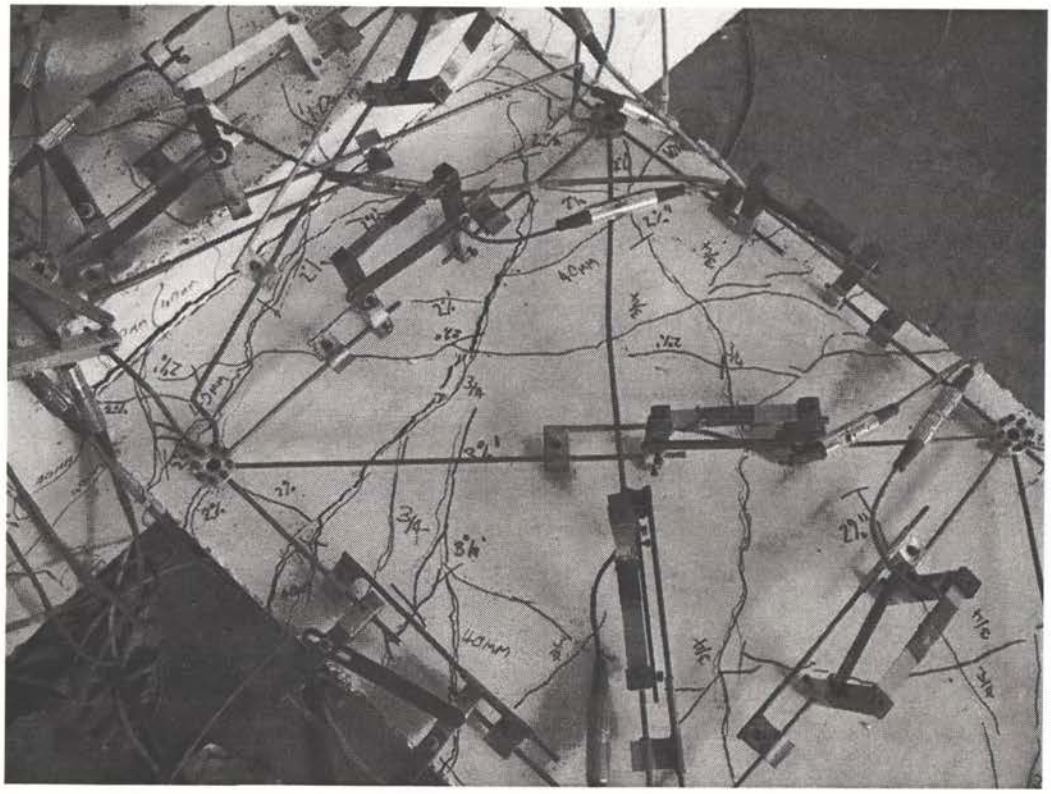

**Figure 5-8 Left hand plastic hinge after first half-cycle to 3% drift**

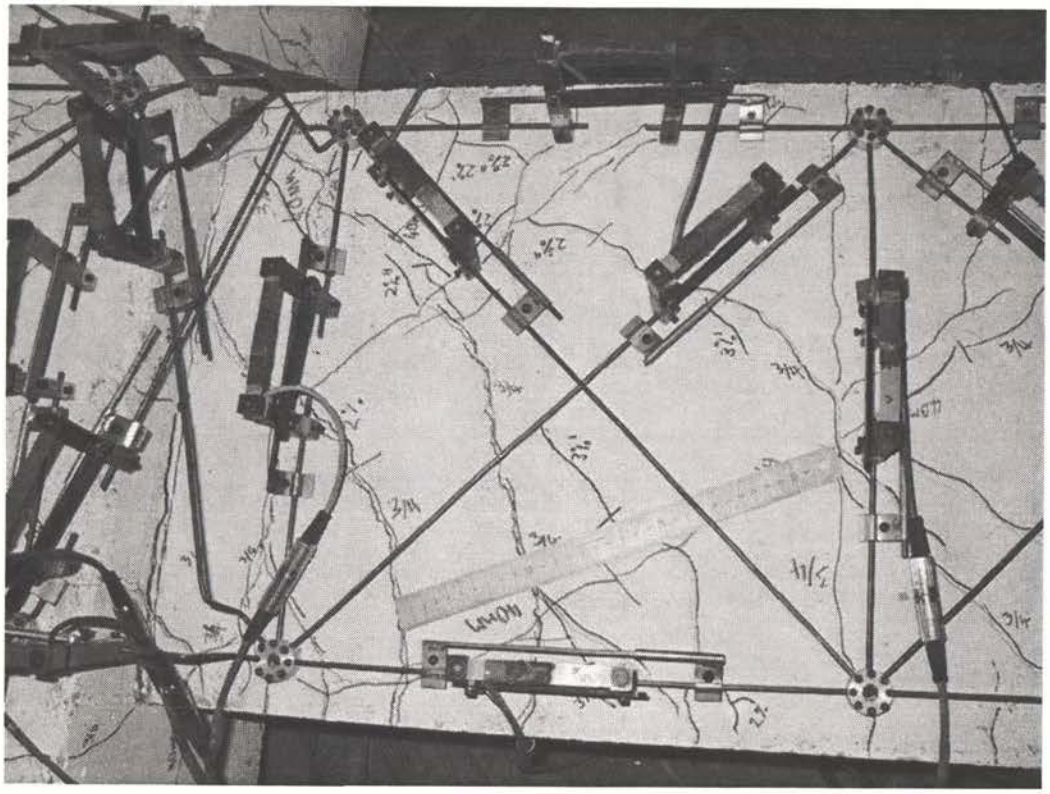

**Figure 5-9 Right hand plastic hinge zone after first half-cycle to 3% drift**

**3% Pull I**

As noted above, well developed plastic hinges were evident on both sides of the joint zone. Again, little damage was noticed outside of the plastic hinges. During this half-cycle splitting cracks developed above the reinforcement of both beams.

**3% Push II**

No significant damage was noticed during this half-cycle. Stirrups were visible through the crack at the beam-column interface from this cycle onwards.

**3% Pull II**

Many new splitting cracks were observed during this cycle, on the left hand top side of the column, in the tension side of the right hand beam, and the compression side of the left hand beam. This crack is illustrated in Figure 5-10. The plastic hinge zones continued to absorb the majority of new damage.

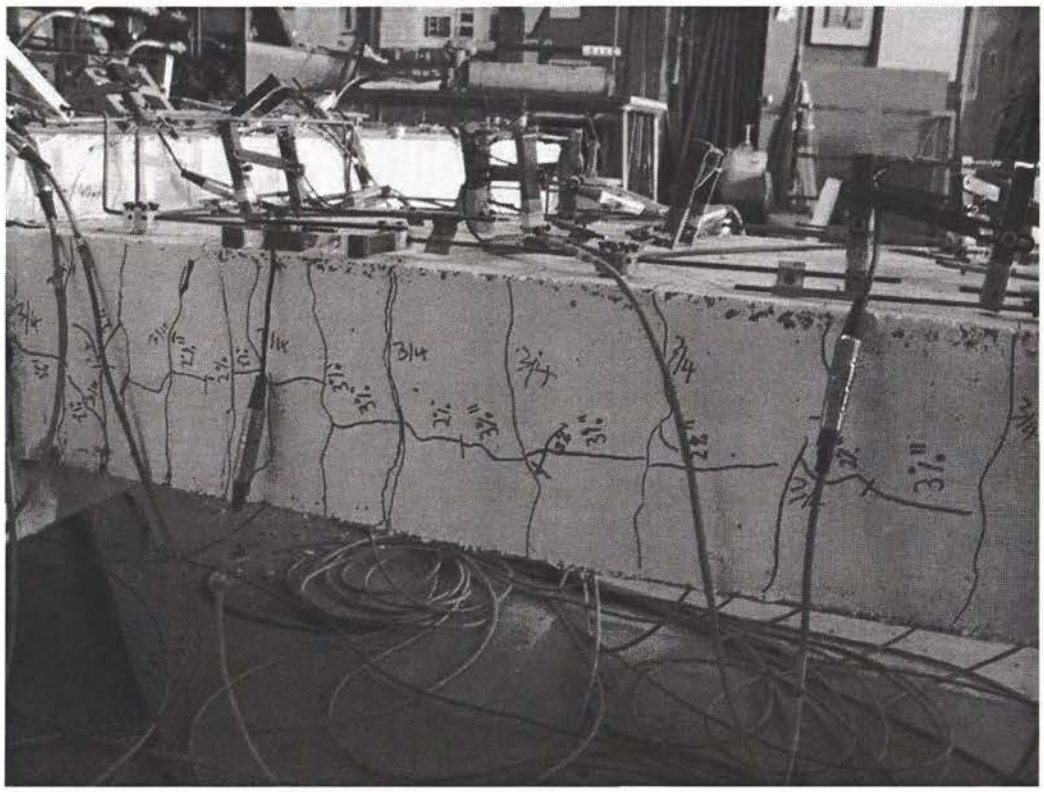

**Figure 5-10 Splitting crack in left hand beam during 3% pull two half-cycle**

**4% Push I**

The most obvious damage to occur during this half-cycle was a significant loosening of the cover concrete in the plastic hinge zones. Coincident with this was the dropping of concrete from the underside of the beam as the same loosening occurred.

The cracks at the beam-column interface were over 10 mm wide at this stage.

**4% Pull I**

A large chunk of concrete fell from the tension side of the top beam during this cycle. This is illustrated in Figure 5-11. The splitting cracks in the beams continued to extend.

**4% Push II**

The right hand beam twisted through an angle of approximately three degrees. Significant spalling of concrete occurred in both plastic hinge zones, and reinforcing bars were visible in these areas. The bars of the right hand beam appeared to have buckled.

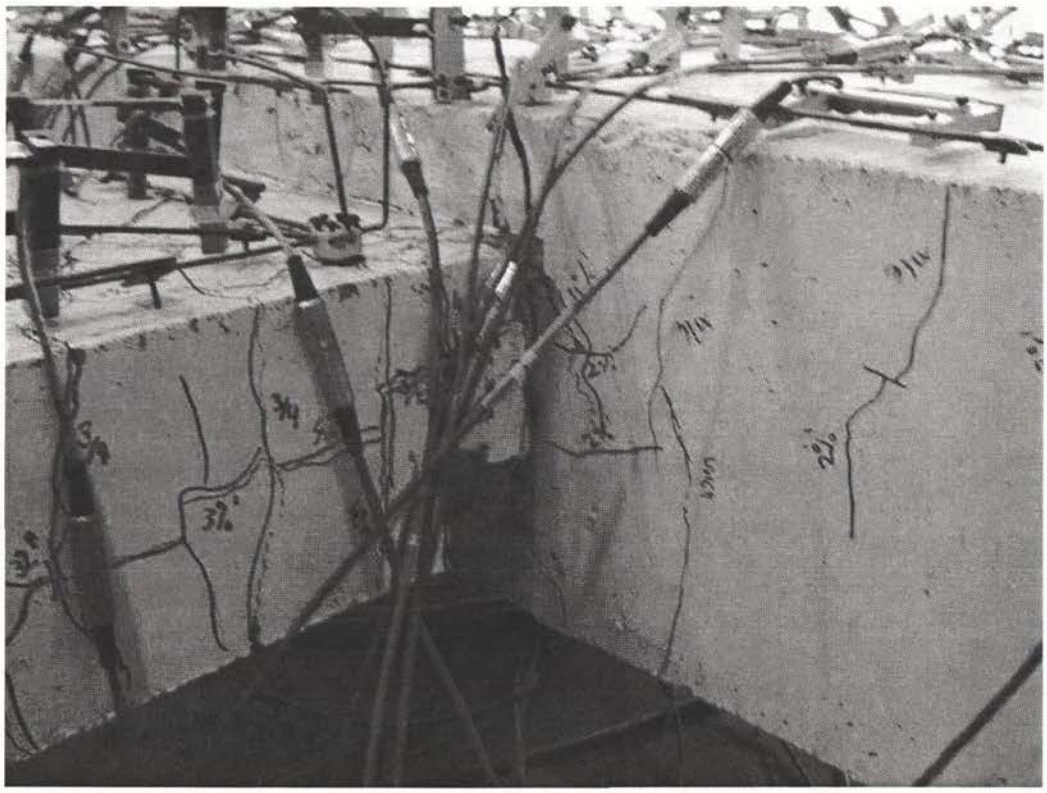

**Figure 5-11 Right hand plastic hinge zone showing area where concrete fell away during 4% pull cycle one**

**4% Pull II**

The concrete of both plastic hinge zones had broken up considerably by the end of this cycle, as can be seen in Figure 5-12 and Figure 5-13. Two bars were clearly exposed in the right hand plastic hinge zone.

**5% Push I**

Both beam twisted severely in this half-cycle (see Figure 5-14 and Figure 5-16), and gauges were removed from around the beam-column interface to prevent damage to these. The concrete of the left hand plastic hinge zone was essentially destroyed at this stage (see Figure 5-15). The break up of the concrete in the right hand hinge zone was not as severe, but the reinforcing bars in compression were fully exposed and badly buckled as shown in Figure 5-17.

**5% Pull I**

Due to the advanced state of damage to the unit, testing was halted following completion of this cycle. It was evident that the apparent good condition of the concrete in the right hand plastic hinge zone during the previous cycle was an illusion. Upon reversal of the loading direction large quantities of concrete fell from the right hand hinge, obviously crushed badly during the previous cycle (see Figure 5-18).

It now appeared that the plastic hinge zone of the left hand beam was in better condition, as is shown in Figure 5-19. It is seen that the damage to the left hand hinge was limited largely to the cover concrete, leaving the confined core intact in comparison to the right hand hinge.

The final condition of unit 1 can be seen in Figure 5-20. It is emphasised that after the first few half-cycles almost all damage was concentrated in the plastic hinge zones, and that no crack in the column or joint region exceeded 1 mm in width.

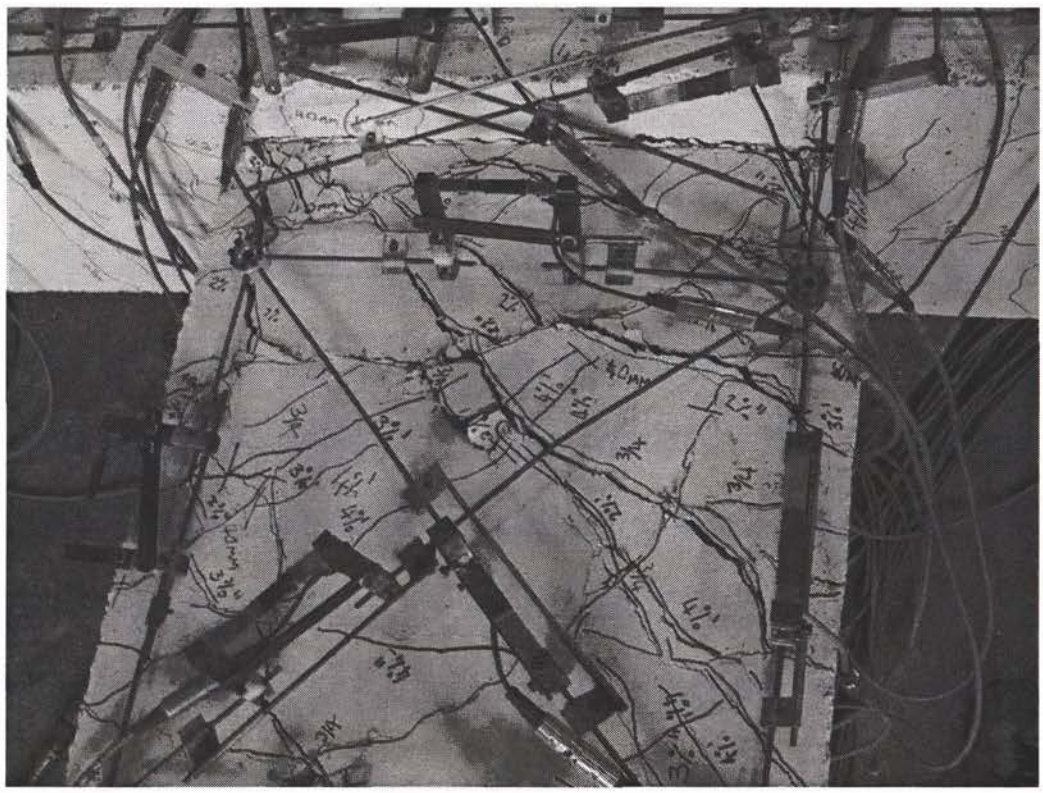

**Figure 5-12 Left hand plastic hinge zone at conclusion of 4% drift cycles**

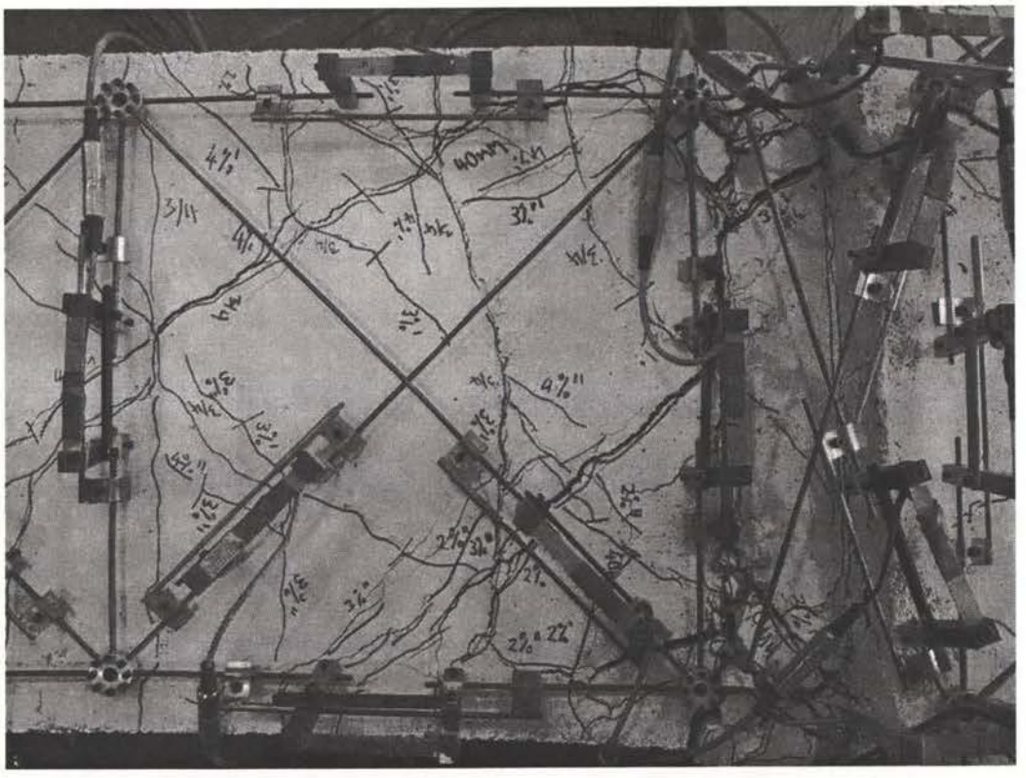

**Figure 5-13 Right hand plastic hinge zone at conclusion of 4% drift cycles**

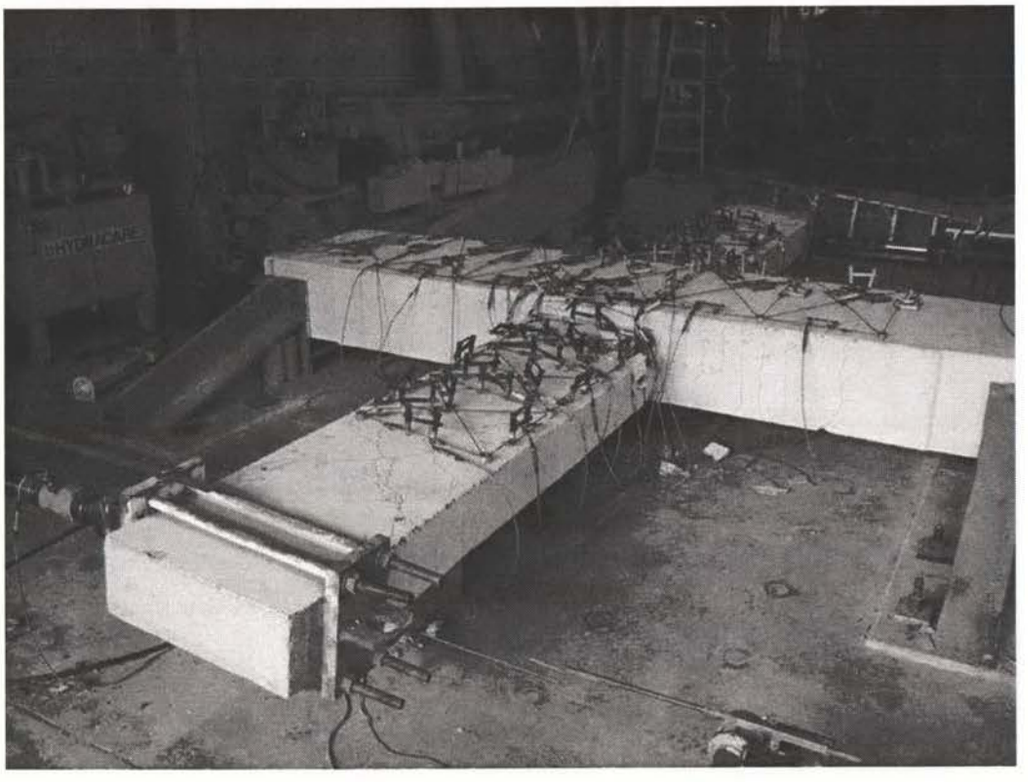

**Figure 5-14 Left hand beam at 5% drift, push direction**

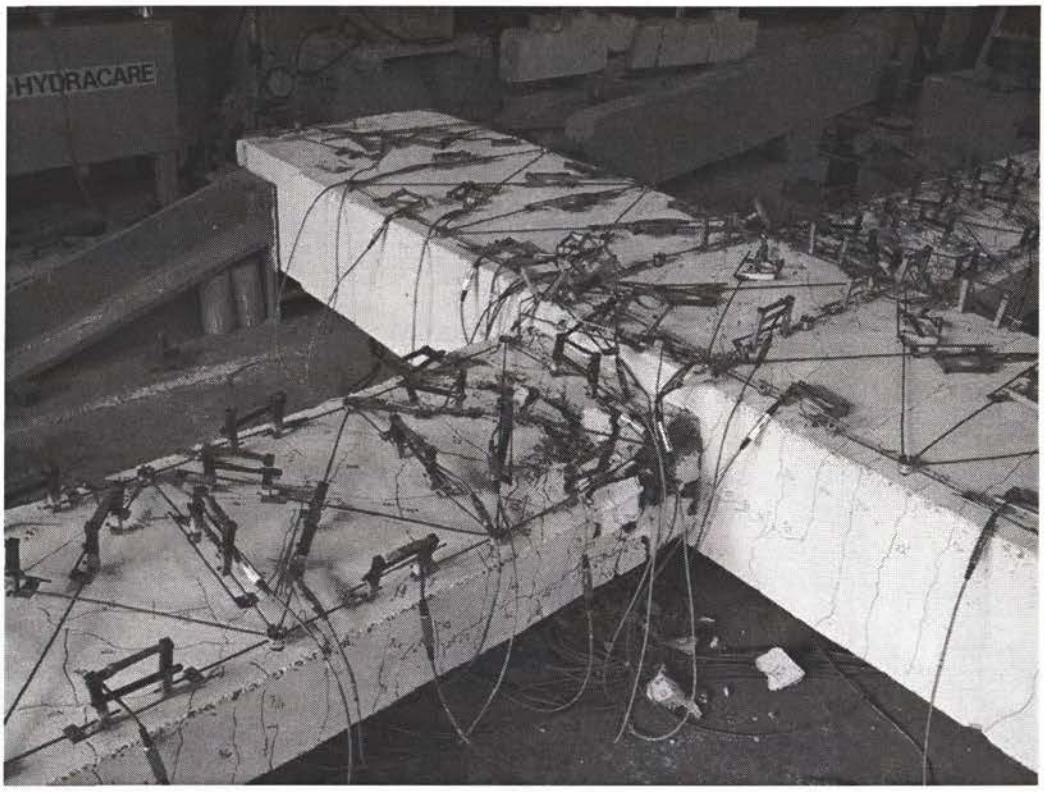


**Figure 5-15 Plastic hinge zone of left hand beam at 5% drift, push direction**

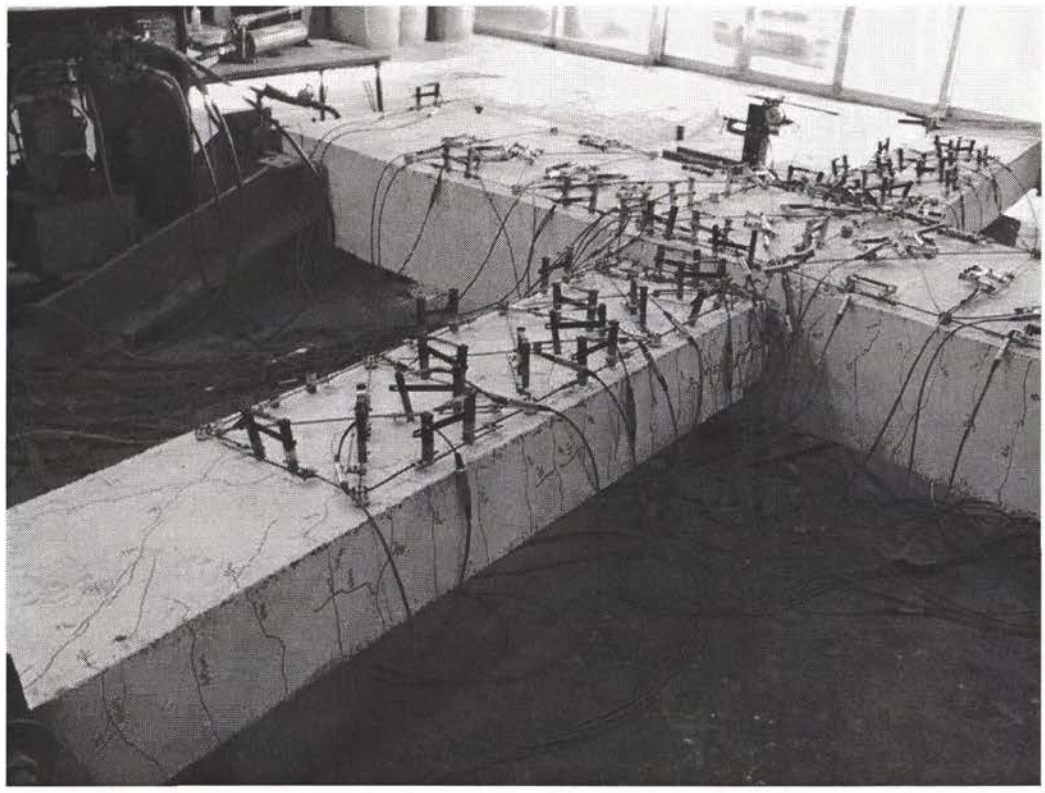

**Figure 5-16 Right hand beam at 5% drift, push direction**

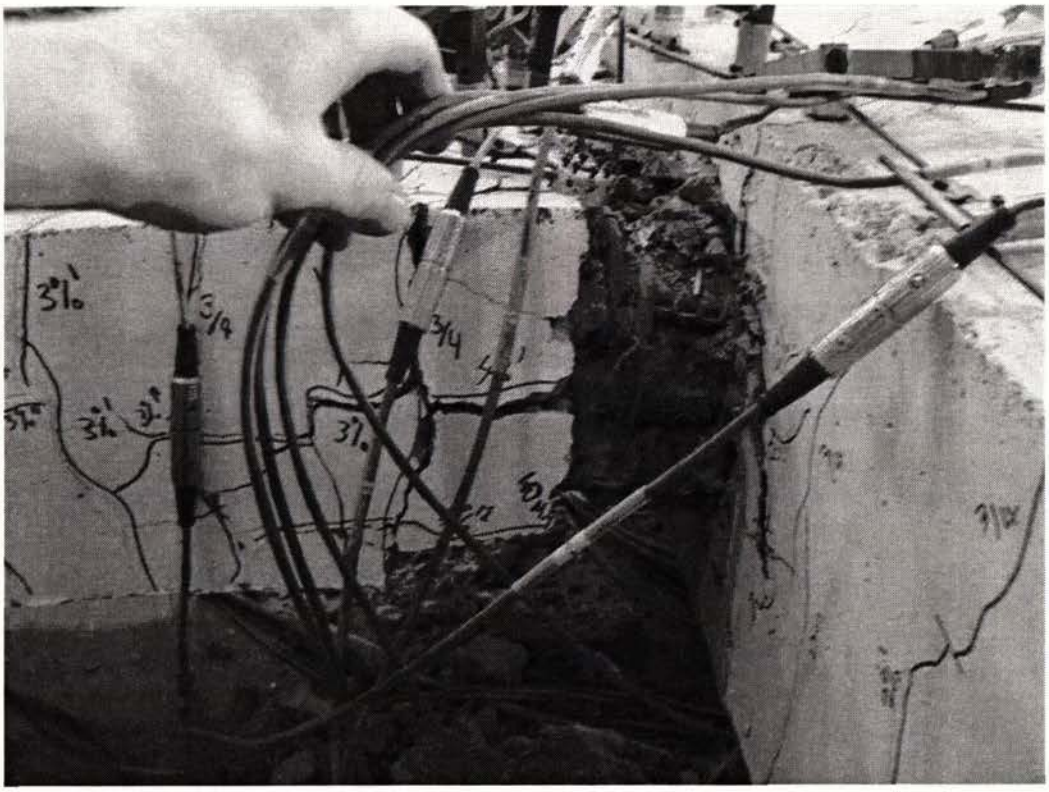

**Figure 5-17 Buckling of bars in right hand plastic hinge zone during 5% push cycle one**

**Figure 5-18 End condition of right hand plastic hinge zone showing loss of concrete**

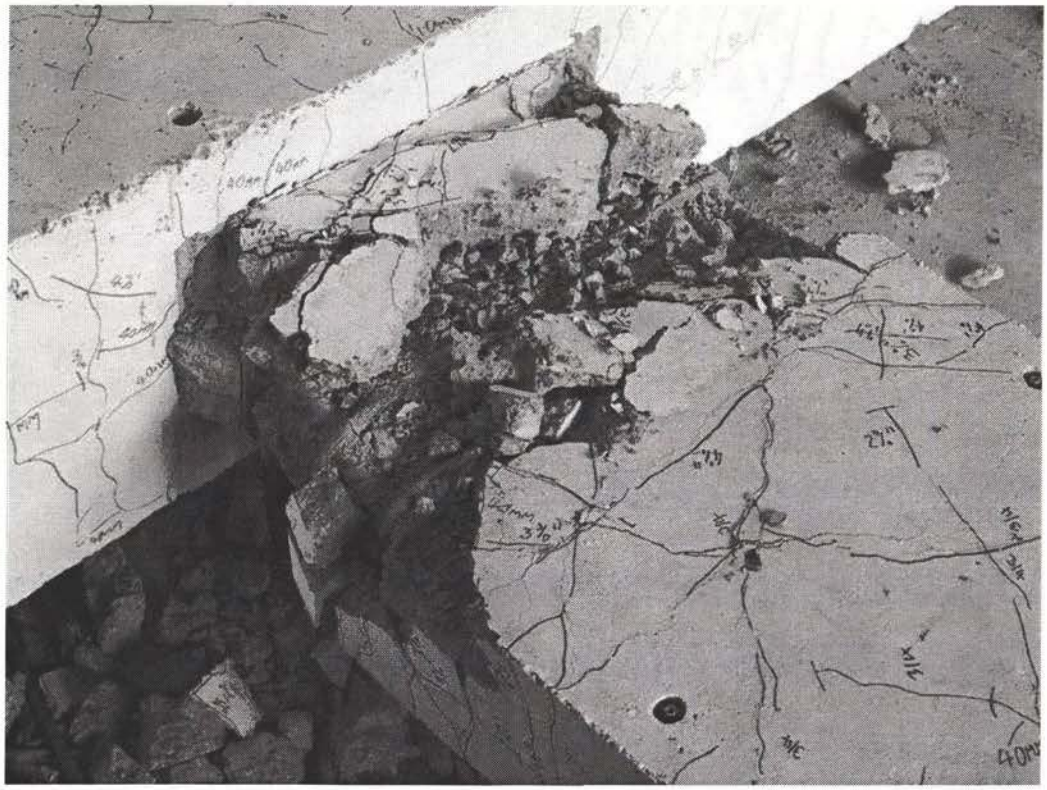

**Figure 5-19 End condition of left hand plastic hinge zone with loose concrete removed**

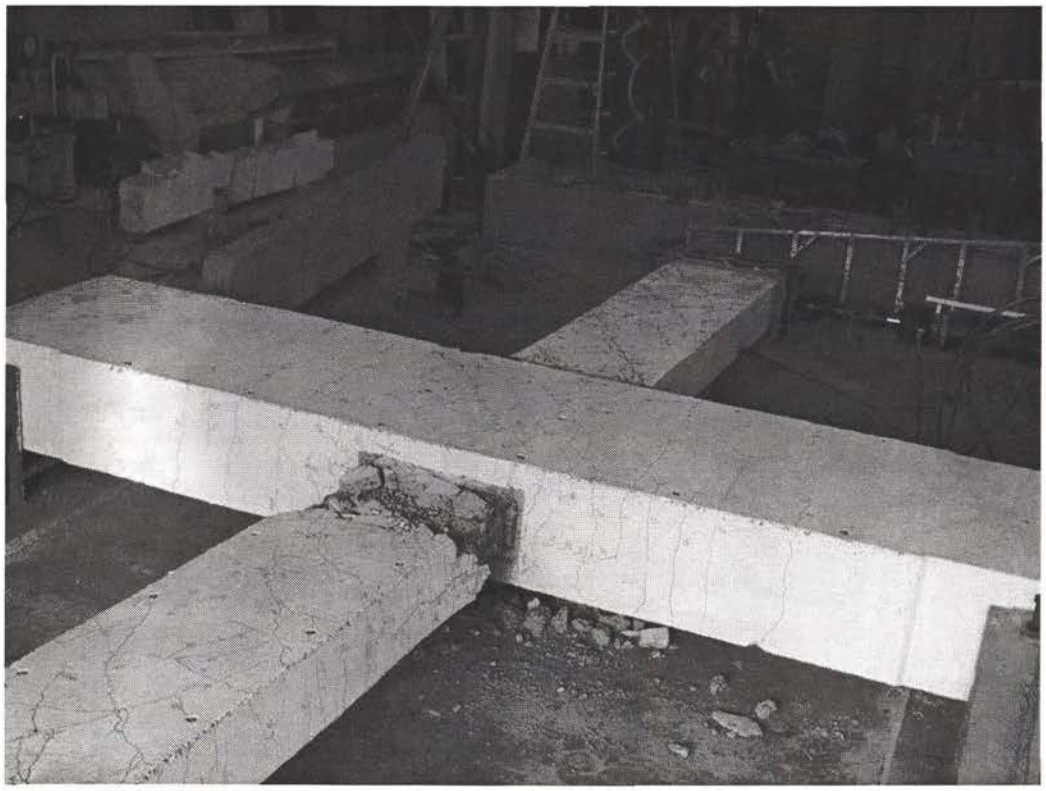

**Figure 5-20 Final condition of unit 1 with gauges removed for clarity**

## 5.2 Unit 2B

**¾ $F_n$ Push**

As for the test of unit 1B, all gauges were checked to ensure they were working. The initial readings for the steel rulers to be used as backup in case of power failure were 295 mm and 293 mm for the left and right beams respectively.

In contrast to the test of unit 1B, the first cycle to ¾ $F_n$ went entirely as planned. Flexural cracking of the beams was noted, along with shear cracks in the joint region. One crack formed adjacent to the joint zone on the tension sides of the top and bottom columns. The residual width of these cracks when the load was removed was approximately 0 mm, indicating the whole test unit had remained within its elastic strength range as planned.

**¾ $F_n$ Pull**

More cracks formed during the pull half-cycle than in the previous push half-cycle. Three shear cracks formed in the joint region, the largest of which (running diagonally from corner to corner of the joint) measured 0.1 mm in width. The pattern of flexural cracking of the beams occurred as was expected, with crack widths of approximately 0.05 mm. Aside from the aforementioned cracks adjacent to the joint region, the columns were still essentially undamaged. The condition of the unit at the end of the elastic half-cycles is shown in Figure 5-21.

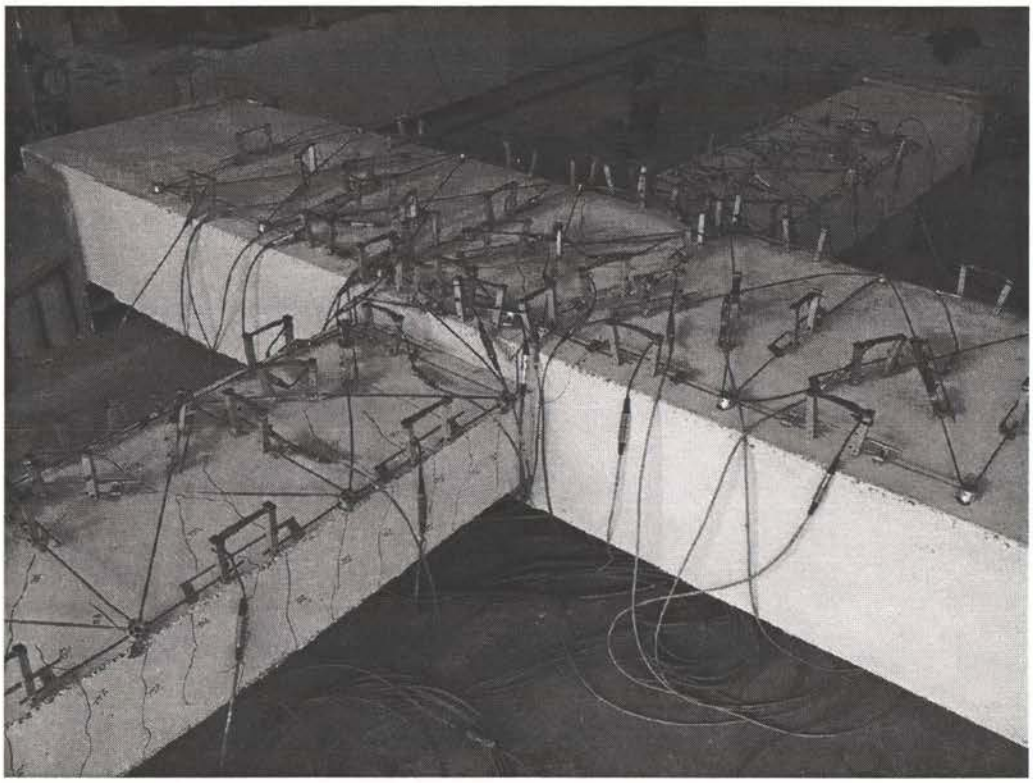

**Figure 5-21 Unit 2B after completion of elastic half-cycles**

The displacements reached at the end of the ¾ $F_n$ half-cycles, and the estimated yield displacements are presented in Table 5-1. The estimated yield displacement of a beam tip, $\Delta_y$, was calculated as follows:

$$\Delta_y = \frac{\Delta_{3/4F_n} \cdot F_n}{F_{3/4F_n}} \qquad \text{eq. 19}$$

where $\Delta_{3/4Fn}$ is the displacement at the peak of the ¾ $F_n$ half-cycle, $F_n$ is the actuator force required develop the nominal moment capacity of the beam, and $F_{3/4Fn}$ is the force at the peak of the ¾ $F_n$ half-cycle. The estimated yield drift was calculated from the estimated yield displacement by summing the estimated yield displacement of the left and right beam tips and dividing by the width between the beam tips (~4900 mm)

**Table 5-1 Estimation of unit 2B yield displacement from ¾ $F_n$ half-cycles**

| Cycle | Beam | $\Delta_{3/4Fn}$ | $F_{3/4Fn}$ | $F_n$ | $\Delta_y$ |
|---|---|---|---|---|---|
| | | (mm) | (kN) | (kN) | (mm) |
| Positive | Left | 17.26 | 118.2 | 161.5 | 23.63 |
| | Right | 18.70 | 117.5 | 159.9 | 25.56 |
| Negative | Left | -16.53 | -119.3 | 161.5 | 22.39 |
| | Right | -19.47 | -124.1 | 159.9 | 25.08 |

The estimated yield drift calculated from these values was 1%. Based on this information, it was decided to continue with the loading cycle as planned (see Figure 4-4).

**2% push I**

Extensive shear and flexural cracking occurred in both beams during this cycle. Splitting cracks were also noted in the right hand beam, probably due to the thin cover concrete provided. More shear cracking occurred in the joint zone (see Figure 5-22), and minor flexural cracking occurred in the column. The main cracks at the beam-joint interface opened to approximately 2-3 mm. Very minor concrete crushing was seen.

**2% Pull I**

This cycle was similar to the preceding push half-cycle. Splitting was seen in the left beam, and small splitting cracks occurred on the face of each column. Shear cracking extended along the length of both beams, and it was apparent that plastic hinges had formed in both beams. Less compression damage was visible than for the first half-cycle to 2% drift.

During this half-cycle the left hand jack froze. The problem was solved without affecting the test, and remedial measures were taken at the end of the cycle to enable better control of the right jack, which seemed to be running ahead of the left jack (in contrast to the testing of unit 1B).

**2% Push II**

As expected very little new damage was noted during this half-cycle. No new damage occurred in the joint zone, and little new shear cracking of the beams was visible. Cracks in the plastic hinge zones opened to 1.2 mm, while the shear cracks in the joint region measured approximately 0.5 mm.

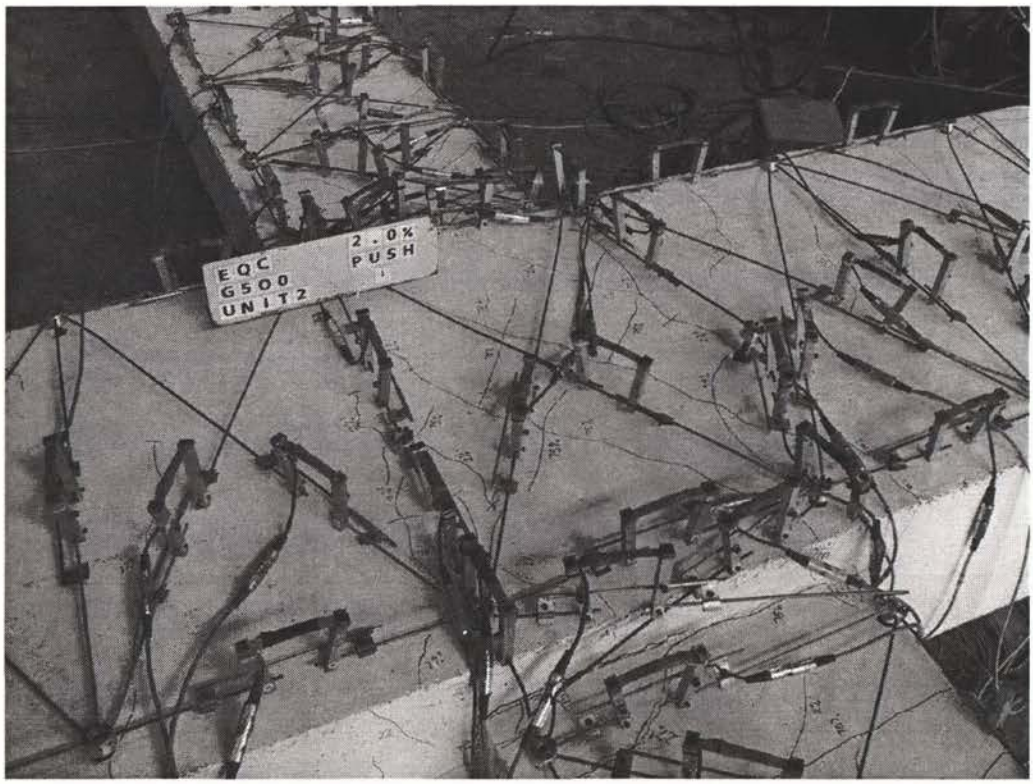


**Figure 5-22 Joint shear cracking at conclusion of first half-cycle to 2% drift**

No loss of stiffness was evident indicating that longitudinal reinforcement slip was not occurring. The left beam remained stronger than the right beam throughout the first three inelastic half-cycles.

**2% Pull II**

The stiffness of the unit was lower than during the first pull half-cycle to 2%, but the magnitude of the ultimate load that was developed was similar. There was no significant cracking during this cycle, and no sign of slippage of the longitudinal reinforcement. The cover concrete in the plastic hinge zones appeared to be breaking up during this cycle. The condition of the unit at after the final 2% drift half-cycle can be seen in Figure 5-23.

**3% Push I**

Again, few new cracks were noted, and most damage was confined to the plastic hinge zones. The concrete of the left hand plastic hinge was breaking into distinct blocks, while the right hand hinge seemed to maintain cohesion more (see Figure 5-24 and Figure 5-25). The cracks at the column face opened to approximately 5 mm.

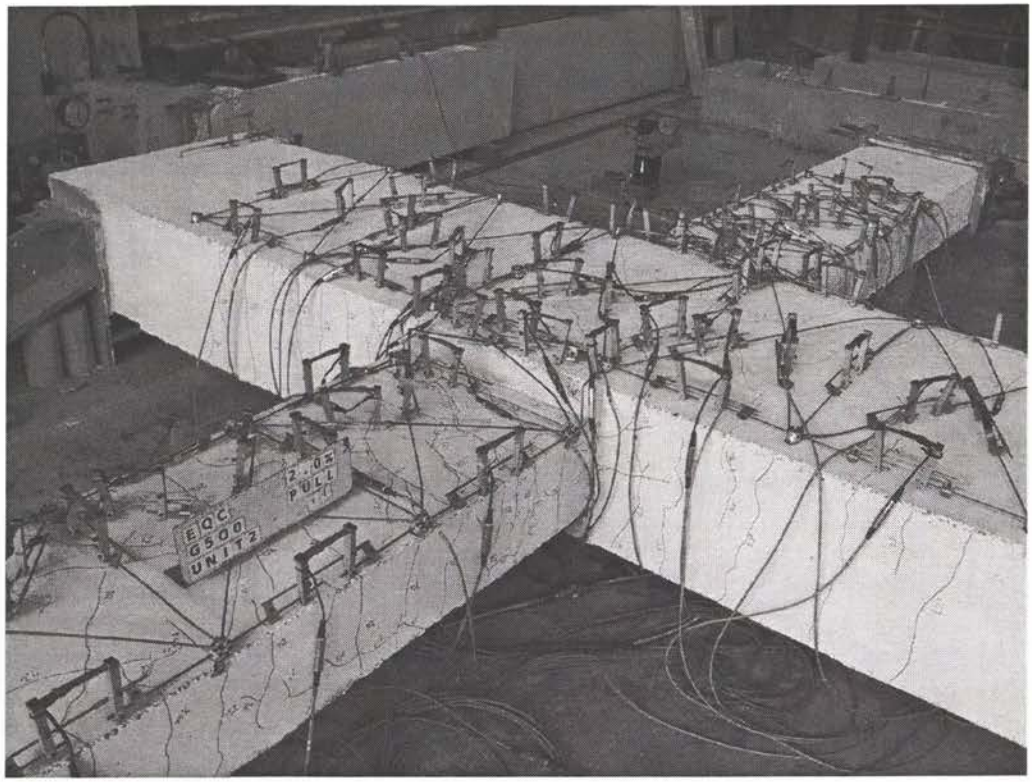


**Figure 5-23 Condition of unit 2B after final 2% drift cycle**

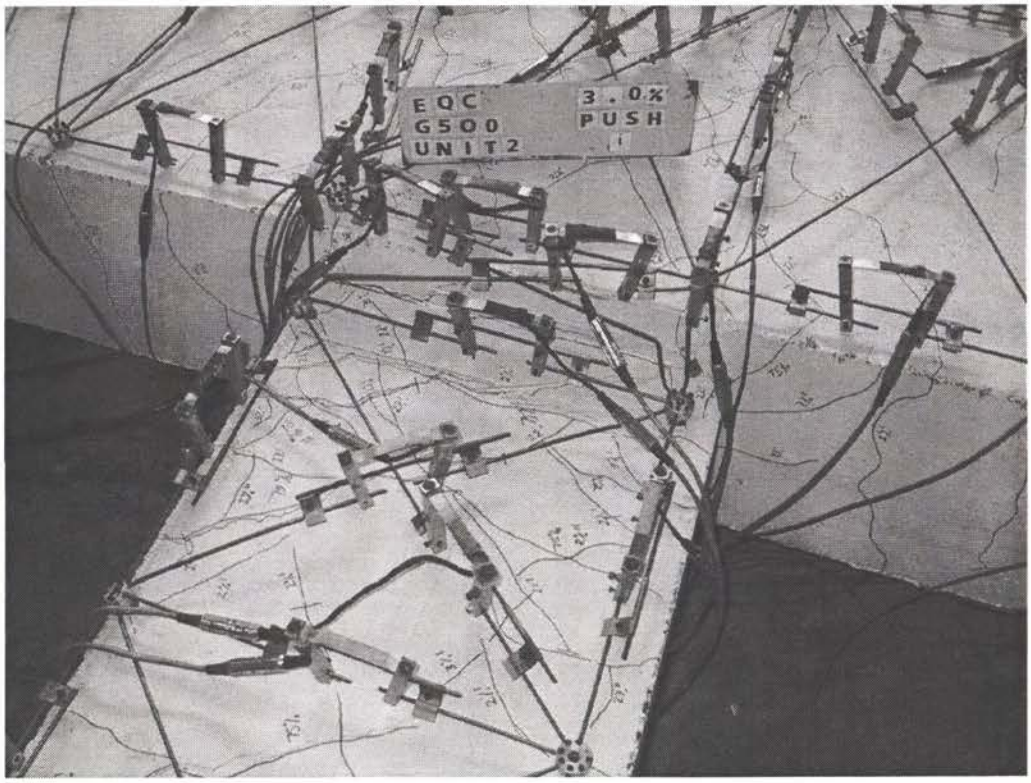


**Figure 5-24 Right hand plastic hinge zone after first half-cycle to 3% drift**

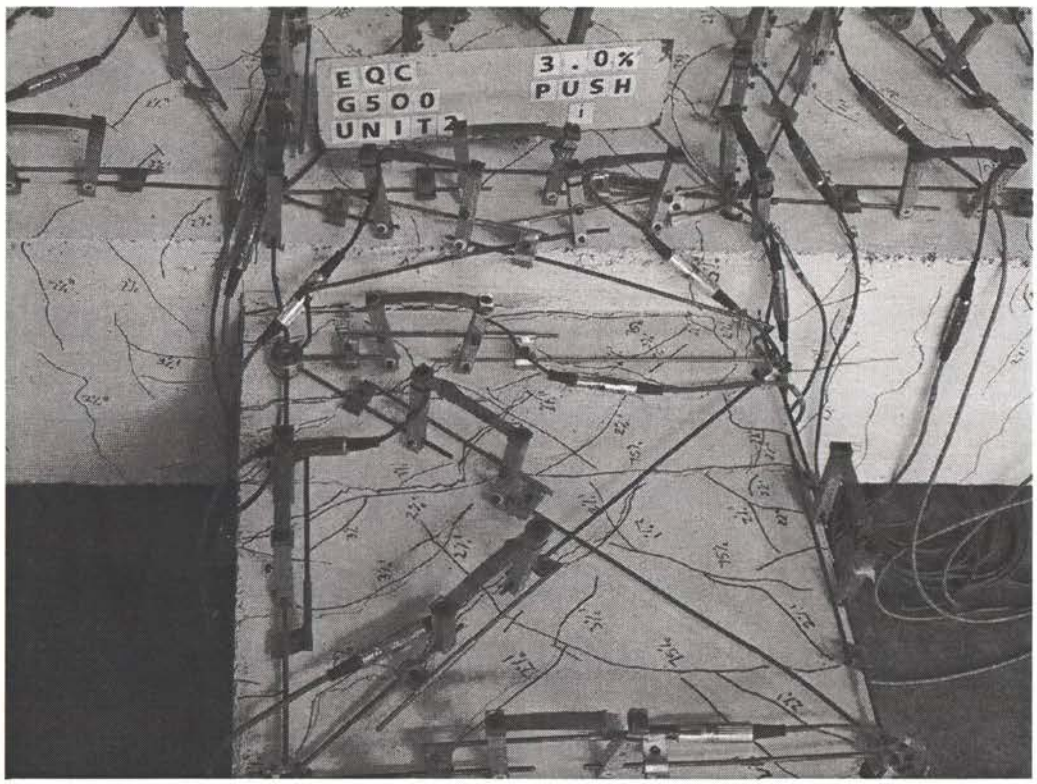


**Figure 5-25 Left hand plastic hinge zone after first half-cycle to 3% drift**

**3% Pull I**

Small extensions were seen on several shear cracks along the right hand beam, and the right hand plastic hinge zone began showing signs of breaking into blocks, as the left hand beam had done in the previous half-cycle. A long crack of 4 mm width opened up in the left hand plastic hinge zone. The largest cracks in the right hand hinge were 2 mm wide. The cracks in the joint zone remained limited to 0.5 mm width.

The cover concrete over the first stirrup in the right hand plastic hinge was found to be loose. When measured, it was found to be approximately 8 mm thick, slightly less than the designed value. The hysteresis loops produced by the data logging software indicated a large quantity of energy absorption still occurring, and no sign of bar slip.

**3% Push II**

The first signs of significant concrete crushing were noted during this cycle. Shear cracks in the right hand beam extended, and both plastic hinge zones were extensively cracked at this stage. For the first time during the test new cracks were found on the compression edge of the beams, a further indication that concrete crushing was occurring (see Figure 5-26). In contrast to the advanced stage of damage to the beams, the joint and columns still showed no signs of further damage.

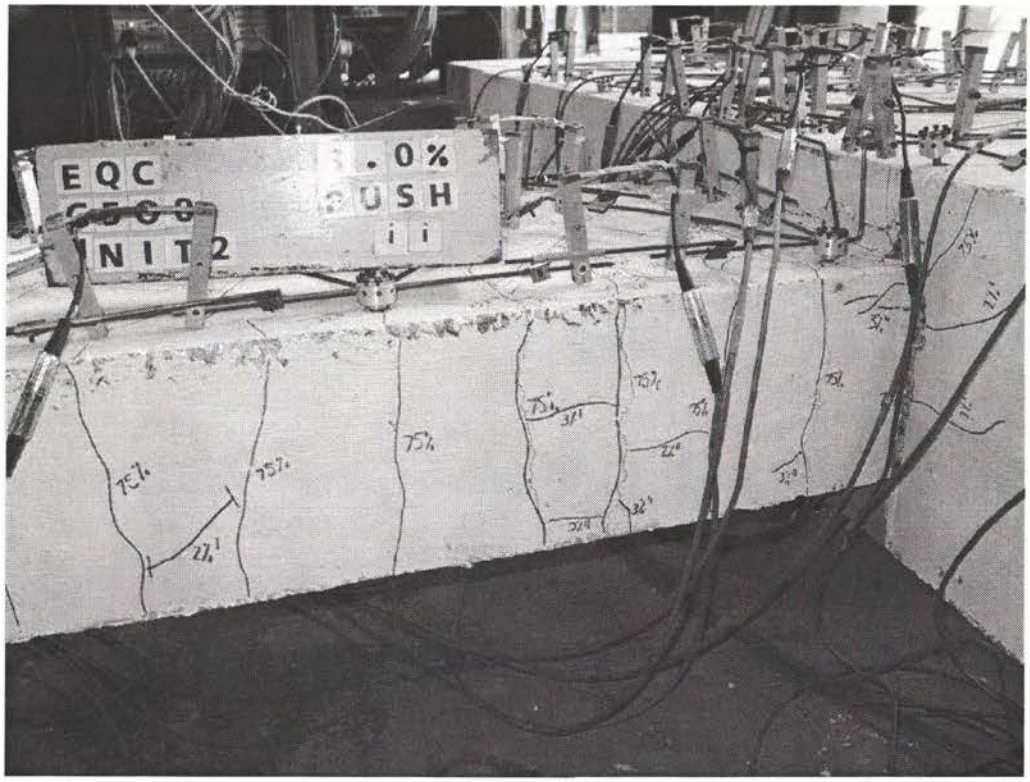


**Figure 5-26 Right hand plastic hinge zone at end of second 3% drift half-cycle, showing signs of concrete crushing**

After the load was released the residual crack widths on various parts of the unit were noted. It was found that those in the beams remained open 2 mm, with a 3 mm residual width at the beam-joint interface. The cracks in the joint remained open approximately 0.1 mm, while those in the column closed completely.

**3% Pull II**

The unit followed a similar pattern of damage as for the last few half-cycles, with damage concentrated in the plastic hinge zones.

**4% Push I**

Concrete fell from the underside of the unit during this cycle, leaving stirrups exposed in the plastic hinge zones. The pattern of cracking shown in Figure 5-27 probably indicated that the top reinforcing bars in the beams were on the verge of slipping.

**4% Pull I**

Several small areas of concrete buckled out of the face of the left-hand plastic hinge during this half-cycle, although few new cracks formed in this cycle. From the appearance of the unit it seemed that all cracks that could form had formed by this stage.

**4% Push II**

As expected, the right hand beam began to twist torsionally during this cycle. The left beam did not twist, but it appeared that the shear deformation in the plastic hinge zone was considerable. Large quantities of cover concrete were dislodged from both beams.

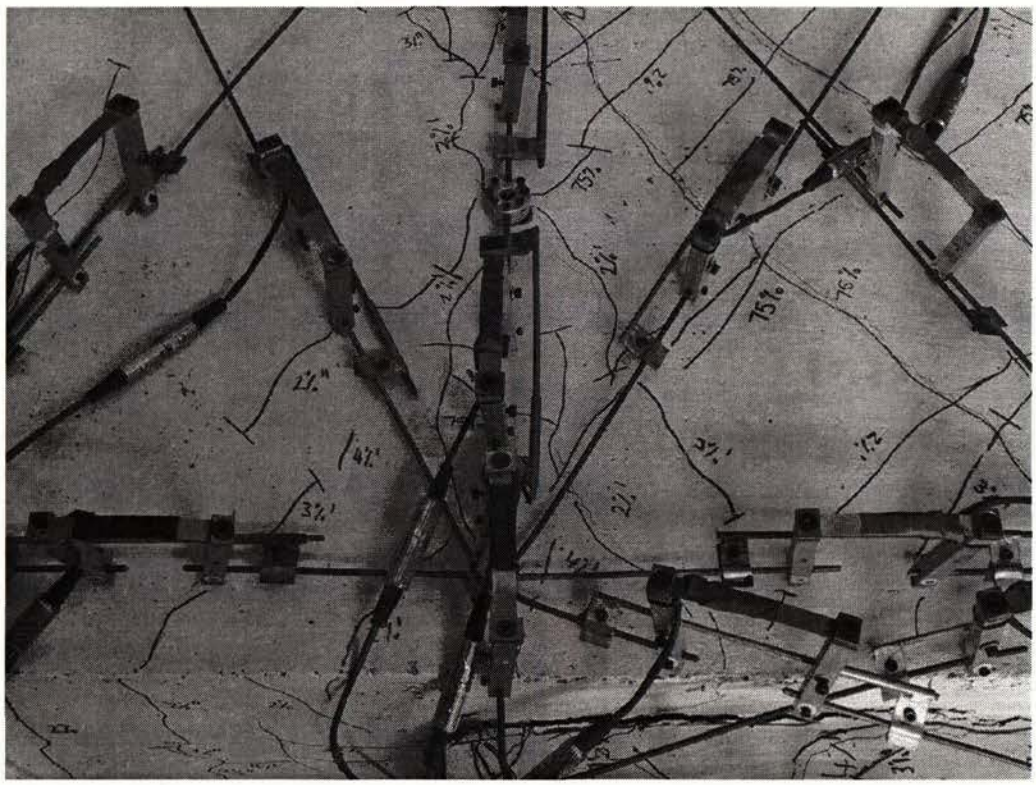

**Figure 5-27 Crack pattern indicating imminent reinforcement slip**

During this load cycle the peak loads of both beams were lower than during the first push half-cycle to 4%. This was the first instance during the test where strength decreased.

**4% Pull II**

This cycle marked the first occasion where unit 2B failed, i.e. did not achieve 80% of the peak load sustained in previous pull cycles. The right beam was severely twisted during this cycle, but the left beam still did not twist. Both plastic hinge zones lost large quantities of concrete, including some core concrete.

Despite the unit having technically reached failure during this cycle it was decided to continue testing until it was not possible to displace the beams further. The condition after the first failure of the unit is shown in Figure 5-28.

**5% Push I**

Both beams twisted to a large degree during this cycle (approximately 10 degrees, see Figure 5-29), meaning that obtaining meaningful displacements at the load points became difficult. In addition, gauges in the plastic hinge zone were removed to prevent damage to them.

The strength of the unit was significantly less than during previous cycles. The core concrete was visibly fractured, and virtually all cover concrete had fallen from the plastic hinge zones at the end of this half-cycle.

**5% Pull I**

The right beam twisted again during this half-cycle, while the left translated in a shear type movement (see Figure 5-30). This was caused by the virtual absence of cohesive concrete in the left hand plastic hinge zone, allowing formation of a shear hinge. It was decided that further cycling of the unit would not provide any meaningful information, and the test was halted.

After completion of the testing the gauges were removed from the unit, providing a clearer view of the final condition of the unit. This is shown in Figure 5-31 and Figure 5-32.

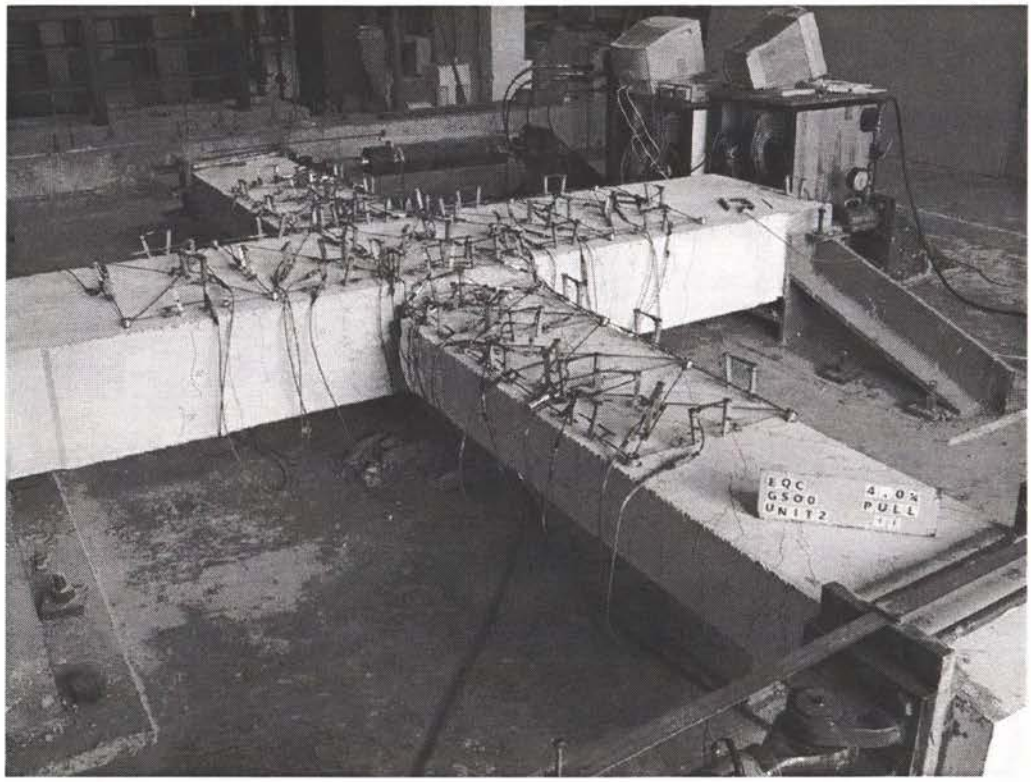


**Figure 5-28 Condition of unit 2B after failure during 4th half-cycle to 4% drift**

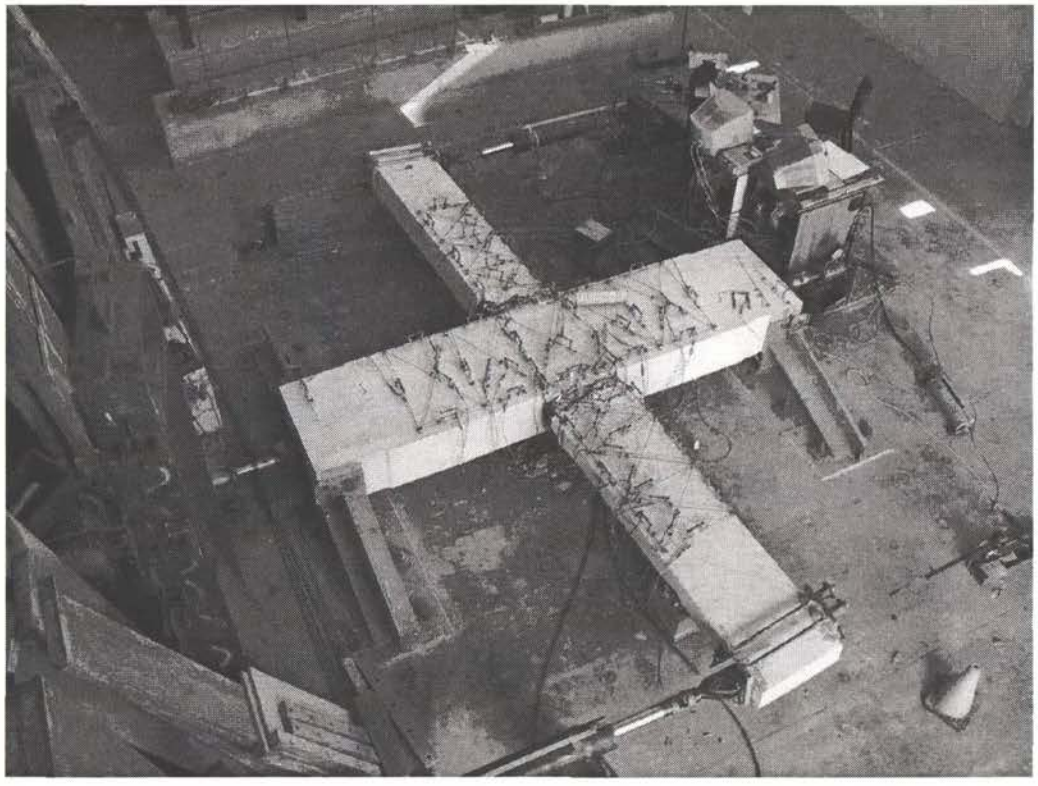

**Figure 5-29 Unit 2B at 5% drift showing torsional distortion of both beams**

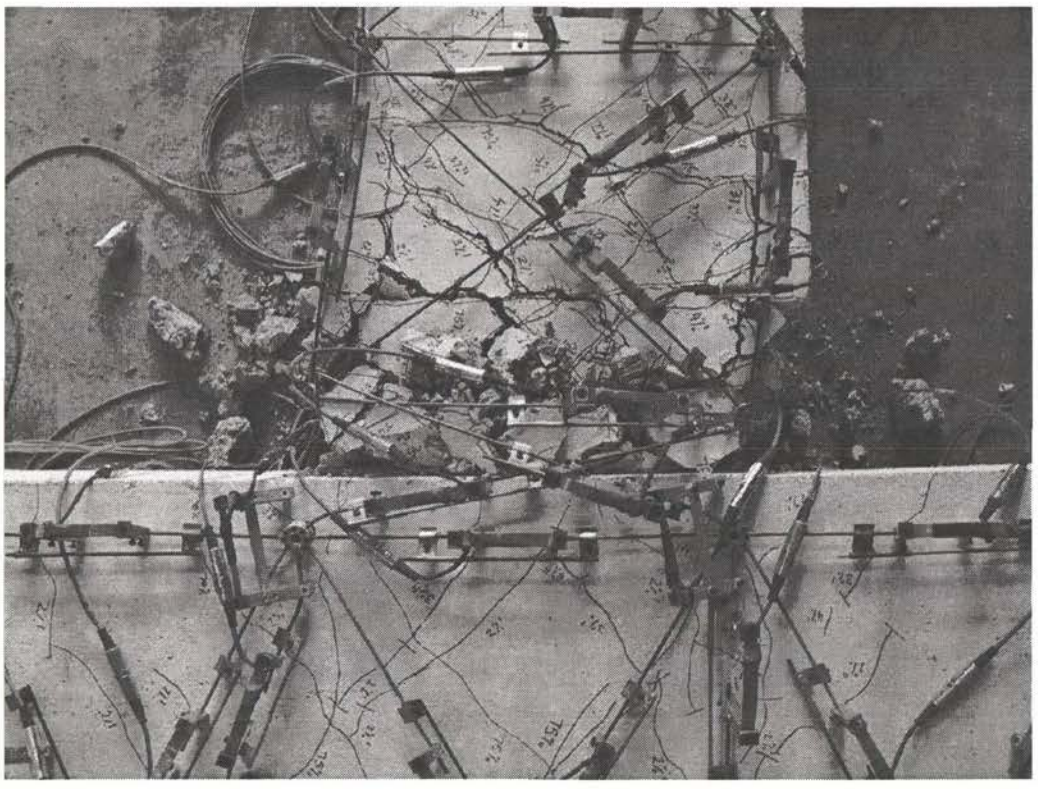

**Figure 5-30 Large shear deformation of left hand plastic hinge zone during second half-cycle to 5% drift**

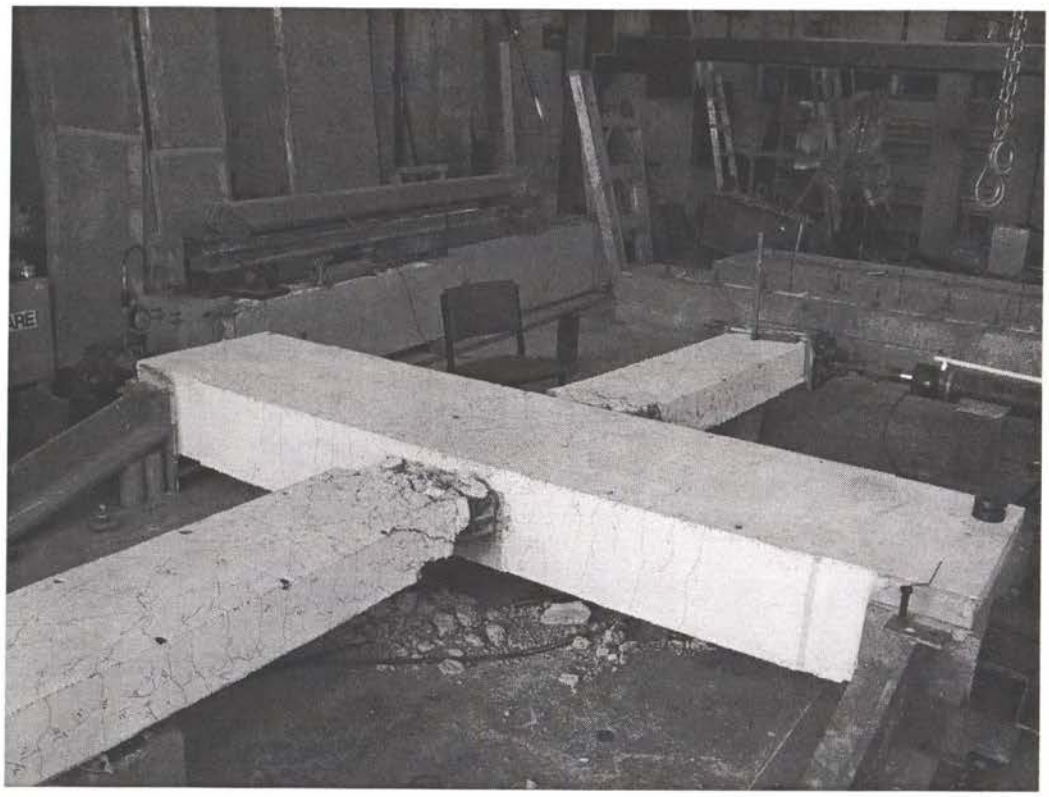

**Figure 5-31 Condition of unit at completion of testing (from left hand side)**

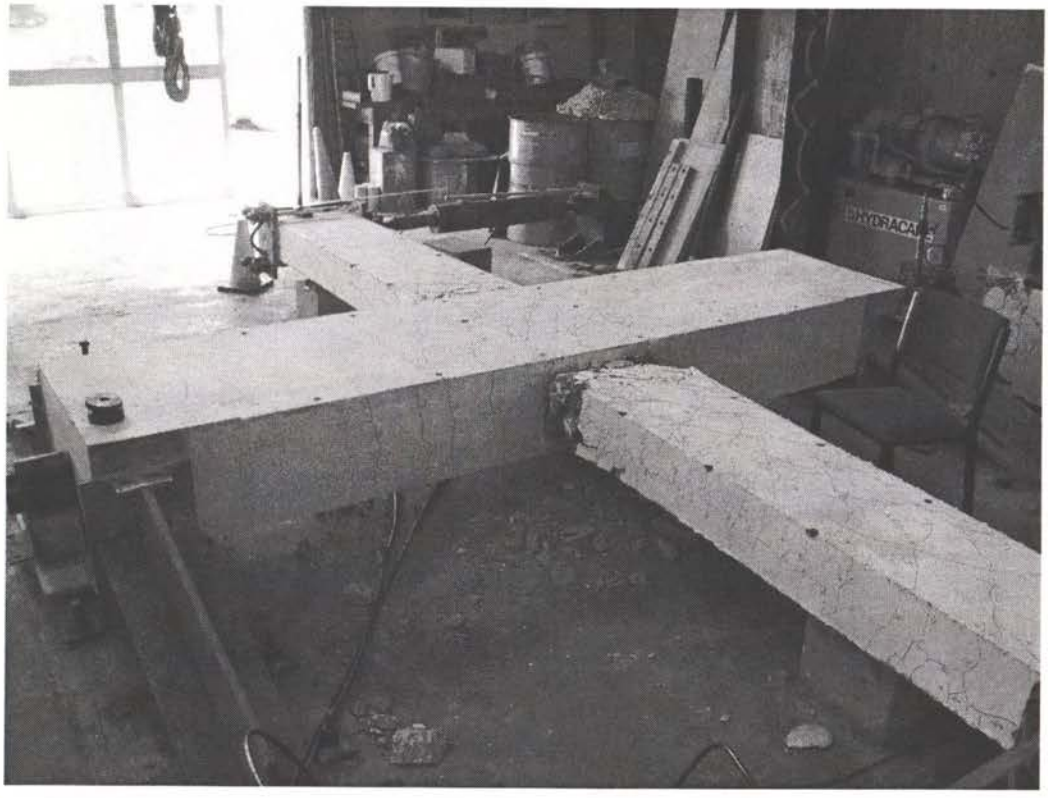

**Figure 5-32 Condition of unit at completion of testing (from right hand side)**

## *5.3 Unit 3B*

**Pre-test observations**

As mentioned in section 4.3, a computer controlled hydraulic system was developed at the University of Auckland. This system was developed to replace the existing, manually controlled, system. The testing of unit 3B represented the first time the new system had been used to control a test with two independent actuators.

Set-up of the new system was similar to the old system. Movement of the beam-column unit relative to the floor was prevented by loading the single acting jacks at the column ends to approximately 62 kN each. The rulers mounted over the reversing actuators at the beam ends were checked, and initial readings of 276 mm and 310 mm were noted for the left and right beams respectively.

The initial condition of the unit was checked, and it was noted that there were a number of cracks present on the faces of the beams, presumably from forces induced when manoeuvring the unit into the restraints. These cracks were marked in pink. Finally, all gauges were tested to ensure the readings they gave were realistic.

**0.4% Push**

As expected there was very little change in the condition of the unit at this stage. Minor flexural cracks in the beams and at the joint edges were the only noticeable damage. It was found that two gauges were not reading accurately, and these were swapped.

**0.4% Pull**

The pattern of cracking during this cycle was effectively identical to that in the previous half-cycle. No damage to the column was observed, and there was no sign of yielding.

**0.8% Push i**

Due to the new control system being used for the first time it was decided to conduct a further elastic half-cycle in each direction. During this cycle the displacement of the previous cycle was doubled to 0.8% drift.

The flexural cracking in the beams extended further towards the actuators as the load increased during this half-cycle. Shear cracks also formed in the beams and in the joint region. In addition, minor flexural cracks formed in the columns. None of the cracks in the concrete exceeded 0.2 mm. This indicated that no inelastic deformation had occurred at this stage.

**0.8% Pull i**

More shear and flexural cracking occurred in the beams of the unit. Shear cracking of the joint and flexural cracking of the column also continued to occur. Despite a lack of evidence of inelastic displacement, cracks indicative of the initial stages of bond failure formed around the bottom beam reinforcing bars where they passed through the joint.

Between the peaks of this and the previous cycle problems occurred with the left-hand actuator. The problem seemed to prevent the actuator from reaching the targeted displacement.

**0.8% Push ii**

Due to the problems experienced with the left-hand actuator during the previous cycle it was decided that a second pair of half-cycles to 0.8% drift would be conducted to try and determine the cause of the problem.

During this half-cycle the problem of an actuator not achieving the required displacement occurred in the other (right-hand) actuator.

Some crack extension occurred in the left-hand beam, and there was more shear cracking outside the potential plastic hinge region (in the region with greater stirrup spacing). There was almost no change in the condition of the right-hand beam. This matched expectations, since the displacement reached was less than during the previous half-cycle.

**0.8% Pull ii**

The displacement control problem again transferred from one side to the other, now occurring with the left-hand actuator. There was in general very little new cracking, the exception being the formation of two new cracks in the joint region.

Following this half-cycle the left-hand actuator was uncoupled from the test unit. Experimentation revealed that there was no physical reason why either actuator could not reach the programmed displacements. Despite the left-hand actuator not achieving 20 mm displacement when required during this half-cycle, it was found that the actuator would extend beyond 20 mm if 25 mm displacement was entered into the controlling computer. The actuator would not however extend to the full 25 mm required in this case. The only explanation found was that the control system did not appear to be releasing the pressure in the return line of the actuator. This valve was tested and found to be functional. It was therefore decided to remove the new control system and conduct the remainder of the test with the old manually controlled system.

**1% Push i**

Due to ongoing problems during the previous half-cycles, the fluctuations these caused in the data readings and the fact that the unit had still not been subjected to any inelastic displacement, it was decided to re-zero all of the gauges and begin a new data file. Any significant errors this introduced could be removed by comparing and altering the data to match the readings immediately prior to re-zeroing the gauges. In addition, all gauges were rechecked and several were changed.

Significant new shear cracking of the beams occurred during this half-cycle. The shear cracks now extended across approximately 80% of the depth of the beam. No cracking yet existed close to the

loading points at the ends of the beams. There was also more flexural cracking of the columns and new shear cracks in the joint region. The position and orientation of some of these joint cracks supported the view that the bottom beam bar might slip at an early stage.

**1% Pull i**

This half-cycle resulted in similar extension of shear cracks to the previous half-cycle, although there was less new cracking in the joint zone. This was a result of more cracks having formed in the joint zone during previous half-cycles in this direction of loading. As expected, flexural cracking extended further along the columns as the moment increased.

**1% Push ii**

Overall there was virtually no change in the condition of the unit. Some new cracks in the columns occurred, but the state of the beams remained identical. As expected, the stiffness of the unit on reloading was reduced somewhat.

**1% Pull ii**

Again there was little new crack formation. More new cracks formed in the left-hand beam than in the right-hand one, but the displacement of the left beam was slightly larger. Shear cracks outside the plastic hinge region of the left-hand beam opened to approximately 0.5 mm. At the conclusion of the half-cycles to 1% drift the unit was clearly still within its elastic range.

**2% Push i**

This half-cycle caused a considerable increase in damage to the test unit. Shear cracks in the beams extended significantly, and flexural cracking in the newly formed plastic hinges opened to approximately 1.1 mm. The shear crack widths were not greater than 0.5 mm. A few small new cracks occurred in the joint region, where crack widths were less than 0.3 mm.

**2% Pull i**

Some new cracking occurred in the joint region, and it was obvious that the unconfined cover concrete in the plastic hinge zones was beginning to break apart. New and extended shear cracks formed in the beams, while there were few new cracks in the columns. The new cracks nearest to the column restraints appeared to be shear cracks rather than flexural cracks. One crack was found on the compression edge of a plastic hinge zone.

**2% Push ii**

Aside from an increase in damage to the plastic hinge zones and a number of new cracks in the joint and columns, this half-cycle was uneventful.

**2% Pull ii**

Again there was little new damage to the test unit. Some minor spalling of concrete occurred in the left-hand plastic hinge region.

**3% Push i**

Almost all the new damage in this half-cycle was confined to the beams, and specifically the plastic hinge regions. This indicated that the capacity design procedure used to design the unit was working

as planned. By this stage the plastic hinge zones were heavily cracked in all directions, although there was as yet no major spalling. Crack widths in the plastic hinge zones were up to 3 mm, while those in the joint and columns remained less than 0.3 mm and 0.1 mm respectively.

**3% Pull i**

Again new damage was restricted to the plastic hinge zones. Some crushing of concrete occurred in the right-hand plastic hinge. There was some crack extension in the joint region, most notably around the top and bottom edges of the joints.

**3% Push ii**

Few new cracks occurred in the left-hand plastic hinge. The right-hand plastic hinge continued to break up, but maintained strength. In addition, several new cracks formed on the compression side of the right-hand beam. Shear cracks from the joint region had now extended well into the columns.

**3% Pull ii**

This half-cycle brought the first significant signs of concrete spalling from the underside of the plastic hinge regions. Due to the absence of uncracked concrete, no new cracks formed on the surfaces of the plastic hinges.

During this and the previous half-cycle, cracks formed on the column face above and below the right-hand beam (Figure 5-33). This was considered to be an indication that bond failure was beginning to occur.

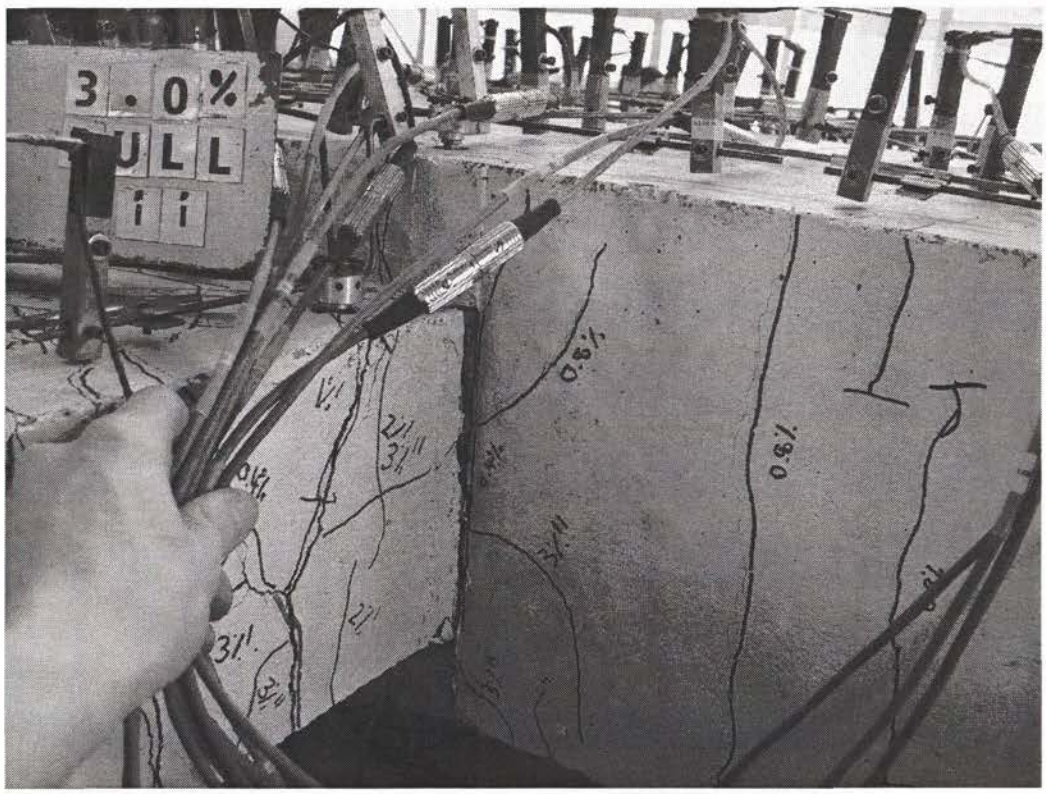


**Figure 5-33 Cracks on column face during fourth half-cycle to 4% drift**

**4% Push i**

Again there was little new cracking during this cycle, despite the increased displacement involved. All the new cracks that did occur were located in the plastic hinge regions, and there was increased crushing of the cover concrete in these regions also. Crack widths increased significantly compared to the cycles to 3% drift. In particular there was wide opening of splitting cracks in those areas of the joint adjacent to reinforcement in tension.

Measurement of various cracks gave the following results:

| | |
|---|---|
| Shear cracks in the beams | 0.8 mm |
| Plastic hinge regions | up to 4 mm |
| Crack at beam-joint interface | 7 mm |
| Splitting cracks in the joint | 1 mm |
| Joint shear cracks | 0.4 mm |

**4% Pull i**

Little new cracking was noted anywhere on the test unit. There was extension of some cracks in the column, adjacent to the joint region. Readings from the gauges installed to measure reinforcement slip indicated this may be happening, although strength and stiffness remained satisfactory.

**4% Push ii**

This half-cycle was the first in which strength loss occurred relative to the previous half-cycle for the same direction of loading. Gauge readings again indicated that bar slip was occurring, and this was supported by the continued extension of cracks around the joint region.

Cover concrete was now falling from the plastic hinge regions, and the only new cracking was that visible on the compression sides of the plastic hinge regions.

**4% Pull ii**

Bond failure had definitely occurred by the conclusion of this half-cycle. Large quantities of concrete were pulled from the right-hand side of the joint by the top beam reinforcing bars as they slipped (Figure 5-34). There was also similar but less severe damage to the left-hand side of the joint where the lower reinforcing bars exited the joint.

This half-cycle brought a more significant (~20%, hence close to failure) strength reduction than the previous cycle. There was no sign of the plastic hinge buckling that affected the testing of units 1B and 2B at this stage of testing.

On release of the load a large amount of concrete fell from the unit.

**5% Push i**

No new cracking occurred during this cycle, although there was a large loss of concrete from the left-hand side of the unit.

**5% Pull i**

This half-cycle was not fully completed as the actuator on the right-hand beam reached the limit of its stroke. The stiffness of the unit was approximately zero for a significant portion of the half-cycle, clearly demonstrating that no bond existed between the beam reinforcement and the joint zone concrete. Testing was concluded with this half-cycle.

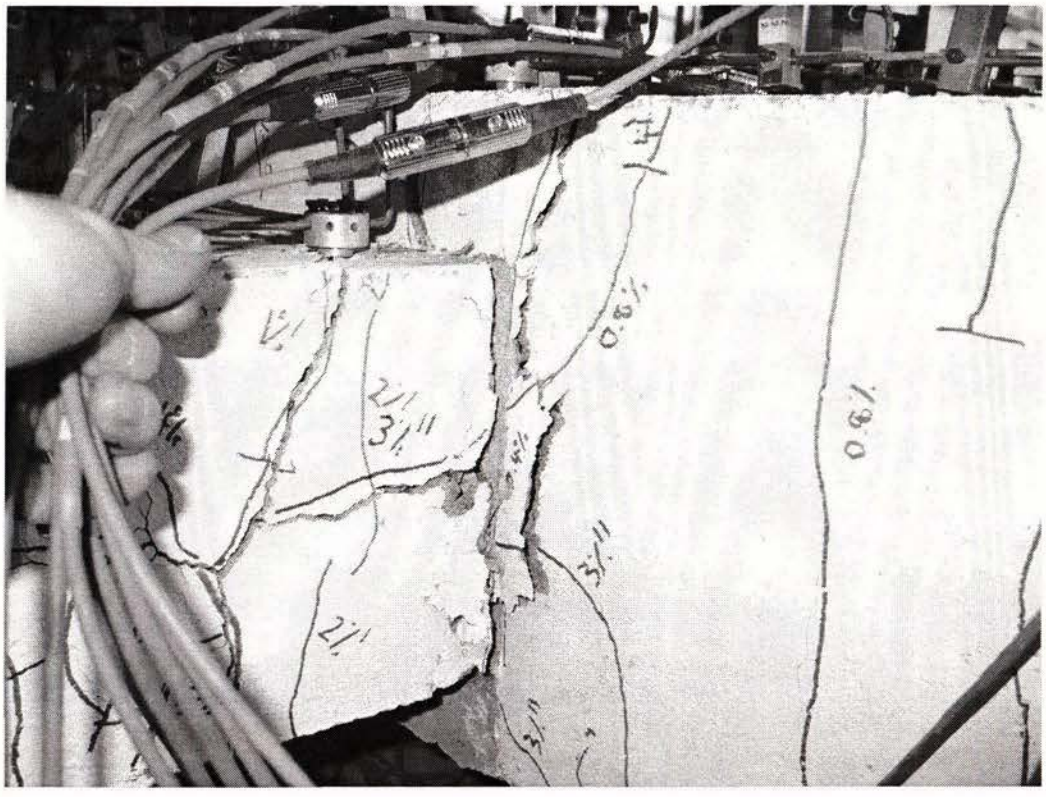


**Figure 5-34 Concrete being pulled from the joint zone by slipping beam reinforcement, fourth half-cycle to 4% drift**

## 5.4 Unit 4B

**Pre-test observations**

Due to the problems encountered with the new computer controlled hydraulic system and the short interval between testing of units 3B and 4B (restricting the time available to trouble shoot the new system), it was decided to control the testing of unit 4B using the same manual control system as for units 1B and 2B and the latter stages of unit 3B.

As for the preceding tests, all gauges were checked immediately prior to the commencement of testing, and the single acting jacks at the column ends were loaded to approximately 60 kN to prevent movement of the test unit.

**0.5% Push i**

This half-cycle, to approximately 40% of the estimated yield drift, caused flexural cracks along approximately three quarters of the length of the beams. Splitting cracks formed at the edges of the joint region where reinforcing bars in tension entered the joint region, and in addition a single shear crack formed in the joint region.

**0.5% Pull i**

Compared to the initial half-cycle there was slightly more flexural cracking during this half-cycle. A number of shear cracks formed in the joint region, and the first cracking of the column occurred in the form of a single crack on each tension side.

**0.5% Push ii**

New crack formation was limited to a single crack in the top column, and a pair of flexural cracks in the left-hand beam.

**0.5% Pull ii**

Again there was only limited new cracking during this half-cycle.

**1% Push i**

As expected, this half-cycle resulted in a significant increase in cracking all over the unit, but no sign of yielding. The joint region was now cracked in many places, including a major diagonal tension crack across the central area (Figure 5-35). Shear and flexural cracking extended over much of the beams, and there was more flexural cracking in the columns as well.

**1% Pull i**

It was noticed during this half-cycle that the load sustained by both beams was higher than for the previous half-cycle (in the other direction of loading). Significant shear cracking occurred at the end of both beams, and there was more new damage in the joint region. Flexural cracks extended further along both beams, and formed across the central half of the columns.

**1% Push ii**

The load sustained in this half-cycle was unchanged from the first to 1% drift in this direction. There was little new damage.

**1% Pull ii**

Only minor crack elongation occurred during this half-cycle.

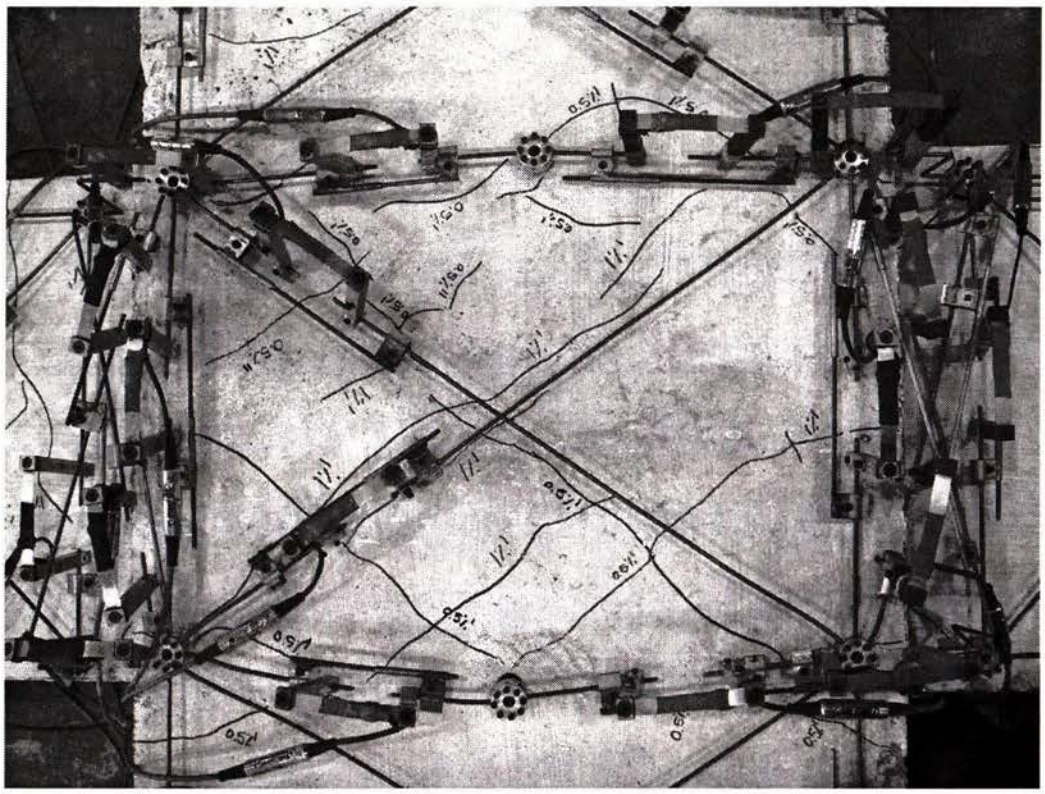

**Figure 5-35 Typical damage to joint region at low drift levels**

**2% Push i**

The increased displacement (and hence force) of this half-cycle again brought significant new shear cracking at the beam ends. Nearer the columns existing flexural cracks grew under increased shear loads. In addition, new flexural cracks developed close to the column faces. Some new cracks formed in the column, but the only new damage in the joint zone was a small extension of existing cracks.

Even at this relatively early stage of testing there was evidence that the yielding of beam reinforcement was penetrating into the column, approximately to the point where the beam and outer column reinforcement crossed.

**2% Pull i**

Less cracking occurred during this half-cycle than during the previous one. This was probably due to the smaller increase in maximum load measured in this direction than had been measured in the push

direction of loading. Most of the new cracks formed at the beam ends. Several new cracks formed in the joint region.

It appeared at this point that the concrete of the plastic hinge regions was breaking into distinct "chunks" under the cyclic actions of the test.

**2% Push ii**

Several new cracks formed in the joint region during this half-cycle. It was also noticed that there was an absence of cracking in the lower right hand corner of the joint (Figure 5-36). Splitting cracks formed in the right-hand beam, but overall there was little new damage.

**2% Pull ii**

Few new cracks formed during this half-cycle. There was almost no change in the condition of the joint region. Splitting cracks formed on the bottom side of the left-hand beam, corresponding to those that formed in the right beam during the previous half-cycle. It was thought that these cracks indicated that the cover concrete in this area was very thin.

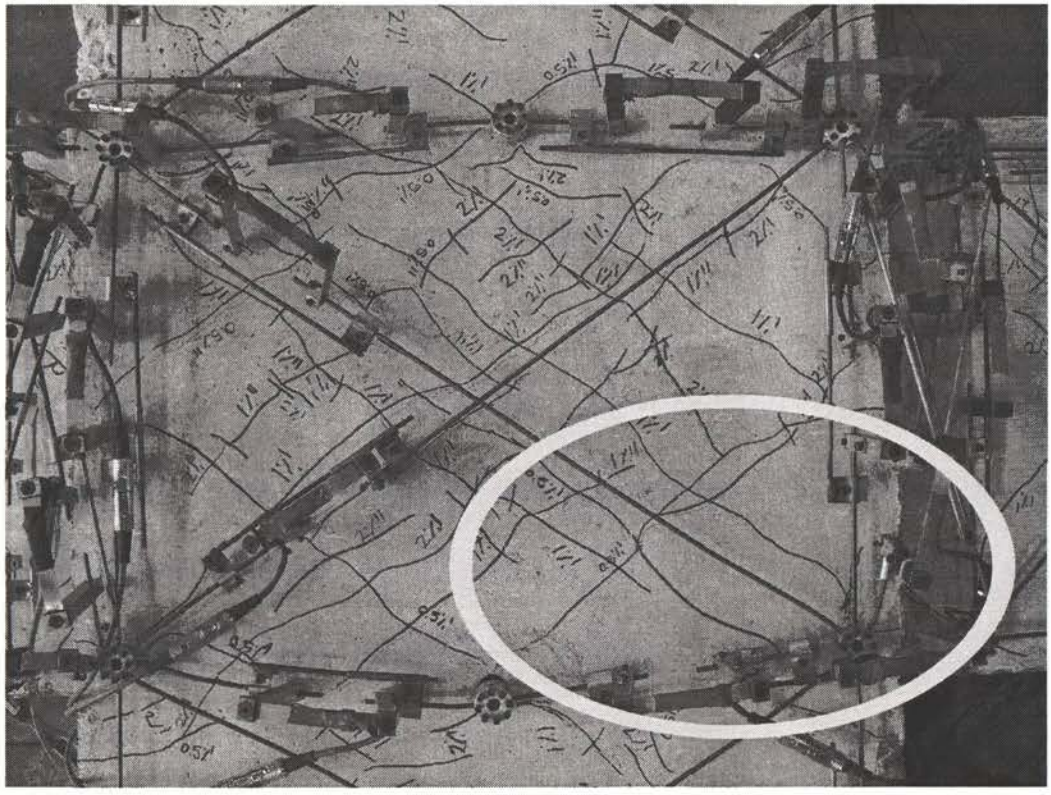

**Figure 5-36 Joint zone during third half-cycle to 2% - Note uncracked area (circled)**

**3% Push i**

New cracking during this half-cycle was mostly restricted to the plastic hinge zones. In these areas crack widths were up to 2 mm, and the main crack at the beam-column interface was approximately 4 mm wide. Cracks in the joint region were around 2 mm wide.

The splitting cracks in the right hand beam that formed during the previous half-cycle in this direction extended further along the beam in this half-cycle. Splitting also occurred on the top surface of the left-hand beam for the first time.

**3% Pull i**

Extensive new cracking occurred in the right-hand plastic hinge region during this half-cycle. In addition, the shear cracks in the joint zone now began extending into the adjacent areas of the column.

**3% Push ii**

New damage in this half-cycle was limited to a few crack extensions in the joint zone and a number of minor new cracks in the plastic hinge zones.

**3% Pull ii**

Again, new damage was very minor. A pair of new cracks opened in the joint zone, and small new cracks occurred in the plastic hinges.

**4% Push i**

During this half-cycle the splitting cracks around the entry point of the beam reinforcement to the joint zone opened significantly. Minor spalling of concrete occurred in the plastic hinge regions, but few new cracks formed.

**4% Pull i**

Few new cracks formed anywhere on the unit. A large piece of mortar fell from the left-hand plastic hinge. This had been used to repair pre-test damage to the cover concrete in this area. As occurred in the test of joint 3B, the beam reinforcement seemed to be pulling chunks of concrete from the joint region during this cycle (Figure 5-37).

**4% Push ii**

This half-cycle resulted in the first noted strength reduction. This drop was less than 20% of the peak strength, so testing was continued. Several new cracks formed in the plastic hinge regions, increasing the "crazing" effect in this area. Concrete continued to pull off the edge of the joint region as the beam reinforcement slipped through it. The gauges measuring reinforcement movement indicated that slip was definitely occurring.

**4% Pull ii**

The strength drop noted during this half-cycle again measured less than 80% of the previous maximum strength. Few new cracks formed, but there was significant breaking up of concrete in the right hand plastic hinge zone. This and the large blocks of concrete now being moved by the slipping beam reinforcement (see Figure 5-38) gave the impression that the test unit had reached the limits of its performance.

**5% Push i**

Failure occurred during this cycle, with strength clearly dropping by more than 20% of the peak. Measured slip of the beam reinforcement was around 7 mm. Some spalling occurred in the right-hand plastic hinge region, and much of the remaining concrete appeared loose and likely to fall during further cyclic loading.

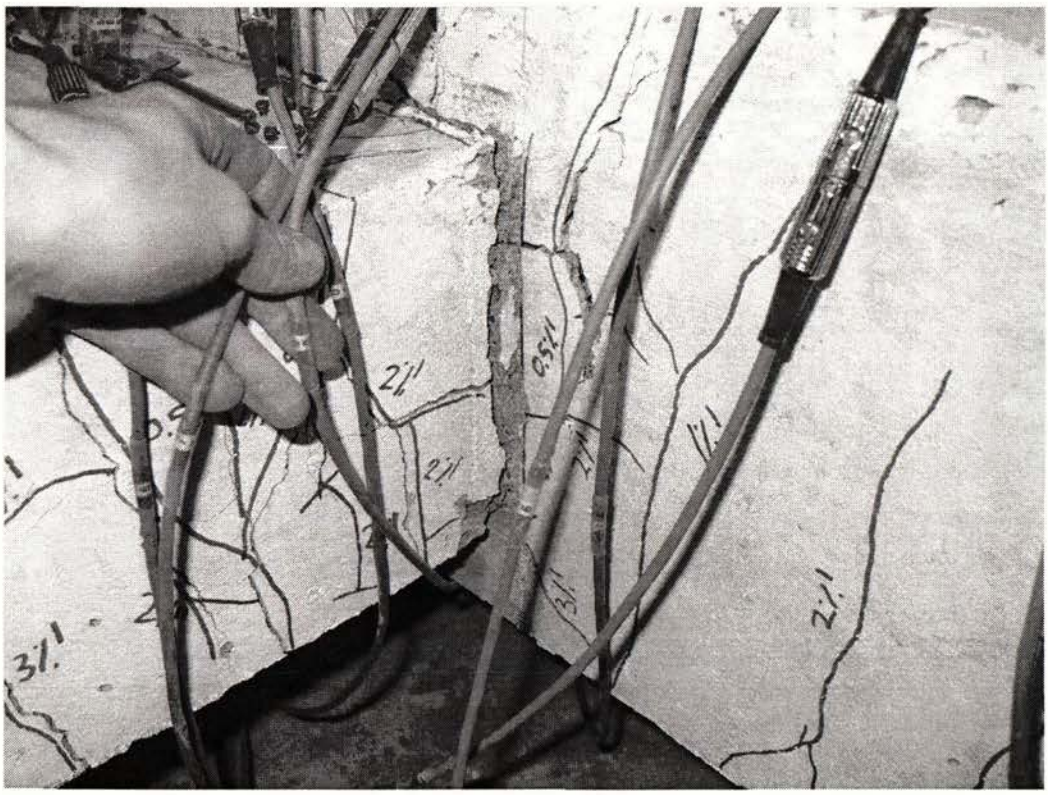

**Figure 5-37 Evidence of concrete being pulled from the joint zone during second half-cycle to 4% drift**

**5% Pull i**

The cover concrete on the top edge of both plastic hinge regions spalled completely during this cycle. Large "cones" of concrete pulled from both sides of the joint as significant bar slip continued.

**5% Push and pull ii**

Concrete continued to spall during these two half-cycles, and the test unit failed to approach the previous maximum loads sustained. Both cycles were completed, but failure was clearly evident prior to the commencement of either half-cycle.

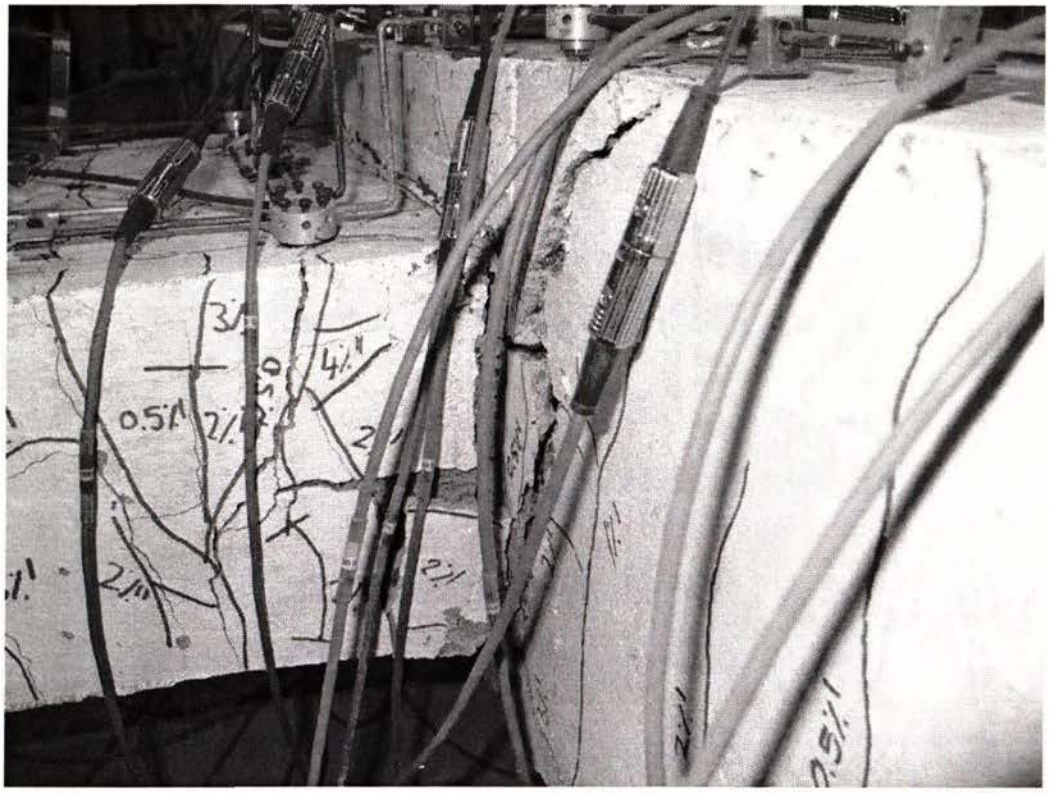

**Figure 5-38 Further damage to joint zone caused by bar slip - fourth half-cycle to 4% drift**

# 6 Analysis of Experimental Results

This chapter provides an analysis of the global performance of units 1B-4B, along with focussed analysis of the performance of certain aspects of the test units. The results of testing units 1B-4B are also compared to previous test results, particularly recent testing at the University of Auckland that investigated bond failure in internal beam-column joints [1, 2].

## *6.1 Hysteretic Response*

Figure 6-1 to Figure 6-4 show the hysteretic response of units 1B-4B, plotted as storey drift against storey (column) shear force.

Also shown on Figure 6-1 to Figure 6-4 is the nominal storey shear of each unit (the storey shear that would be developed when both the left and right beam reach their NZS 3101:1995 design strength, based on measured material strengths, $M_n$) and the predicted yield storey shear (the storey shear developed when both beams simultaneously reach their expected yield strength, based on measured material strengths, $M_y$). For units 2B-4B there is little difference between these two values (2-4% difference). However, for unit 1B there is an 8% difference between the two values. Due to the lower concrete strength of unit 1B, the area of compressed concrete in the beams was deeper than for units 2-4B. This lead to the (significant quantity of) compression reinforcement experiencing a greater strain, and thus contributing significantly to the strength of the section. Compression reinforcement is typically ignored when calculating nominal strength of beams, and hence the actual yield strength of unit 1B was underestimated by this calculation.

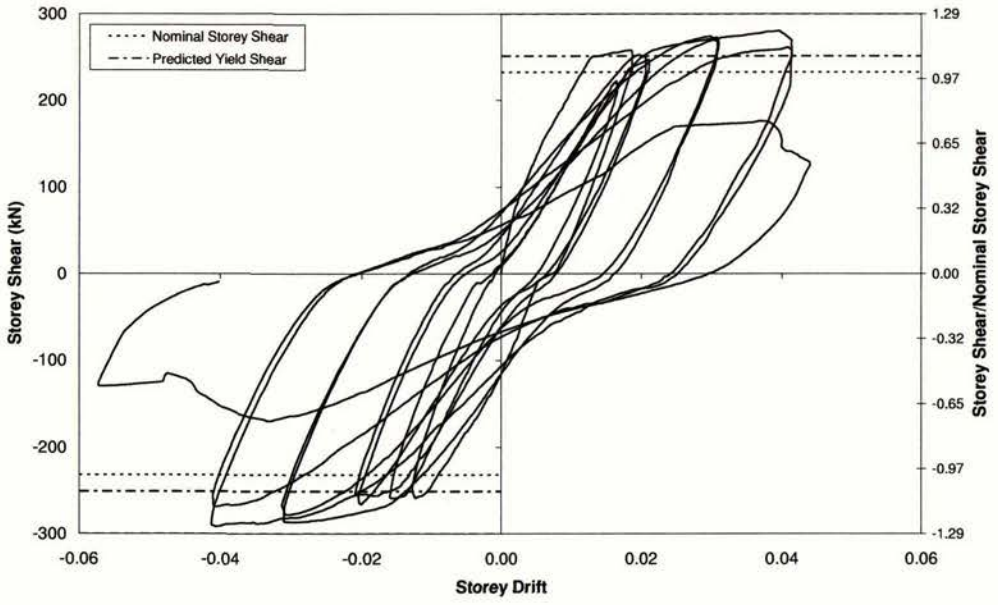


**Figure 6-1 Storey shear vs. storey drift, unit 1B**

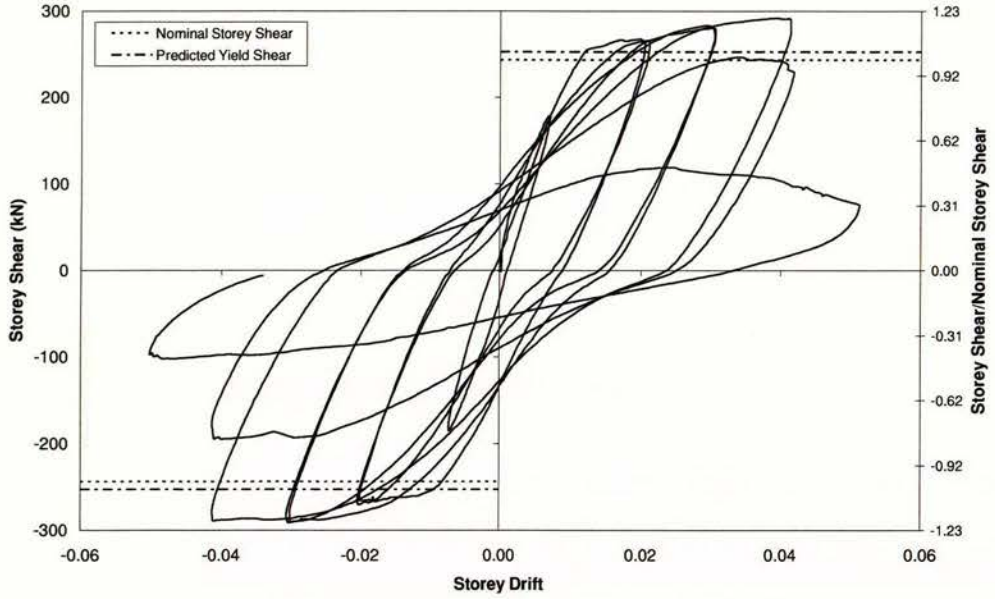


**Figure 6-2 Storey shear vs. storey drift, unit 2B**

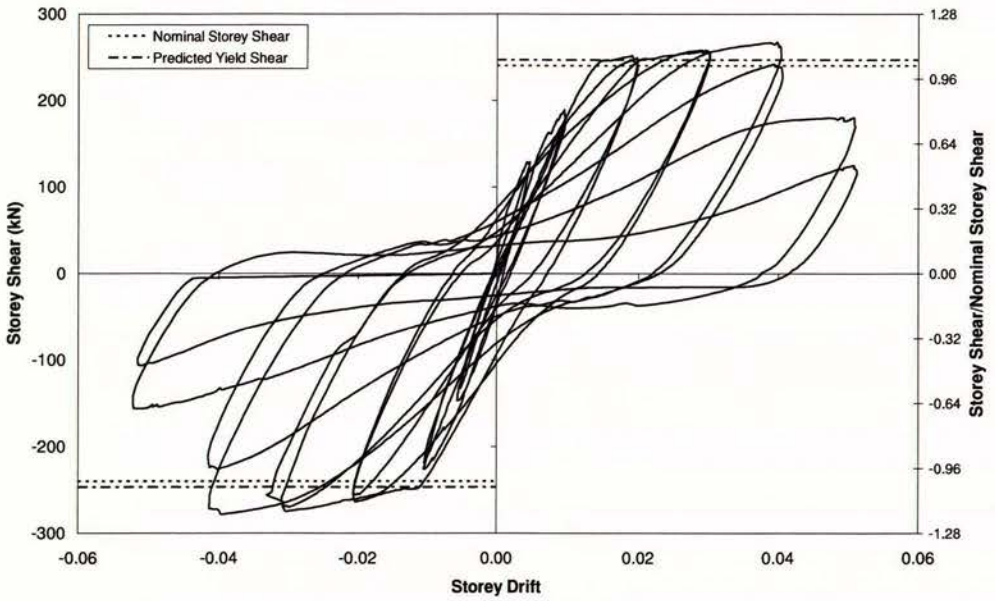


**Figure 6-3 Storey shear vs. storey drift, unit 3B**

In assessing the performance of units 1B-4B it is important to recall the dimensions of the units. Specifically, that units 1B&2B had nominally identical dimensions, as did units 3B&4B. The similarity of behaviour exhibited by these matched pairs can be seen in Figure 6-5 showing the envelopes of storey shear (plotted relative to the yield shear of each unit) against storey drift. It is seen that for positive displacement, units 1B&2B follow similar envelopes, and that these show greater stiffness than the envelopes for units 3B&4B, which also exhibit similar form. For negative displacement, the

agreement is not so clear. Further discussion of the stiffness of units 1B-4B can be found in section 6.2.

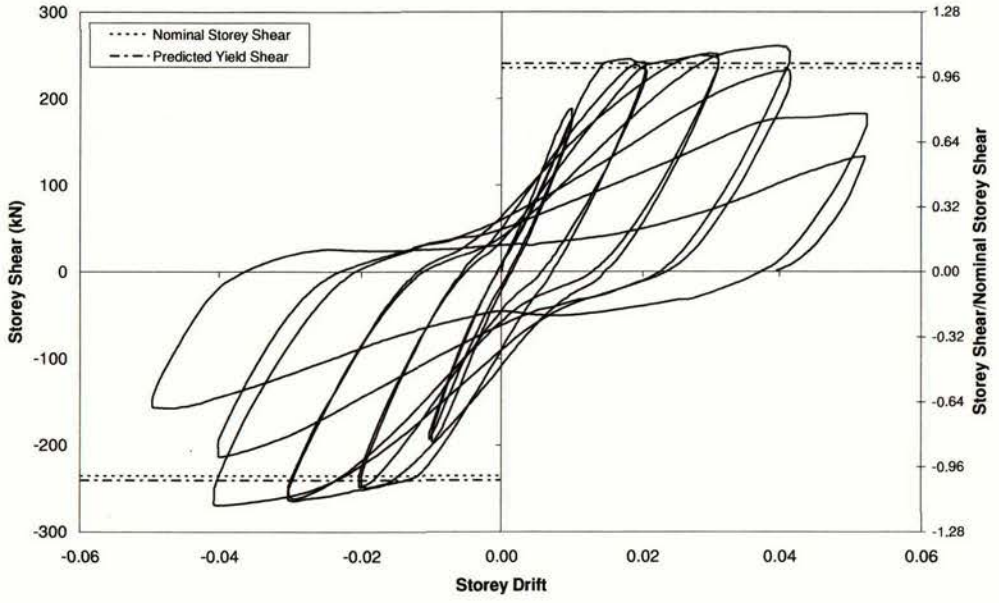


**Figure 6-4 Storey shear vs. storey drift, unit 4B**

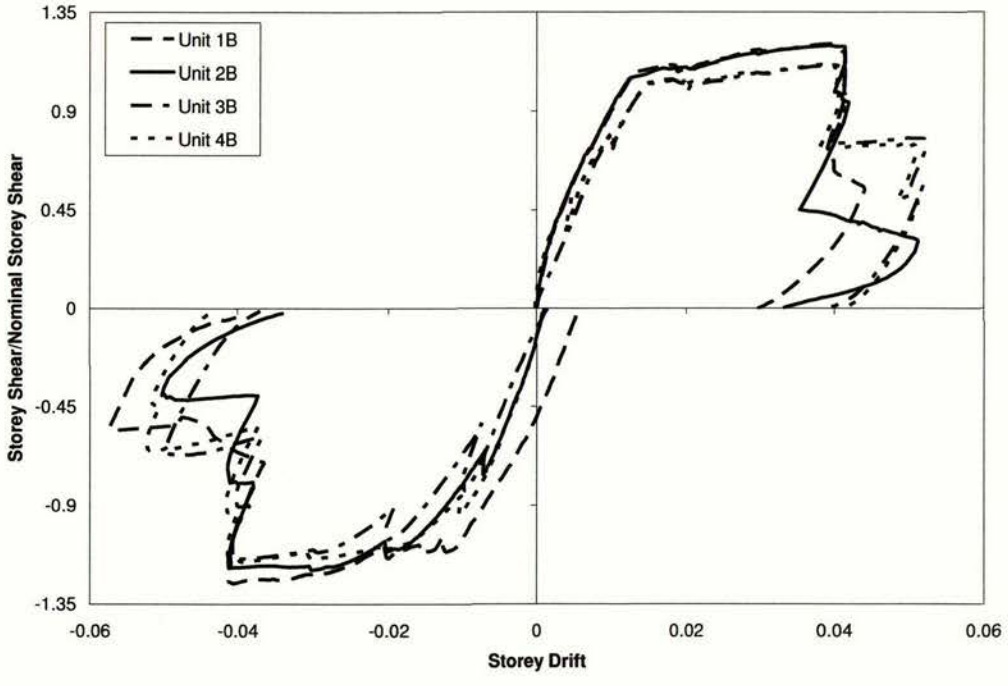


**Figure 6-5 Envelopes of hysteretic response, units 1B-4B**

The envelopes of negative displacement are less well defined than for positive loading in Figure 6-5 because they do not represent the maximum force sustained at a given drift. Instead, an attempt was made to preserve information about what loads were reached the first time a drift level was reached.

Figure 6-6 shows the maximum force developed for each drift level. It is seen that this smoothes some of the differences seen in Figure 6-5, in particular improving correlation between the response of units 1B&2B, since unit 1B had already undergone inelastic displacement prior to the first cycle of negative displacement (see section 5.1). The downside to showing the maximum force at a drift level is that this approach removes information on the initial stiffness of the units.

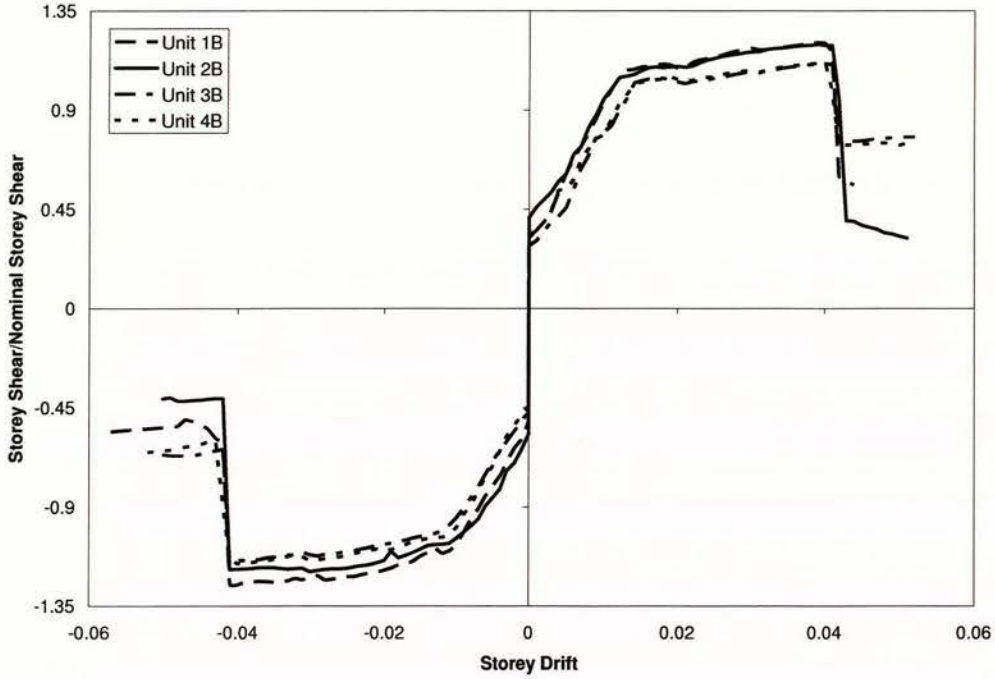


**Figure 6-6 Envelopes of maximum response, units 1B-4B**

Not visible in the envelopes shown above is the increased pinching of the hysteretic loops of units 3B&4B compared to units 1B&2B (see Figure 6-1 to Figure 6-4). In the later cycles (those to 4% drift or more), it is seen that the trace of the hysteretic curve on reloading is almost horizontal (i.e. stiffness~0) in the case of units 3B&4B, whereas for units 1B&2B the units retained some stiffness at low load levels until the conclusion of the tests. Zero stiffness at low load levels is characteristic of interior beam-column joints that have experienced a complete anchorage failure [3].

It can be seen from Figure 6-1 to Figure 6-4 that all four units performed acceptably well up to 4% drift, although the strength of two of the units (most obviously 2B) dropped by more than 20% (technical failure) during the last (forth) half cycle to 4% drift. This is beyond the maximum drift level allowed by New Zealand design standards. At 5% drift the strength of all units dropped considerably, due to either bond failure (units 3B&4B) or buckling of the plastic hinge regions (units 1B&2B). More discussion of the failure of units 1B-4B can be found in section 6.3.

## 6.2 Stiffness of Beams and Columns

In order to evaluate the behaviour of structures it is necessary to determine elastic properties of the component members of the structure (such as the effective moment of inertia ($I_e$) and yield displacement of the sections). For homogeneous materials such as steel this is straight forward, as the properties do not change significantly over the life of the structure. However, for reinforced concrete sections the determination of these properties is significantly more complicated due to the variable nature and non-isotropic properties of the material, and hence the need to assess the level of cracking in the section at the time the properties are expected to be important.

**Comparison of Yield Drift with Predicted Value**

Priestley [50] has suggested that the yield storey drift of reinforced concrete moment resisting frames can be predicted as:

$$\theta_y = 0.5\varepsilon_y \frac{l_b}{h_b} \qquad \text{eq. 20}$$

where $\theta_y$ is the yield storey drift of the frame, $\varepsilon_y$ is the yield strain of the beam reinforcement ($=f_y/E_{steel}$), $l_b$ is the length of the beam between column centres, and $h_b$ is the beam depth. For units 1B-4B, $h_b$ was 500 mm, giving predicted yield displacements as shown in Table 6-1.

**Table 6-1 Actual and predicted yield drifts, units 1B-4B**

| Unit | $f_y$ | $l_b$ | $\theta_y$ predicted | $\theta_y$ experimental | $\theta_{y\,exp}/\theta_{y\,pre}$ | $\theta_y$ (Lin) |
|---|---|---|---|---|---|---|
| | (MPa) | (mm) | | | | |
| 1B | 552 | 4892 | 0.0135 | 0.0132 | 0.978 | 0.0170 |
| 2B | 552 | 4905 | 0.0135 | 0.0122 | 0.901 | 0.0171 |
| 3B | 537 | 4877 | 0.0131 | 0.0145 | 1.107 | 0.0165 |
| 4B | 537 | 4892 | 0.0131 | 0.0143 | 1.092 | 0.0166 |
| | | | | Average | 1.020 | |
| | | | | S.D. | 0.085 | |

It is seen in Table 6-1 that the yield drifts predicted by eq. 26 are in good agreement with the yield drifts that occurred during testing. Both the average value and standard deviation (S.D.) of $\theta_{exp}/\theta_{pre}$ indicate better agreement between experimental and predicted values than was obtained from the calibration of eq. 20. The differences between actual and predicted values are due to the assumptions made by Priestley [50], including the proportions of yield displacement attributable to different types of deformation. The proportion of displacement due to shear and flexural deformation is discussed in section 6.5.

Lin [58] suggested a method to include the influence of axial load in eq. 20. Using this modified equation resulted in significantly poorer prediction of yield drift. These values are listed in the last column of Table 6-1.

**Effect of Frame Flexibility on the Design Process**

In the New Zealand earthquake loading standard [10] the maximum allowable inter-storey drift under any circumstances is 2.5%. In many cases this is reduced to between 1.5% and 2.0%. Similar limits exist in the replacement for the current loading standard [59] and in several overseas loadings codes [60-62]. Given the high drifts at yield displayed by these beam-column joint units it is readily apparent that for structures where these form the primary lateral force resisting system the maximum appropriate displacement ductility would be approximately $\mu = 2$, and that in some situations the designer would be obligated to design the building as a nominally ductile ($\mu = 1.25$) structure. Using a reduced displacement ductility in the design of a building implies that the structure will attract greater forces during a seismic event. It is therefore necessary to increase the strength of the structure, which will require the use of more reinforcement, thus further worsening the congestion resulting from the use of grade 500E beam longitudinal reinforcement in moment resisting frames that was discussed in section 3.3. This restriction on structural ductility caused by utilising high strength reinforcement in yielding components of structures has been discussed previously [50-52], but its significant effect on the design process warrants repeat mention.

## *6.3 Drift and Displacement Ductility at Failure*

**Causes and Characteristics of Failures**

Units 1B-4B were designed using the capacity design procedure required by New Zealand design standards [4, 10]. It was therefore expected that the mode of failure could be predicted accurately for all units. It was theoretically impossible for shear failures to occur, or for flexural failure of the column to occur, since the test units' capacity with respect to these failure types exceeded the actions that could be generated in the units by their "fuse" failure type.

Capacity design typically requires this "fuse" failure to be the flexural capacity of the beams of moment resisting frames. For units 1B-4B it was expected that the bond of the beam reinforcement would fail before the flexural capacity of the beams was reached, since the units did not provide the column depths required by the New Zealand concrete design standard [4].

As was mentioned in section 6.1 bond failure did not occur in units 1B&2B. For these two units the cause of failure was buckling of the beam longitudinal reinforcement in the plastic hinge zones, resulting in both beams twisting. This occurred during cycles to 5% drift. Bond failure did occur in units 3B&4B, and was noticeable in the hysteretic response of the units during cycles to 5% drift.

Figure 6-7 shows the proportion of strength maintained between successive cycles beyond 4.0% drift in the same direction of loading. The cycles to 4.0% drift marked the point at which the strength of the test units began to decrease – prior to this the strength of the units increased with each cycle. It has been typical in New Zealand to define failure to have occurred during a cycle if it is the first cycle in

which the force sustained is less than 80% of the maximum force previously sustained in that direction [57].

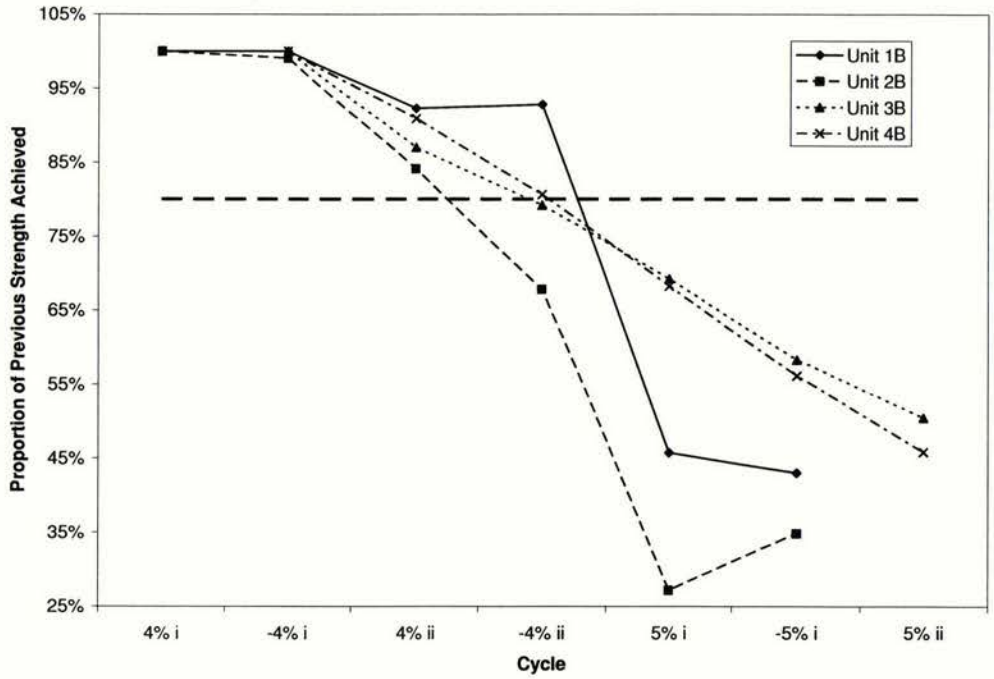


**Figure 6-7 Proportion of previous strength attained in successive cycles**

It is evident from Figure 6-7 that unit 1B failed during the first cycle to 5% drift in the positive direction, unit 2B failed during the second cycle to 4% drift in the negative direction, and that units 3B&4B were on the limit of failure during the second cycle to 4% drift (negative direction), but can realistically be said not to have failed until the first cycle to 5% drift (positive direction).

It can also be observed from Figure 6-7 that the failures of units 1B&2B was much more severe than those of units 3B&4B. While the strength of units 3B&4B dropped at a rate of approximately 10% per half-cycle, units 1B&2B both showed sudden strength drops of approximately 50% in one half cycle. This can be attributed to the sudden nature of the buckling failure they experienced compared to the gradual increase of bond slip that occurred in units 3B&4B. Translated to the performance of an entire structure, the sudden failure of units 1B&2B would most likely have more negative impact than the (relatively sustainable) bond failure of units 3B&4B.

**Maximum Achieved Displacement Ductility**

In section 6.2 it was shown that the inter-storey drift of units 1B-4B at yield was between 1.2 and 1.45. Table 6-2 shows the displacement ductility of units 1B-4B at failure. It is important to note that, following the logic of section 6.2, these values are not representative of realistic design values and are presented for interest only.

**Table 6-2 Displacement ductility of units 1B-4B**

| Unit | Yield Drift | Failure Drift | Displacement Ductility |
|---|---|---|---|
| 1B | 0.0132 | 0.05 | 3.79 |
| 2B | 0.0122 | 0.04 | 3.28 |
| 3B | 0.0145 | 0.05 | 3.45 |
| 4B | 0.0143 | 0.05 | 3.50 |

## *6.4 Bond Performance*

As has been mentioned previously, bond failure occurred in only two of the four beam-column joint units tested. In order to assess the bond performance of the four test units, gauges were installed in the joint region specifically to measure the slip of the beam longitudinal reinforcement as testing progressed (see section A.5). The readings from these gauges for units 1B-4B are shown in Figure 6-8. Note that there are two different vertical scales in Figure 6-8, one for units 1B&2B and one for units 3B&4B, and that the vertical scales shown at the left apply for both graphs running across the page.

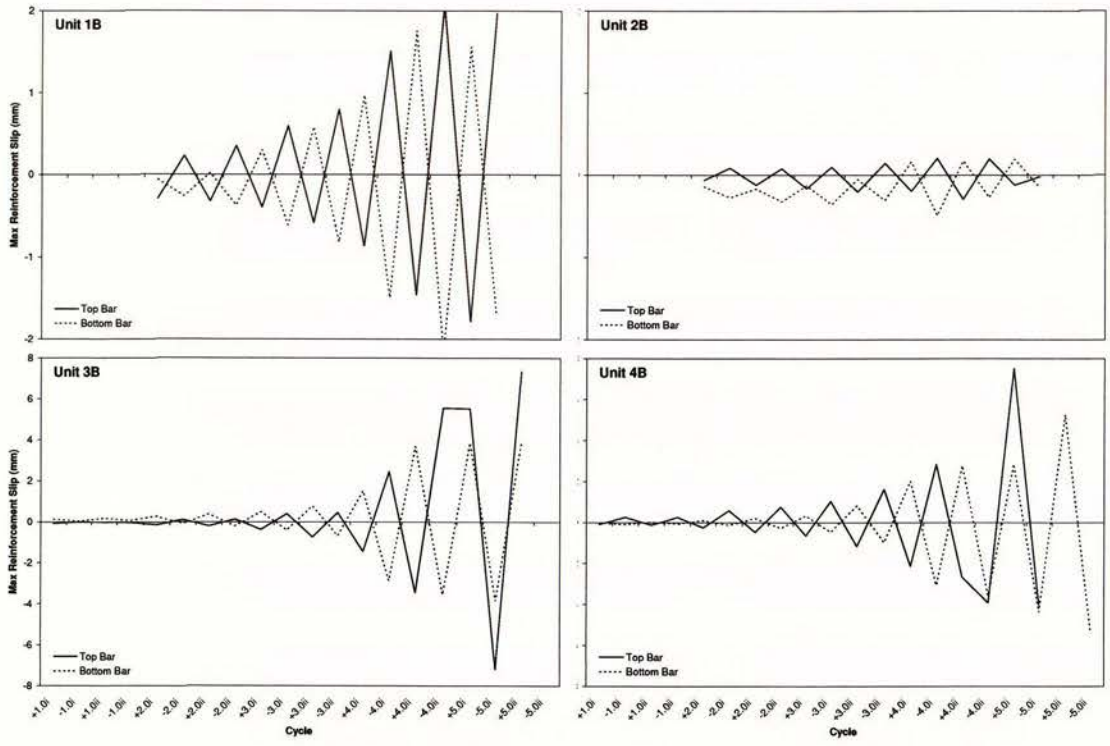


**Figure 6-8 Beam reinforcement slip, units 1B-4B**

The most important aspect of Figure 6-8 is that bar slip was limited at drift levels allowable in design (up to approximately 3.0%). Taking into account the different vertical scales, it is clear that both the top and bottom beam reinforcement of units 3B&4B slipped considerably more at later stages of testing than that in units 1B&2B. In particular, the reinforcement of unit 2B stayed almost static within the joint throughout testing. This can be explained by unit 2B having a considerably higher concrete

strength than unit 1B ($f'_c$ = 40.6 MPa compared to 31.2 MPa). The better bond performance of units 1B&2B compared to units 3B&4B and units previously tested at the University of Auckland [1, 2], which experience bond failure at drift levels of 1.6 to 4.0% (see Table 6-3), was less predictable.

Table 6-3 compares the column depths used for units 1B-4B (and other beam-column joint units tested recently at the University of Auckland) with those required by NZS 3101:1995 amendment 3 [4]. Note that the values for units 1B-4B are different than the design values presented in Table 4-1. This is because the values below are calculated using measured material properties, rather than specified properties. Accordingly, $\alpha_o$ (reinforcement overstrength factor) is taken as 1.15 only, since only strain hardening needs to be accounted for (not variability of material strength as is the case in a design situation. Additionally, F (the factor introduced in amendment 3) is taken as 0.7 below, rather than the draft value of 0.8 used in Table 4-1. All other α factors are as for Table 4-1.

**Table 6-3 Comparison of sub-assembly column depths to NZS3101:1995 requirements**

| Unit | $d_b$ | $f_y$ | $f'_c$ | F | $\alpha_o$ | $h_{c\ req.}$ | $h_{c\ used}$ | $h_{c\ used}/h_{c\ req.}$ | Bond failure drift |
|---|---|---|---|---|---|---|---|---|---|
| | (mm) | (MPa) | (MPa) | | | (mm) | (mm) | | (%) |
| 1B | 25 | 552 | 31.2 | 0.7 | 1.15 | 1049 | 800 | 0.76 | - |
| 2B | 25 | 552 | 40.6 | 0.7 | 1.15 | 919 | 800 | 0.87 | - |
| 3B | 25 | 537 | 44.8 | 0.7 | 1.15 | 851 | 675 | 0.79 | 4.0 |
| 4B | 25 | 537 | 42.8 | 0.7 | 1.15 | 871 | 675 | 0.78 | 4.0 |
| Young 1 | 16 | 519 | 49.2 | 0.7 | 1.15 | 502 | 520 | 1.03 | 4.0 |
| Amso 1 | 16 | 588 | 29.3 | 0.7 | 1.15 | 738 | 520 | 0.70 | 1.6 |
| Amso 2 | 16 | 588 | 40.4 | 0.7 | 1.15 | 628 | 520 | 0.83 | 2.5 |
| Amso 3 | 16 | 588 | 40.9 | 0.7 | 1.15 | 624 | 520 | 0.83 | 4.0 |

Taking into account the relative lack of bar slip in units 1B-4B at drift levels that have relevance to "real-world" building performance (see Figure 6-8), and the fact that none of the four units met current New Zealand design requirements (see Table 6-3), it seems that these design requirements are slightly conservative. This is desirable, and the continued use of these design guidelines is recommended.

Looking at the performance of the units in more detail reveals some discrepancies. Due to the relatively high concrete strength and large column size used it would be expected that unit 2B would perform the best (as was the case). However, units 1B, 3B and 4B were expected to perform similarly based on the proportion of required column depth provided. It also appears that units 1B&2B performed better than would be expected, since both had columns of significantly smaller depth than required.

It seems there are two probable causes for units 1B&2B performing beyond expected levels. Both units were initially designed with grade 300 column reinforcement. However, the 20 mm reinforcement delivered for the columns was grade 500 reinforcement. This lead to the columns having significantly greater flexural strength and vertical shear reinforcement than required. This is shown in Table 6-4. Regrettably no spare 20 mm reinforcement was delivered, so it was not possible to test the actual reinforcement strength. Based on tests for other grade 500 reinforcement, the yield strength of the 20 mm bar has been estimated as 560 MPa in the calculations below. For units 3B&4B the measured reinforcement strength of 584 MPa was used.

**Table 6-4 Comparison of required and actual column moment and vertical joint shear reinforcement capacities**

| Unit | $M_{col\ req}$ | $M_{col}$ | $M_{col}/M_{col\ req}$ | $V_{jv\ req}$ | $V_{jv}$ | $V_{jv}/V_{jv\ req}$ |
|---|---|---|---|---|---|---|
| | (kNm) | (kNm) | | (kN) | (kN) | |
| 1B | 410.4 | 840.9 | 2.05 | 579.0 | 942.5 | 1.63 |
| 2B | 425.4 | 860.7 | 2.02 | 441.5 | 942.5 | 2.13 |
| 3B | 406.1 | 492.6 | 1.21 | 533.8 | 704.3 | 1.32 |
| 4B | 404.2 | 491.0 | 1.21 | 556.5 | 704.3 | 1.27 |
| Young 1 | 269.7 | 326.4 | 1.21 | 443.7 | 625.9 | 1.41 |
| Amso 1 | 177.5 | 195.6 | 1.10 | 284.0 | 226 | 0.80 |
| Amso 2 | 328.0 | 379.0 | 1.16 | 768.5 | 716.5 | 0.93 |
| Amso 3 | 180.7 | 198.0 | 1.10 | 284.0 | 226 | 0.80 |

For units 1B&2B the large excesses of column moment and vertical joint shear capacities seen in Table 6-4 resulted in reduced cracking of the concrete around the beam reinforcement where it passed through the joint zone. Hence both probably improved the bond performance of the test units. It is not possible to identify the proportion to which these two effects influenced the results of these tests since the column moment- and vertical joint shear capacity are so closely linked. This linkage occurs because NZS 3101:1995 allows interior column longitudinal reinforcement to be included in the effective area of vertical joint shear reinforcement. Due to the large column depths and the maximum allowed spacing of column longitudinal reinforcement (<200 mm c/c) no additional vertical joint shear reinforcement was required for units 1B-4B. It would be prudent in any further series of beam-column joint tests to decouple the vertical joint shear capacity from the column moment capacity. This could be achieved by the use of different sizes and grades of reinforcement for the end and intermediate column bars. It is noted that for units 1B&2B the excess moment capacity of the columns was approximately that required by NZS 3101:1995 if dynamic amplification factors are taken into account [63, 64] and to values recently recommended by overseas researchers [65].

**The effect of vertical joint shear reinforcement on bond performance**

An attempt has been made to determine the effect of vertical joint shear reinforcement on bond failure in interior beam-column joints. Many of the test units included in a database assembled by Fenwick

and Megget [3] have been re-analysed to determine how the quantity of joint shear reinforcement compared to that required by NZS 3101:1995 [4]. Figure 6-9 and Figure 6-10 are plots showing the ratio of column depth used to column depth required by NZS 3101 (including amendment 3) versus respectively the ratio of horizontal and vertical joint shear reinforcement provided to that required for those units analysed [1, 2, 58, 66-75].

The specifications of the units described in the aforementioned references were put into a spreadsheet developed to analyse how closely beam-column joints met the requirements of the New Zealand concrete design standard [4]. Parameters included were the gross dimensions of the unit, quantity and strength of beam and column longitudinal reinforcement, and joint shear reinforcement. Units found to contain less than three fourths of the horizontal shear reinforcement required by the New Zealand concrete design standard were discarded as it was felt that joint shear failure would be likely to govern the response of the units. The database analysed includes approximately 40 beam-column joint tests.

It appears from Figure 6-9 that the quantity of horizontal joint shear reinforcement present in a joint does not affect the occurrence of bond failure (disregarding the fact that if too little joint shear reinforcement was present then a bond failure would not occur before joint shear failure occurs). Looking at Figure 6-10, it appears possible there is a link between the quantity of vertical joint shear reinforcement provided and the minimum column depth required to prevent bond failure. The dashed line in Figure 6-10 represents a possible divide between joints in which bond failure is or is not likely. While there is currently insufficient evidence to recommend design guidelines based on Figure 6-10, the dashed line discussed could be used to determine desirable column reinforcement levels for future beam-column joint tests. A more detailed assessment of the influence of vertical joint shear reinforcement and column moment capacity could improve understanding of when bond failure is likely to occur in interior beam column joints.

## *6.5 Components of Displacement*

The force-displacement curves shown in section 6.1 provide a useful summary of the behaviour of the four beam-column joints tests described in this report. It is also interesting to decompose the total displacements into their component parts. For interior beam-column joints, the important components are beam and column flexure and shear displacements, and joint shear displacements. These components are calculated from the readings of the gauges shown in Figure 4-2 using methods described in Appendix A.

Figure 6-11 to Figure 6-14 show the components of displacement for units 1B-4B at the peaks of different loading steps. Positive loading cycles are plotted above the horizontal axis and negative loading peaks below the horizontal axis. The heavy dashed line in each plot represents the corrected

turn potentiometer readings (see section A.3 for details of correction factors), to which the combined total of beam and column shear and flexure and joint shear displacements should be compared.

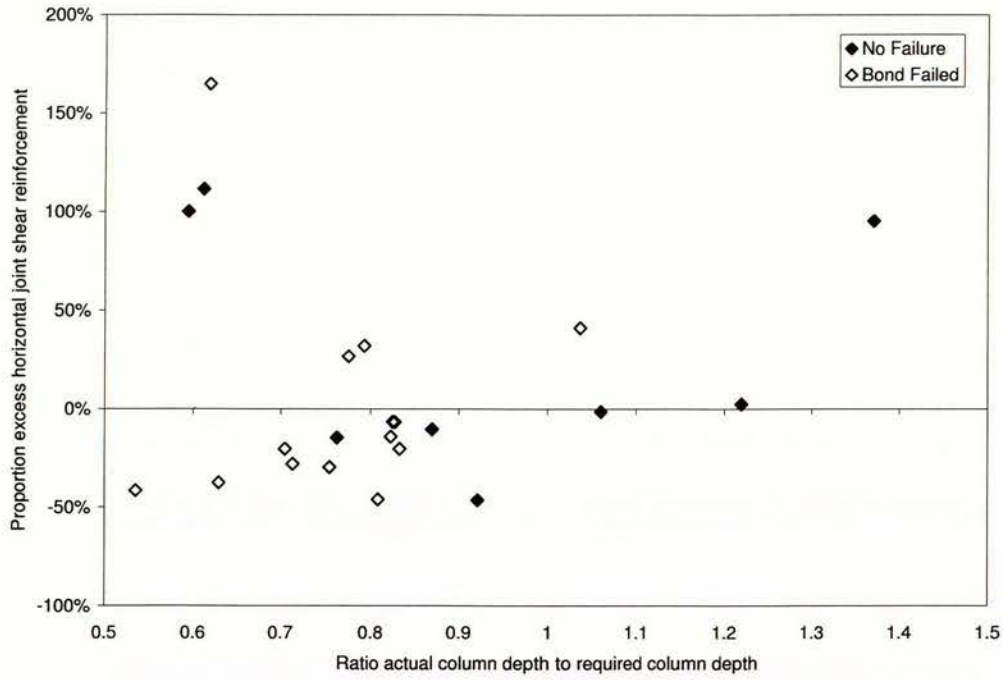


**Figure 6-9 Effect of horizontal joint shear reinforcement on bond strength**

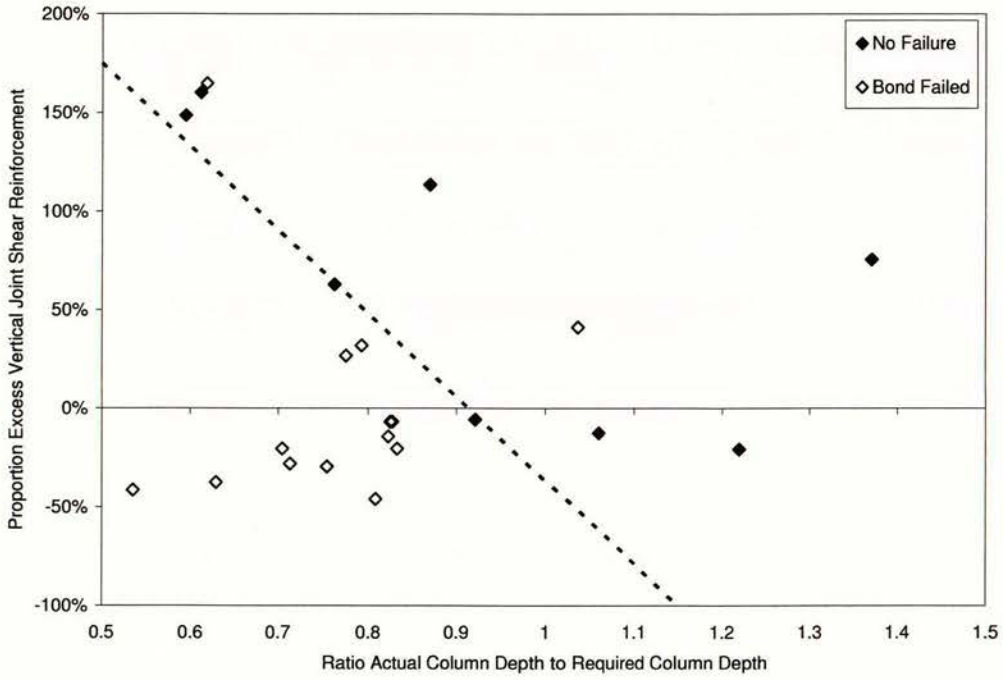


**Figure 6-10 Effect of vertical joint shear reinforcement on bond strength**

It can be seen that the agreement between the turn potentiometer readings and the sum of the displacement components is good for most of the beams. In general the error between the two values is less than 10% (see Figure 6-15), the two exceptions being the right beams of units 3B&4B. The readings for all beams are questionable during the later cycles, particularly those to 5% drift. At this stage of testing significant buckling of the beam longitudinal reinforcement in the plastic hinge zone began to take place, and the portal gauges were at the limits of their linear measurement capabilities.

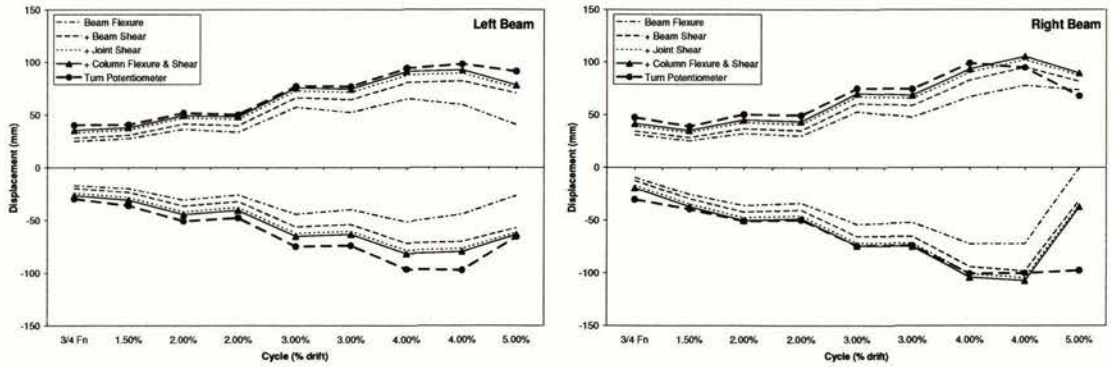


**Figure 6-11 Components of displacement for left- and right-hand beams, unit 1B**

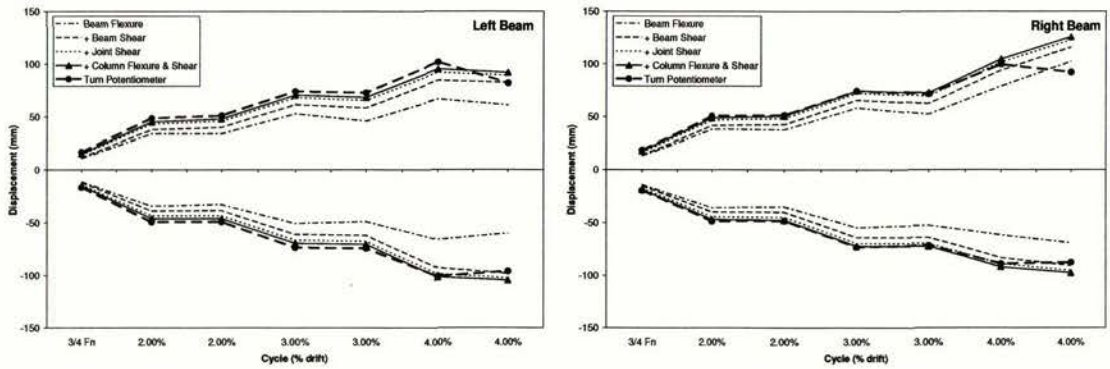


**Figure 6-12 Components of displacement for left- and right-hand beams, unit 2B**

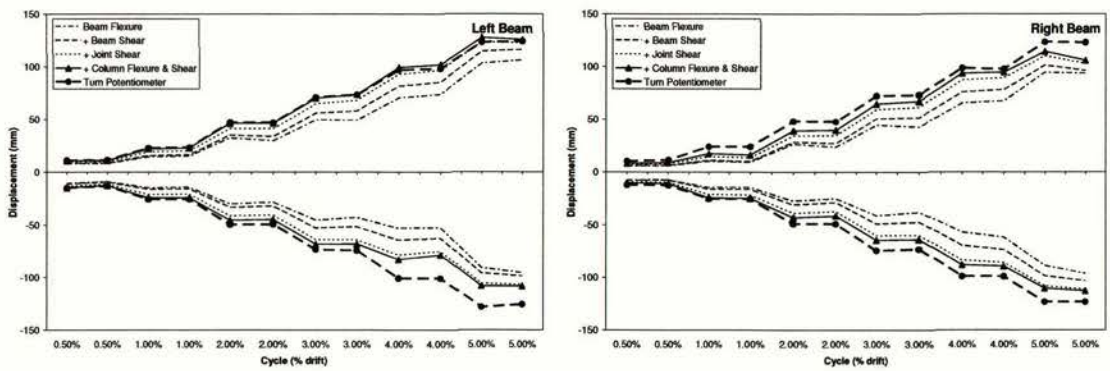


**Figure 6-13 Components of displacement for left- and right-hand beams, unit 3B**

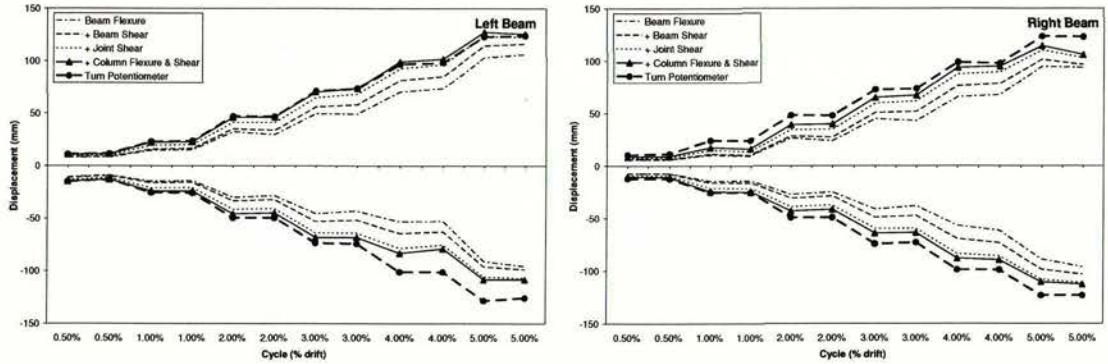


**Figure 6-14 Components of displacement for left- and right-hand beams, unit 4B**

It is interesting to compare the proportion of displacement attributable to each component. To aid this comparison Figure 6-15 shows the components of displacement of units 1B-4B as a percentage of the corrected turn potentiometer reading. An average of component values for positive and negative half-cycles for the left and right beams is plotted for each complete cycle. Additionally the closure error has been plotted. Note that values are plotted only for cycles to two, three and four percent drift – earlier cycles differed between the test units, and later cycles (to five percent drift) were felt to give unreliable readings as mentioned above.

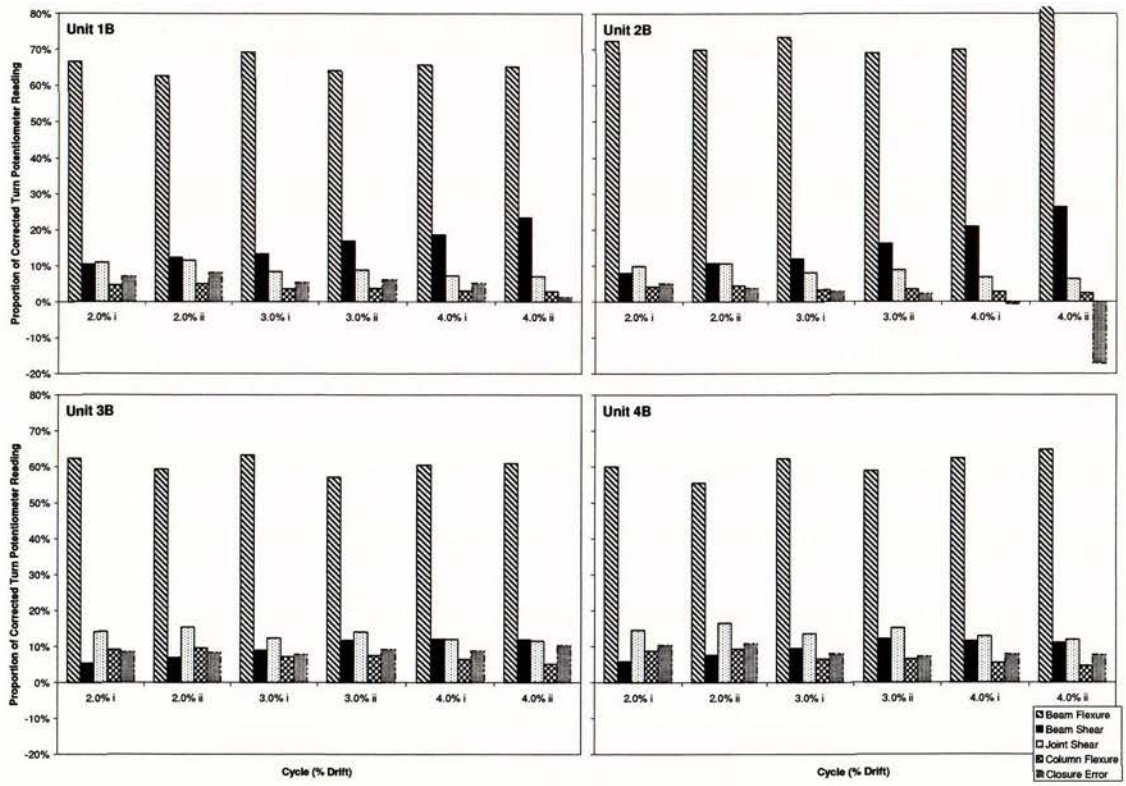


**Figure 6-15 Components of displacement as proportion of turn potentiometer reading, units 1B-4B**

As was evident in several earlier graphs, there are obvious similarities between the units with identical geometry – units 1B&2B and units 3B&4B. Unsurprisingly the components of displacement due to beam deformations are more significant for units 1B&2B (with larger, stiffer columns) – beam flexural displacement accounts for approximately 70% of the total displacement of units 1B&2B, but only 60% of the total displacement of units 3B&4B, clearly dominating the response of all units. For all four units the proportion of displacement attributable to beam flexure stayed approximately constant throughout testing, while displacement due to beam shear increased. This is particularly noticeable for units 1B&2B, while the beam shear displacements in units 3B&4B increased more gradually at first, and then remained roughly constant for the later cycles.

For all units column shear displacement was insignificant, never exceeding half a percent of the total displacement, and hence is not shown in Figure 6-11 to Figure 6-15. As testing proceeded the proportions of both column flexure and joint shear displacements dropped. This was expected since the response of these elements was designed to remain elastic, and hence deformation was proportional to force, which remained similar after plastic hinges formed in the beams.

# 7 Conclusions

- Four beam-column joint sub-assemblies were built and tested between October 2003 and August 2004. The four units were designed in accordance with the New Zealand Concrete Design Standard [4], and were of similar dimensions to units previously tested at the University of Auckland [1, 2].
- Previous testing at the University of Auckland had shown that existing design rules did not specify adequate column depths to prevent bond failure of grade 500E longitudinal beam reinforcement passing through interior beam-column joints. The aim of the four tests described in this report was to provide information on the bond performance of large diameter grade 500E reinforcement.
- The performance of the joints was satisfactory at drift levels corresponding to New Zealand design limits, indicating that current New Zealand design rules are slightly conservative. This is desirable, and the continued use of these design rules is recommended.
- Bond failure occurred in only two of four joints tested. This was despite:
  - All four units being cycled to drift levels that significantly exceeded New Zealand and overseas drift limits.
  - None of the four test units having column sizes equal to those specified by current New Zealand design requirements.
- It is thought that the better than expected bond strength developed by units 1B&2B was caused by the large quantity of column reinforcement included in these units. This reinforcement gave the columns a large excess of moment and vertical joint shear capacity over that required, which would have reduced damage to the joint zone concrete as testing progressed and thus improved bond conditions.
- A study of previous beam-column joint tests has examined how the quantity of horizontal and vertical joint shear reinforcement affects bond performance of interior beam-column joints. The study suggests that large quantities of vertical joint shear reinforcement improves joint zone bond characteristics. No relationship was evident between bond performance and horizontal joint shear reinforcement. The database of test results analysed provides insufficient evidence to base design recommendations on.
- Where a moment resisting frame is the primary lateral force resisting system in a structure, the use of grade 500E beam flexural reinforcement is not currently a sensible design option due to:
  - The large number of reinforcing bars required compared to grade 300E reinforcement;
  - The high interstorey drift levels that can be expected at first yield, and the resulting low ductility levels that can be used in design.

  It is therefore recommended that designers not use grade 500E longitudinal reinforcement in the beams of moment resisting frames.

# Appendix A Converting Portal Gauge Readings into Components of Displacement

## *A.1 Details of Instrumentation*

The four beam-column joint test units described in this report were extensively instrumented with load cells, turn potentiometer gauges and portal gauges. This appendix outlines how the readings from the portal gauge transducers were converted into measures of shear and flexural deformation, how reinforcement slip in the joint region was measured and how correction factors were calculated to account for translation and rotation of the test unit within the column mounting brackets.

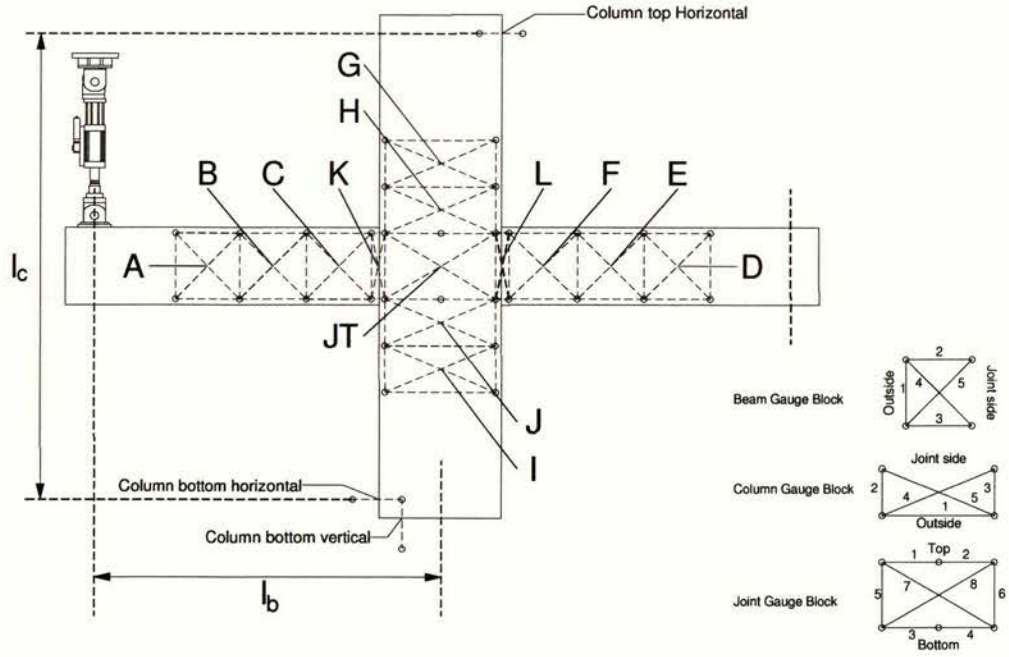


**Figure A-1 Detailed layout of portal gauge transducers showing numbering scheme**

Figure A-1 shows in more detail the gauge layout used (compared to Figure 4-2 seen previously). As can be seen, the gauges were placed in a grid type pattern, and each block of five gauges was assigned an alphabetical label from A through L, with the joint region labelled as group JT and containing eight gauges.

Within each gauge group the gauges were numbered from one through to five (or eight in the case of the joint region). Gauge one in any beam or column gauge group ran across the outside of the group, gauges two and three formed the outside edges of the group and gauges four and five were the diagonal gauges.

Additional gauges worth noting are those marked at the column top and bottom in Figure A-1. These gauges spanned between the test unit and the column restraints, and thus gave measurements indicating how the unit was moving relative to the (fixed) restraints.

The length between the mounting points of all gauges was measured to enable displacement measurements to be converted into strain measurements. The widths and height of each gauge group was defined as $w_x$ and $h_x$ respectively, where x is the gauge group letter. A number of additional measurements were made. Those marked P through to S in Figure A-1 were measured from the outside of the most outward gauge group on the respective beam or column to the midpoint of either the actuator (beams, P & Q) or the restraint frames (columns, R & S).

## *A.2 Calculating Shear and Flexural Displacement Components*

For all displacement calculations described below it is assumed that changes in angle are small.

**Joint Shear**

In considering the deflection of the beam tips due to joint shear, several components must be considered. In Figure A-2 it can be seen that joint deformations caused by both horizontal and vertical shear forces affect the displacement of the beam and column tips. It is important to note that the translational and rotational effects occur in opposition – for instance the beam rotation is upwards in Figure A-2 and the beam translation is downwards. This occurs as a result of the internal forces seen in Figure 2-2.

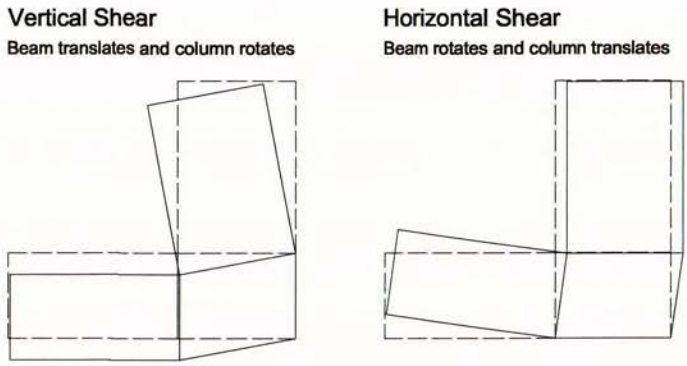


**Figure A-2 Effects of horizontal and vertical joint shear**

It is evident from Figure A-3 a) that if the beam-column joint was fixed only at the centroid of the joint region then both the beam and column tips would deflect from their original position. During the beam-column joint tests described in this report the column tips were prevented from displacing. Since the deformation of the joint zone remains the same the displacement that would have occurred at the column tips is shifted (by rigid body rotation) to the beam tips. This is illustrated in Figure A-3 b). If $\delta_{col}$ is a column tip displacement that is prevented from occurring, the induced displacement at a beam tip is:

$$\delta_{beam} = \delta_{col} \frac{l_b}{l_c} \qquad \textbf{eq. 21}$$

where $l_b$ and $l_c$ are as defined in Figure A-1. This conversion is used in this section and also in the following sections on column shear and flexural displacements.

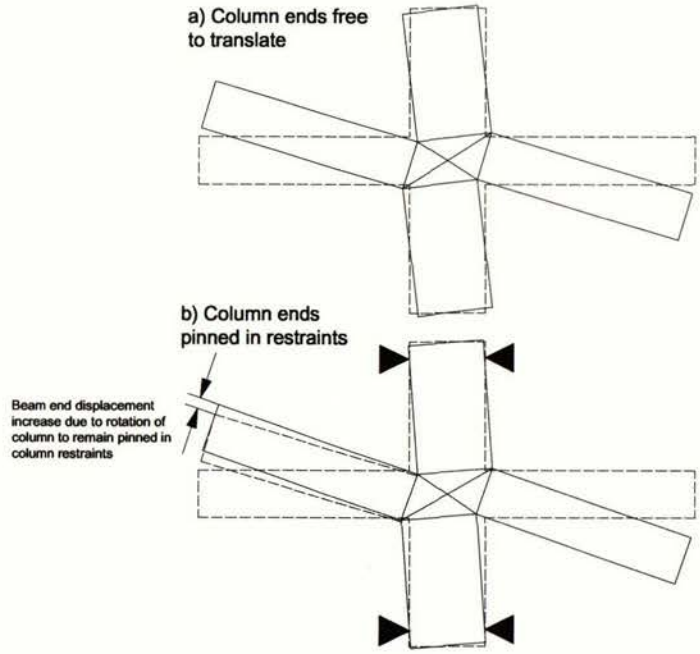


**Figure A-3 Load point deflections resulting from joint shear deformation**

In order to simplify the calculation of beam tip displacements due to joint shear deformation, it is assumed that the angles marked α in Figure A-4 are equal, and that h' and w' are equal to the original joint gauge block dimensions $h_j$ and $w_j$.

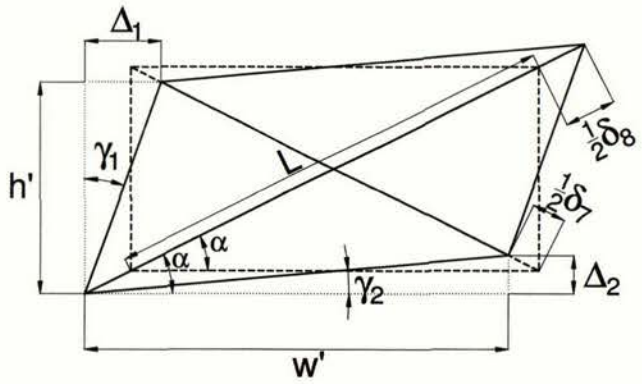


**Figure A-4 Shear deformation of joint zone gauge group**

Based on the geometry in Figure A-4, it can be seen that:

$$\Delta_1 = \cos\alpha\left(\frac{\delta_8 - \delta_7}{2}\right) = \frac{w_{joint}}{L}\left(\frac{\delta_8 - \delta_7}{2}\right) \quad \text{(a)}$$

$$\Delta_2 = \sin\alpha\left(\frac{\delta_8 - \delta_7}{2}\right) = \frac{h_{joint}}{L}\left(\frac{\delta_8 - \delta_7}{2}\right) \quad \text{(b)}$$

**eq. 22**

where $\delta_7$ and $\delta_8$ are the gauge readings for the joint zone diagonal gauges. It is also true that for small angles:

$$\gamma_1 = \frac{\Delta_1}{h'} = \frac{w_j}{L.h_j}\left(\frac{\delta_8 - \delta_7}{2}\right) = \frac{\delta_8 - \delta_7}{2L.\tan\alpha} \quad \text{(a)}$$

$$\gamma_2 = \frac{\Delta_2}{w'} = \frac{h_j}{L.w_j}\left(\frac{\delta_8 - \delta_7}{2}\right) = \frac{\delta_8 - \delta_7}{2L}\tan\alpha \quad \text{(b)}$$

**eq. 23**

where $\gamma_1$ and $\gamma_2$ are the horizontal and vertical shear deformations respectively.

Referring to Figure A-2 and recalling the opposite signs of rotational and translational member displacement, the displacement of each beam (left or right) or column (top or bottom) tip is:

$$\delta_{beam} = \gamma_1\left(l_b - \frac{h_c}{2}\right) - \gamma_2\frac{h_c}{2} \quad \text{(a)}$$

$$\delta_{column} = \gamma_2\left(\frac{l_c - h_b}{2}\right) - \gamma_1\frac{h_b}{2} \quad \text{(b)}$$

**eq. 24**

where $h_c$ and $h_b$ are the depth of the column and beam respectively, $l_b$ is the length from the column centreline to the beam tip and $l_c$ is the height between column restraints. Converting the two column tip displacements (top and bottom) to beam tip displacements and then summing gives the total (left or right) beam tip displacement, $\Delta_{JS}$

$$\Delta_{JS} = \delta_{beam} + (\delta_{col.top} + \delta_{col.bottom})\frac{l_b}{l_c}$$

$$\Delta_{JS} = \gamma_1\left(l_b - \frac{h_c}{2}\right) - \gamma_2\frac{h_c}{2} + \frac{[\gamma_2(l_c - h_b) - \gamma_1 h_b]Z}{l_c}$$

**eq. 25**

**Beam and Column Flexural Displacements**

Flexural displacements are approximated by calculating the angle of rotation between the inner and outer edge of a gauge group and multiplying this angle by the distance from the centre of the gauge group and the centre of the actuator or column restraint.

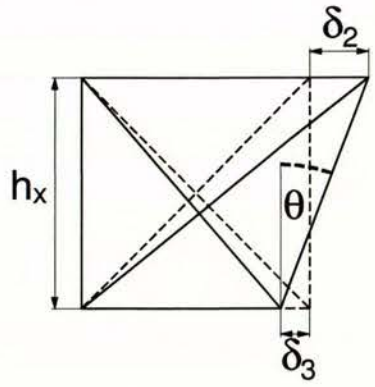


**Figure A-5 Definitions used to determine rotation in a gauge group**

Figure A-5 shows the displacements ( $\delta_2$ and $\delta_3$, the change in length of gauge 2 and 3 respectively) used to determine the rotation ($\theta$) over the length of gauge group 'x', of height $h_x$. For situations were

group 'x' is a beam gauge group, $h_x$ is the height of the group. For column groups, $h_x$ is the width of the gauge group. For both types of groups this is the length of gauge 1.

The flexural rotation within a gauge group 'x' is:

$$\theta = \frac{\delta_2 - \delta_3}{h_x} \qquad \textbf{eq. 26}$$

and the displacement at the end of the beam or column caused by this rotation is:

$$\Delta_{Flex-X} = \theta . D_x \qquad \textbf{eq. 27}$$

where $D_x$ is the distance from the centre of the gauge group to the beam or column tip. For the beam gauge groups the total displacement at beam tip due to beam flexure is determined by summing the flexural displacement due to each gauge group on the beam, i.e.

$$\Delta_{BF.left} = \Delta_{Flex-A} + \Delta_{Flex-B} + \Delta_{Flex-C} + \Delta_{Flex-K} \quad \text{(a)}$$

$$\Delta_{BF.right} = \Delta_{Flex-D} + \Delta_{Flex-E} + \Delta_{Flex-F} + \Delta_{Flex-L} \quad \text{(b)} \qquad \textbf{eq. 28}$$

For gauge groups on the columns (groups G, H, I and J from Figure A-1) it is necessary to convert the displacement at the column ends into an equivalent displacement at the beam tips. This conversion is accomplished as follows:

$$\Delta_{CF} = [\Delta_{Flex-G} + \Delta_{Flex-H} + \Delta_{Flex-I} + \Delta_{Flex-J}]\frac{l_b}{l_c} \qquad \textbf{eq. 29}$$

where Z is the distance from the column centreline to the left or right beam tip respectively, and $H_{unit}$ is the height between the centres of the column restraints (assumed to be the points of zero moment).

**Beam and Column Shear Displacements**

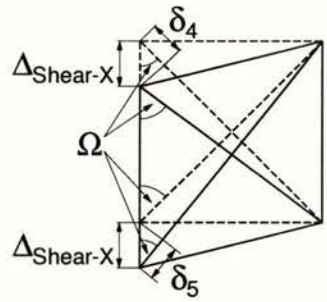


**Figure A-6 Definitions used to determine shear displacement in a gauge group**

To determine the magnitude of shear displacements that occurred in a gauge group it is assumed that the dimension of the gauge group parallel to the shearing force does not change, and therefore that the two shear displacements marked $\Delta_{Shear-X}$ in Figure A-6 are equal. For the purposes of this explanation it is assumed that $\delta_5$ is an extension (and hence a positive portal gauge reading) and that $\delta_4$ is a contraction (and the portal gauge reading is negative). Due to the small geometry changes of gauge blocks during testing it is assumed that the angle $\Omega$ remains constant, and is given by:

$$\Omega = \tan^{-1}\left(\frac{w_x}{h_x}\right) \qquad \textbf{eq. 30}$$

where $w_x$ and $h_x$ are respectively the width and height of the gauge group. From Figure A-6 it can be seen that:

$$\cos(\Omega) = \frac{\delta_5}{\Delta_{Shear-X}} = \frac{-\delta_4}{\Delta_{Shear-X}} \qquad \textbf{eq. 31}$$

Rearranging eq. 30 and summing to provide an average value of $\Delta_{Shear\text{-}X}$ gives:

$$\Delta_{Shear-X} = \frac{\delta_5 - \delta_4}{2\cos(\Omega)} \qquad \textbf{eq. 32}$$

The total displacement due to beam shear at a beam tip is simply the sum of the shear displacements of the gauge blocks on that beam (A, B, C and K on the left beam, D, E, F and L on the right beam).

The displacement of a load point due to column shear is given by the following:

$$\Delta_{CS} = [\Delta_{Shear-G} + \Delta_{Shear-H} + \Delta_{Shear-I} + \Delta_{Shear-J}]\frac{l_b}{l_c} \qquad \textbf{eq. 33}$$

with definitions as for equation eq. 29.

## *A.3 Calculating Correction Factors for the Turnpot Readings*

It is necessary to correct the readings of total beam displacement obtained from the turnpot gauges to allow for rigid body movement of the beam-column joint within the column restraints. This movement is separated into two parts – lateral translation of the unit parallel to the column, and rotation of the unit, as seen in Figure A-7. Since the turn potentiometers read parallel to the column, lateral translation parallel to the beams will not affect their readings.

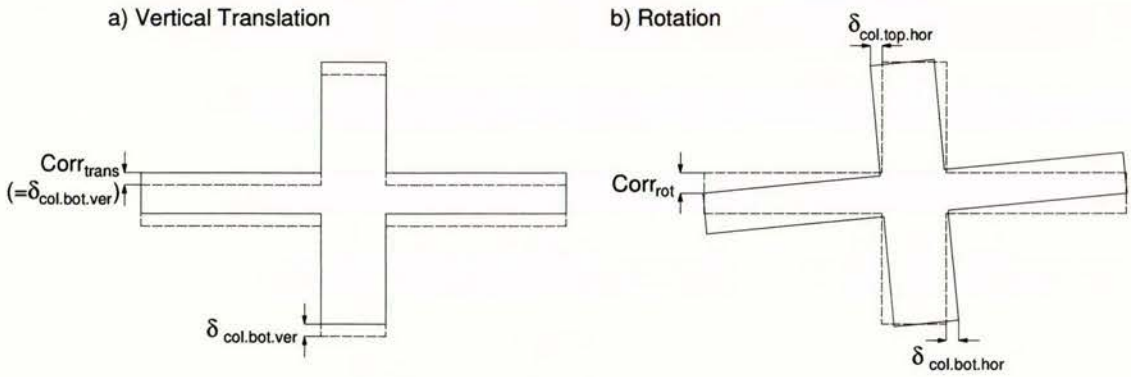


**Figure A-7 Correction factors for overall movement of test unit**

**Translation Correction Factor**

Translation of the unit parallel to the column was measured by a single portal gauge transducer, marked "column bottom vertical" in Figure A-1. This was installed so that the gauge gave a positive reading if the column moved upwards (as defined in Figure 4-5).

To correct the readings of beam end deflections, this reading was applied as follows:

$$Corr_{trans.left} = \delta_{col.bot.ver} \quad \text{(a)}$$
$$Corr_{trans.right} = -\delta_{col.bot.ver} \quad \text{(b)} \qquad \textbf{eq. 34}$$

where $Corr_{trans.x}$ is the correction factor applied to the turnpot reading for the left or right hand beam, and $\delta_{col.bot.ver}$ is the change in length of the portal gauge column bottom vertical.

**Rotation Correction Factor**

Two portal gauges were installed to measure the rotation of the unit within the column restraints. These are marked column top horizontal and column bottom horizontal in Figure A-1. The gauges were installed so that a positive gauge reading (an extension of the gauge length) resulted from a positive (anti-clockwise) rotation of the beam-column joint.

The correction factor required was calculated from these readings as follows:

$$Corr_{rot} = (\delta_{col.top.hor} + \delta_{col.bot.hor})\frac{l_b}{l_c} \qquad \textbf{eq. 35}$$

i.e. the correction factor for the left or right beam is the total displacement of the column ends divided by the column height (to give an angle of rotation) multiplied by the distance from the centreline of the column to the centreline of the double acting actuator on the respective beam.

## *A.4 Comparison of displacement components with total beam tip movement*

To establish the accuracy of the calculated displacement components, it is necessary to compare them with the beam tip displacements measured by the turn potentiometers. To obtain a value for comparison the components of displacement due to beam and column shear and flexure, joint shear and rigid body rotation were summed for each beam tip, i.e.

$$\Delta_{Total} = \Delta_{JS} + \Delta_{BF} + \Delta_{BS} + \Delta_{CF} + \Delta_{CS} + Corr_{rot} + Corr_{trans} \qquad \textbf{eq. 36}$$

## *A.5 Measuring longitudinal reinforcement slip in the joint region*

In order to fulfil the requirements of this series of tests it was important to measure the movement of the beam longitudinal reinforcement in the joint region. This was done by installing four gauges in the joint region (joint gauge block 1-4 in Figure A-1) for this purpose. As was discussed in section 2.3 it was very unlikely that the bond between the column reinforcement and concrete would fail during testing, and hence no provision was made to measure column reinforcement slip.

At the outer edge of the joint region gauges JT1-JT4 were attached to studs welded to the column longitudinal reinforcement, which was assumed to be a fixed reference. The other end of the gauges (near the centreline of the column) were attached to longer studs that were welded to the beam longitudinal reinforcement (see Figure A-8). Examination of the data recorded during testing of units

1B-4B showed that the change in width of the joint gauge group did not exceed half a percent, showing that the assumption of the column bars being fixed reference points was reasonable.

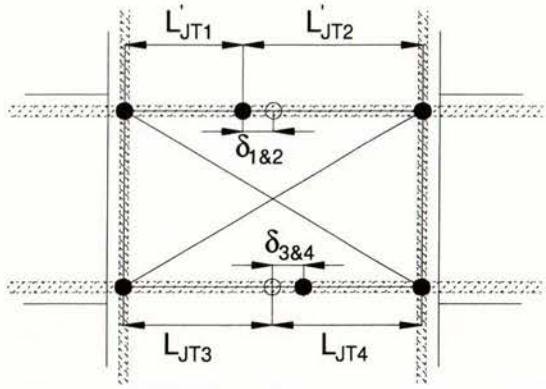


**Figure A-8 Measurement of reinforcement movement in the joint region**

Since the assumption that the column longitudinal bars were unmoving was correct (i.e. $L'_{JT1}+L'_{JT2}$~constant) the readings for gauges JT1 and JT2 ($\delta_{1\&2}$ in Figure A-8) and JT3 and JT4 ($\delta_{3\&4}$) gave a measure of how far the beam longitudinal reinforcement had slipped relative to the column reinforcement and surrounding concrete. Therefore, the distance the reinforcement slipped was taken as the average of these two measurements, i.e.

$$Slip_{top.bar} = \frac{\delta_1 - \delta_2}{2} \quad \text{(a)}$$

$$Slip_{bot.bar} = \frac{\delta_3 - \delta_4}{2} \quad \text{(b)}$$

**eq. 37**

The negative signs take account of the fact that one gauge was expanding (positive reading) and one was contracting (negative reading) while measuring the same movement.

# References


1. Young, K.L. (1998). *Anchorage Plates and Mechanical Couplers in Seismic Resistant Concrete Frames Reinforced with Threaded Bar.* Masters Thesis, Department of Civil and Resource Engineering, University of Auckland, Auckland, New Zealand. 233p.
2. Megget, L.M., R.C. Fenwick, and N. Amso (2003). *Seismic Performance of Internal Beam-Column Joints with 500 Grade Reinforcement. Proceedings of the Pacific Conference on Earthquake Engineering.* Christchurch, New Zealand: University of Canterbury.
3. Fenwick, R.C. and L.M. Megget (2003). *The Influence of Using Grade 500 Reinforcement in Beam Column Joint Zones and on the Stiffness of Reinforced Concrete Structures.* The Cement and Concrete Association of New Zealand & Reinforcing New Zealand Inc. Wellington, New Zealand. 13p.
4. NZS 3101:1995 *The Design of Concrete Structures.* Standards New Zealand: Wellington, N.Z. 256p.
5. Paulay, T. (1988). *Seismic Design in Reinforced Concrete: The State of the Art in New Zealand.* Bulletin of the New Zealand National Society for Earthquake Engineering, **21**(3): pp.208-233.
6. Park, R. and T. Paulay (1975). *Reinforced Concrete Structures.* New York, New York: John Wiley and Sons. 769p.
7. Blume, J.A., N.M. Newmark, and L.H. Corning (1961). *Design of Multistorey Reinforced Concrete Buildings for Earthquake Motions.* Chicago, Illinois: Portland Cement Association. 318p.
8. Hanson, N.W. and H.W. Connor (1967). *Seismic Resistance of Reinforced Concrete Beam-Column Joints.* Proceedings of the American Society of Civil Engineers, **93**(ST5): pp.533-560.
9. Hanson, N.W. (1971). *Seismic Resistance of Concrete Frames with Grade 60 Reinforcement.* Proceedings of the American Society of Civil Engineers, **97**(ST6): pp.1685-1700.
10. NZS 4203:1992 *Code of Practice for General Structural Design and Design Loadings for Buildings.* Standards New Zealand: Wellington, New Zealand. 134p.
11. Hollings, J.P. (1969). *Reinforced Concrete Seismic Design.* Bulletin of the New Zealand National Society for Earthquake Engineering, **2**(3): pp.217-250.
12. Viwathanatepa, S., E.P. Popov, and V.V. Bertero (1979). *Seismic Behaviour of Reinforced Concrete Interior Beam-Column Subassemblages.* Report No. UCB/EERC-79/14, University of California. Berkeley, California. 184p.
13. Fenwick, R.C. (1981). *Seismic Resistant Joints for Reinforced Concrete Structures.* Bulletin of the New Zealand National Society for Earthquake Engineering, **14**(3): pp.145-159.
14. Paulay, T. and M.J.N. Priestley (1992). *Seismic Design of Reinforced Concrete and Masonry Buildings.* New York, New York: John Wiley & Sons, Inc. 744p.
15. Hakuto, S., R. Park, and H. Tanaka (1999). *Effect of Deterioration of Bond of Beam Bars Passing through Interior Beam-Column Joints on Flexural Strength and Ductility.* ACI Structural Journal, **96**(5): pp.858-864.
16. Park, R. (2002). *Some Considerations in the Design of Reinforced Concrete Interior Beam-Column Joints of Moment Resisting Frames.* Journal of the Structural Engineering Society of New Zealand, **15**(2): pp.53-64.
17. ACI-ASCE Committee 352 (1976). *Recommendations for the Design of Beam-Column Joints in Monolithic Reinforced Concrete Structures.* ACI Journal, **73**(7): pp.375-393.
18. Blakeley, R.W.G., L.M. Megget, and M.J.N. Priestley (1975). *Seismic Performance of Two Full Sized Reinforced Concrete Beam-Column Joint Units.* Bulletin of the New Zealand National Society for Earthquake Engineering, **8**(1): pp.38-69.
19. Fenwick, R.C. and H.M. Irvine (1977). *Reinforced Concrete Beam-Column Joints for Seismic Loading Part II - Experimental Results.* Bulletin of the New Zealand National Society for Earthquake Engineering, **10**(4): pp.174-185.
20. Galunic, B., V.V. Bertero, and E.P. Popov (1977). *An Approach for Improving Seismic Behaviour of Reinforced Concrete Interior Joints.* Report No. UCB/EERC-77/30, University of California. Berkeley, California. 94p.
21. Blakeley, R.W.G., F.D. Edmonds, L.M. Megget, and J.H. Wood (1979). *Cyclic Load Testing of Two Refined Concrete Beam-Column Joints. Proceedings of the South Pacific Regional Conference on Earthquake Engineering.*

22. Ciampi, V., R. Eligehausen, V.V. Bertero, and E.P. Popov (1982). *Analytical Model for Concrete Anchorages of Reinforcing Bars Under Generalized Excitations.* Report No. UCB/EERC-82/23, University of California. Berkeley, California. 111p.
23. Cowell, A.D., E.P. Popov, and V.V. Bertero (1982). *Effects of Concrete Types and Loading Conditions on Local Bond-Slip Relationships.* Report No. UCB/EERC-82/17, University of California. Berkeley, California. 61p.
24. Eligehausen, R., E.P. Popov, and V.V. Bertero (1983). *Local Bond Stress-Slip Relationships of Deformed Bars Under Generalized Excitations.* Report No. UCB/EERC-83/23, University of California. Berkeley, California. 169p.
25. Filippou, F.C., E.P. Popov, and V.V. Bertero (1983). *Effect of Bond Deterioration on Hysteretic Behaviour of Reinforced Concrete Joints.* Report No. UCB/EERC-83/19, University of California. Berkeley, California. 184p.
26. Soleimani, D., E.P. Popov, and V.V. Bertero (1979). *Hysteretic Behaviour of Reinforced Concrete Beam-Column Subassemblages.* ACI Journal, **76**(11): pp.1179-1195.
27. Viwathanatepa, S., E.P. Popov, and V.V. Bertero (1979). *Effects of Generalized Loadings on Bond of Reinforcing Bars Embedded in Confined Concrete Blocks.* Report No. UCB/EERC-79/22, University of California. Berkeley, California. 304p.
28. Popov, E.P. (1984). *Bond and Anchorage of Reinforcing Bars Under Cyclic Loading.* ACI Journal, **81**(4): pp.340-349.
29. Filippou, F.C. (1986). *Simple Model for Reinforcing Bar Anchorages Under Cyclic Excitations.* Journal of Structural Engineering, **112**(7): pp.1639-1659.
30. Mukaddam, M.A. and M.B. Kasti (1986). *Reinforced Concrete Joints Under Cyclic Loading.* Journal of Structural Engineering, **112**(4): pp.937-942.
31. Harajili, M.H. and M.A. Mukaddam (1988). *Slip of Steel Bars in Concrete Joints Under Cyclic Loading.* Journal of Structural Engineering, **114**(9): pp.2017-2035.
32. Russo, G., G. Zingone, and F. Romano (1990). *Analytical Solution for Bond-Slip of Reinforcing Bars in R.C. Joints.* Journal of Structural Engineering, **116**(2): pp.336-355.
33. Monti, G., E. Spacone, and F.C. Filippou (1993). *Model for Anchored Reinforcing Bars Under Seismic Excitations.* Report No. UCB/EERC-93/08, University of California. Berkeley, California. 88p.
34. Fleury, F., J.-M. Reynouard, and O. Merabet (1999). *Finite Element Implementation of a Steel-Concrete Bond Law for Nonlinear Analysis of Beam-Column Joints Subjected to Earthquake Type Loading.* Structural Engineering and Mechanics, **7**(1): pp.35-52.
35. Biddah, A. and A. Ghobarah (1999). *Modelling of shear deformation and bond slip in reinforced concrete joints.* Structural Engineering and Mechanics, **7**(4): pp.413-432.
36. Elmorsi, M., M.R. Kianoush, and W.K. Tso (2000). *Modelling Bond-Slip Deformations in Reinforced Concrete Beam-Column Joints.* Canadian Journal of Civil Engineering, **27**(3): pp.490-505.
37. Leon, R.T. (1989). *Interior Joints with Variable Anchorage Lengths.* ASCE Journal of Structural Engineering, **115**(9): pp.2261-2275.
38. Blakeley, R.W.G. (1983). *Beam-Column Joints*, in *Applications of New Zealand Standard Code of Practice for the Design of Concrete Structures NZS 3101:1982.* New Zealand Concrete Society: Wellington, New Zealand. pp.20.
39. Burns, R.J. (1977). *NZSEE Discussion Group on Seismic Design of Ductile Moment Resisting Reinforced Concrete Frames - Introduction and Philosophy.* Bulletin of the New Zealand National Society for Earthquake Engineering, **10**(2): pp.69-71.
40. Park, R. (1981). *Review of Code Developments for Earthquake Resistant Design of Concrete Structures in New Zealand.* Bulletin of the New Zealand National Society for Earthquake Engineering, **14**(4): pp.177-208.
41. Paulay, T., R. Park, and M.J.N. Priestley (1978). *Reinforced Concrete Beam-Column Joints Under Seismic Actions.* ACI Journal, **75**(11): pp.585-593.
42. Smith, I.C. and G.K. Sidwell (1977). *Beam Flexure and Hinge Zone Detailing in Reinforced Concrete Ductile Frames Requiring Beam Sway Mechanisms.* Bulletin of the New Zealand National Society for Earthquake Engineering, **10**(2): pp.72-79.
43. NZS 3101:1982 *Code of Practice for the Design of Concrete Structures.* Standards Association of New Zealand: Wellington, New Zealand. 127p.
44. Paulay, T. and R. Park (1984). *Joints in Reinforced Concrete Frames Designed for Earthquake Resistance.* Report No. 84-9, Department of Civil Engineering, University of Canterbury. Christchurch, New Zealand. 58p.

45. ACI-ASCE Committee 352 (1985). *Recommendations for Design of Beam-Column Joints in Monolithic Reinforced Concrete Structures.* ACI Journal, **82**(3): pp.266-283.
46. ACI 318-05 2005. *Building Code Requirements for Structural Concrete.* American Concrete Institute: Farmington Hills, Michigan. 400p.
47. Park, R. and R. Dai (1988). *A Comparison of the Behaviour of Reinforced Concrete Beam-Column Joints Designed for Ductility and Limited Ductility.* Bulletin of the New Zealand National Society for Earthquake Engineering, **21**(4): pp.255-278.
48. NZS 3402: 1989 *Steel Bars for the Reinforcement of Concrete.* Standards Association of New Zealand: Wellington, N.Z. 15p.
49. O'Grady, C.R. (2002). *The Challenge of Grade 500 Steel.* Journal of the Structural Engineering Society of New Zealand, **15**(1): pp.42-45.
50. Priestley, M.J.N. (1998). *Brief Comments on Elastic Flexibility of Reinforced Concrete Frames and Significance to Seismic Design.* Bulletin of the New Zealand National Society for Earthquake Engineering, **31**(4): pp.246-259.
51. Paulay, T. (2000). *A Note on New Yield Stress.* Journal of the Structural Engineering Society of New Zealand, **13**(2): pp.43-44.
52. Park, R. (2001). *Use of the New Grade 500E Reinforcing Steel.* Journal of the Structural Engineering Society of New Zealand, **14**(1): pp.29-31.
53. Matthews, J., D. Bull, and J.B. Mander (2002). *Preliminary Results from the Testing of a Precast Hollowcore Floor Slab Building. Proceedings of the New Zealand Concrete Society Conference.* Taupo, New Zealand: New Zealand Concrete Society.
54. AS/NZS 4671:2001 *Steel Reinforcing Materials.* Standards New Zealand: Wellington, New Zealand. 33p.
55. DZ 3101.1 rel.2 (2004). *Public Comment Draft Concrete Structures Standard.* Standards New Zealand: Wellington, New Zealand. 274p.
56. Bull, D. and C. Allington (2003). *Overstrength Factor for Pacific Steel Micro-Alloy Grade 500 Reinforcement: April 2002.* Journal of the Structural Engineering Society of New Zealand, **16**(1): pp.52-53.
57. Park, R. (1989). *Evaluation of Ductility of Structures and Structural Assemblages from Laboratory Testing.* Bulletin of the New Zealand National Society for Earthquake Engineering, **22**(3): pp.155-166.
58. Lin, C. (1999). *Seismic Behaviour and Design of Reinforced Concrete Interior Beam Column Joints.* PhD Thesis, Department of Civil Engineering, University of Canterbury, Christchurch, New Zealand. 461p.
59. AS/NZS 1170.4:2003 *Draft Australia/New Zealand Standard, Earthquake Loading, Post Public Comment Draft 8.* Standards New Zealand: Wellington, New Zealand. 66p.
60. Fenwick, R.C., D. Lau, and B. Davidson (2002). *A Comparison of the Seismic Design Requirements in the New Zealand Loadings Standard with other Major Design Codes.* Bulletin of the New Zealand National Society for Earthquake Engineering, **35**(3): pp.190-203.
61. Booth, E.D., A.J. Kappos, and R. Park (1998). *A Critical Review of International Practice on Seismic Design of Reinforced Concrete Buildings.* The Structural Engineer, **76**(11): pp.212-220.
62. King, A.B. (1996). *The Fundamentals of an Earthquake Standard.* Bulletin of the New Zealand National Society for Earthquake Engineering, **29**(3): pp.199-207.
63. Paulay, T. (2002). *Seismic Evaluation of Column-to-Beam Strength Ratios in Reinforced Concrete Frames. Discussion of Paper by Kara L. Dooley and Joseph M. Bracci.* ACI Structural Journal, **99**(5): pp.709-710.
64. Park, R. (2003). *Some Controversial Aspects of the Seismic Design of Reinforced Concrete Building Structures.* Bulletin of the New Zealand National Society for Earthquake Engineering, **36**(3): pp.165-188.
65. Dooley, K.L. and J.M. Bracci (2001). *Seismic Evaluation of Column-to-Beam Strength Ratios in Reinforced Concrete Frames.* ACI Structural Journal, **98**(6): pp.843-851.
66. Birss, G.R., R. Park, and T. Paulay (1978). *The Elastic Behaviour of Earthquake Resistant Reinforced Concrete Interior Beam-Column Joints.* Report No. 78-13, University of Canterbury. Christchurch, New Zealand. 96p.
67. Cheung, P.C. (1991). *Seismic Design of Reinforced Concrete Beam-Column Joints with Floor Slab.* 91-4, University of Canterbury. Christchurch, New Zealand. 328p.
68. Joh, O., Y. Goto, and T. Shibata (1991). *Influence of Transverse Joint and Beam Reinforcement and Relocation of Plastic Hinge Region on Beam-Column Joint Stiffness*

*Deterioration*, in *SP 123 Design of Beam-Column Joints for Seismic Resistance*, J.O. Jirsa, Editor. ACI: Detroit, Michigan. pp.187-223.

69. Milburn, J.R. and R. Park (1982). *Behaviour of Reinforced Concrete Beam-Column Joints Designed to NZS 3101*. Report No. 82-7, University of Canterbury. Christchurch, New Zealand. 108p.
70. Restrepo-Posada, J.I. (1993). *Seismic Behaviour of Connections between Precast Concrete Elements*. Report No. 93-3, University of Canterbury. Christchurch, New Zealand. 385p.
71. Stevenson, E.C. (1980). *Fibre Reinforced Concrete in Seismic Design*. Report No. 80-7, University of Canterbury. Christchurch, New Zealand. 95p.
72. Xin, X.Z. (1992). *Behaviour of Reinforced Concrete Beam-Column Joints Designed using High Strength Concrete and Steel*. 92-3, University of Canterbury. Christchurch, New Zealand. 121p.
73. Kitayama, K., S. Lee, S. Otani, and H. Aoyama (1992). *Behaviour of High-Strength R/C Beam-Column Joints. Proceedings of the Tenth World Conference on Earthquake Engineering*. Madrid, Spain: Balkema.
74. Monti, G. and C. Nuti (1992). *Cyclic Tests on Normal and Lightweight Concrete Beam-Column Sub-Assemblages. Proceedings of the Tenth World Conference on Earthquake Engineering*. Madrid, Spain: Balkema.
75. Noguchi, H. and T. Kashiwazaki (1992). *Experimental Studies on Shear Performances of RC Interior Column-Beam Joints with High Strength Materials. Proceedings of the Tenth World Conference on Earthquake Engineering*. Madrid, Spain: Balkema.